Title
Wrist-Worn Systems for Activity State Recognition: Evaluation of Challenges and Benefits

Author
Nematihosseinabadi, Ebrahim

Publication Date
2017

Peer reviewed|Thesis/dissertation

UNIVERSITY OF CALIFORNIA

Los Angeles

Wrist-Worn Systems for Activity State Recognition: Evaluation of Challenges and Benefits

A dissertation submitted in partial satisfaction

of the requirements for the degree

Doctor of Philosophy in Electrical Engineering

by

Ebrahim Nematihosseinabadi

2017

ABSTRACT OF THE DISSERTATION

Wrist-Worn Systems for Activity State Recognition: Evaluation of Challenges and Benefits

by

Ebrahim Nematihosseinabadi

Doctor of Philosophy in Electrical Engineering

University of California, Los Angeles, 2017

Professor Majid Sarrafzadeh, Chair

This dissertation investigates the limitation and challenges of wrist-worn sensing in activity state recognition including posture and gait quality inference. In spite of all the benefits that come with wrist-worn sensing systems, there are many challenges in inferring activities using them. The most important challenge is the high rate of false positive due to unwanted hand motion when the system is worn on the wrist. Another important challenge is the limitation on the power budget and processing capabilities of a wrist-worn device. Being far from the Center of Mass (COM), inferring posture and gait seem to be a very challenging problem using wrist data. This dissertation tries to provide a deep investigation on these challenges and propose ways to mitigate them. Different time series analysis methods are employed to serve for improvement in both accuracy and power consumption of activity state recognition. Along the way, we introduce some of the systems and algorithms that were built around these ideas and how they can be helpful in tackling the challenges of wrist-worn sensing systems, when it comes to activity state recognition.

The dissertation of Ebrahim Nematihosseinabadi is approved.

Michael Jerrett

Ali Mosleh

Gregory J. Pottie

Majid Sarrafzadeh, Committee Chair

University of California, Los Angeles

2017

To my parents . . .

who—among so many other things—

believed in me more than what I could possibly imagine

and showed me dims of light when my eyes were too blind to see

TABLE OF CONTENTS

LIST OF FIGURES

LIST OF TABLES

ACKNOWLEDGMENTS

I would like to first acknowledge my advisor, Professor Majid Sarrafzadeh, who gave me the opportunity to join his research group. He guided me through my PhD career involving me in a lot of great projects from which I was able to find my research topic. He has been the key to my success in my PhD career in UCLA with his constant availability and involvement in my research endeavors. I also want to thank my committee members, professor Ali Mosleh and professor Greg Pottie for their smart feedback on my dissertation. I want to specially thank professor Michael Jerrett, another member of my committee, with whom I had the honor to work with and learn a lot from in the past two years. He was kind enough to offer me as much time as he could during his busy schedule to help me through my research.

I must also thank Professor Arash Naeim and Professor Daniel Lu in medical school of UCLA whom I collaborated with in different projects and from whom I received an enormous amount of guidance and vision on the medical side of the research. In that regard, I need to thank Christina Batteate and Kristina Vander Wall for partnering with me as my colleagues in those project from environmental science and medical school departments in UCLA. I also want to acknowledge my fellow colleagues in ER lab: Dr. Bobak Mortazavi for providing immense amount of advice when I joined the lab, being instrumental in helping me gain enough knowledge on fundamentals to initiate productive research in the lab. Dr. Mohammad Pourhomayoun from whom I learned so much on the theoretical side of data analytics and algorithm design for examining time series sensory data. Special acknowledgement to Dr. Young Soo Suh whom I had the pleasure to work with for more than one year during which we collaborated on gait analysis research, managing to publish many research articles in the area. I would like to send my utmost gratitude to my colleagues and my friends in ER lab, Dr. Costas Sideris and Dr. Haik Kalantarian who were always pushing me achieving my research

and career goals, providing a suitable environment for productive collaborations which led to many mutual research endeavors in the field.

A great acknowledgement should also be given to Berkley East Convalescent Hospital staff and management for providing an appropriate and adequate environment to transfer our in-lab achievements to real-world situation by letting us build our remote health monitoring platform in their facility. Similarly special thanks to Digital Health Lab in Samsung Research America which provided me with on-the-edge instrumentation and analysis toolboxes during my internship, which led to publishing two great research articles in the area of remote sensing.

Eventually, I need to send my extreme appreciation to my family: My Father, Dr. Abdolali Nemati for teaching me how to be persistent and encouraged in reaching my goals. My Mother, Shamsieh Sadeghifar, for immense amount of love which made the road a lot easier to pursue. My little sister, Marzieh who never ceased to bombard me with her sisterly love and care. And to all my friends in UCLA, Yasen, Navid, Vince, Vahab, Babak, Kaveh, Armin, Pamchal, Arjun, Noor and Sanaz who were always there for me, keeping me motivated during this long journey of getting my PhD, helping me get up when I was loosing hope and providing me with as much help as they could in the research as well as course-taking side of my journey in UCLA.

VITA

2010	B.Sc. in Electrical Engineering, University of Tehran, Iran.
2012	M. Sc. in Electrical Engineering, McMaster University, Canada.
2009-2010	Teaching Assistant, Electrical Engineering, University of Tehran.
2010 to 2012	Research Assistant, Electrical Engineering, McMaster University.
2012 to 2013	University honorary fellowship, UCLA.
2014-2017	Teaching Assistant, Electrical Engineering, UCLA.
2014-2017	Graduate Research Assistant, Computer Science, UCLA.
2015	Best Paper Award, International Conference on Data Analytics
2016	Research Scientist, Samsung Research America, Mountain View, USA.

PUBLICATIONS

A Novel Algorithm for Activity State Recognition Using Smartwatch Data. E. Nemati et al. IEEE-NIH 2017 Special Topics on Healthcare Innovations and PoC Technologies

Opportunistic Environmental Sensing with Smartphones: a Critical Review of Current Literature and Applications. E. Nemati et al. Current Environmental Health Reports

A Method for Preserving Privacy During Audio Recordings by Filtering Speech. D. Liaqat et al. 1st IEEE Life Sciences Conference (LSC) 2017

A dynamic data source selection system for smartwatch platform. E. Nemati et al. Engineering in Medicine and Biology Society (EMBC), 2016 IEEE 38th

Kalman-filter-based walking distance estimation for a smart-watch. Y. S. Suh et al. Connected Health: Applications, Systems and Engineering Tech., 2016 IEEE

Gait velocity estimation for a smartwatch platform using Kalman filter peak recovery. E. Nemati et al. Wearable and Implantable BSN, 2016 IEEE 13th International Conference on

Building continuous arterial blood pressure prediction models using recurrent networks. C. Sideris et al. Smart Computing, 2016 IEEE International Conference on

Can smartwatches replace smartphones for posture tracking?. E. Nemati et al. Sensors Journal 15 (10), 26783-26800

Context-Aware Data Analytics for Activity Recognition. M. Pourhomayoun et al. International Conference on Data Analytics, 2015

A smartwatch-based medication adherence system. H. Kalantarian et al. Wearable and Implantable Body Sensor Networks, 2015 IEEE 12th International Conf. on

A wireless wearable ECG sensor for long-term applications. E. Nemati et al. IEEE Communications Magazine, 2012

CHAPTER 1

Introduction

1.1 Remote Health Monitoring

Classic method of disease treatment has always been fulfilled by patients sensing the symptoms of a disease and then seeking cure for it in the next step. Today's patient-clinician interaction goes beyond this, involving patients in very early stages of sensing symptoms and in many cases even before getting sick. With improvement in transistor and sensor fabrication, light low-profile unobtrusive sensing systems are produced which provides a great deal of information for clinicians about the patient's health status. This opened up a brand new horizon in medicine, which is called remote health monitoring (RHM), helping clinicians predict and diagnose disease in early stages and quickly provide treatment based upon that.

Although it might not be reasonable to remotely monitor all the populations for their health status all the time, being selective for a certain group of society and for a certain span of their lifetime can result into reduction of healthcare cost considerably. This selection requires knowing some prior information about the subjects. However, this information often does not exist or is not cheap to acquire. A lot of times even some simple insight about the patients, such as sex, age or their medical records is enough to pick a group of people for some sort of remote health monitoring systems (RHMS) that leads to maximum health care cost reduction. A group of people who is growing rather quickly over the past few decades in United States [1], that can benefit a lot from RHMS is elderly population. Another population in need, is patients with chronic

disease. More than half of all Americans had one or more chronic health issues in 2014 and 86% of healthcare spending is for patients with one or more chronic disease [2]. Centers for Disease Control and Prevention (CDC) identifies Cardiovascular disease (CVD) to be the most responsible cause of death in 2016 [3]. Cancer is the second cause of death which often stays with the patients in their whole life. However, it could be completely cured depending on the condition of the patients and type of the cancer [4]. RHM can play a tremendous role in both stages of before and after diagnosis for this categories of patients. Preventive medicine, utilizes RHMS to observe, educate and interfere when the needs come.

Advancement in technology has enabled the implementation of various forms of RHMSs including camera-based, RFID based and WiFi-based positioning systems [5, 6, 7]. However, these systems require high initial setup cost and substantial system installation efforts. In addition, individuals may be unreceptive to these systems due to privacy and security concerns. By contrast, wearable systems usually do not impose these issues. However, it is hard to camouflage them in the daily life of patients and that imposes inconvenience and sometime intolerance among certain populations.

Wearable-based RHMSs, which is the focus of this dissertation, have wide variety of applications. These applications range from tracking activity [8, 9] to heart failure [10, 11], weight training [12], exercise intensity measure [13], fall detection [14], etc. with the mission to reduce healthcare costs and improve quality of care. These systems can not only enable an early prevention care model but also provide an unceasing tracker of risky patients especially within categories of chronic, elderly and frail (Frailty is a common geriatric syndrome that embodies an elevated risk of catastrophic declines in health and function among older adults).

1.2 Smartphone vs. Wrist-Worn Sensing

Providing continuous tracking of patients requires wearables that are unnoticeable and super comfortable to be capable of being unobtrusively integrated to people's daily life when it comes to frail and elderly patients. Enforcing wearing a new wearable which a person normally does not carry is too much of a burden for these populations. However, taking advantage of the wearables they already carry seems to be very reasonable. Smartphones, as an inseparable part of human life, has been utilized by researchers as a stand-alone RHMS for the past decade to investigate the amount of information that could be captured. People carry it all the time, they are easy and familiar to work with and they provide many sorts of human interaction interfaces to take advantage of. Not to mention that they are now equipped with a wide variety of sensors. With all these advantages though, still many patients in the categories of frail and elderly (from our experience with them) are against continuously wearing and interacting with it . Smartphones seem heavy to carry for these patients and they are preferred not to be worn in the night. They also seem complicated to work with from the point of view of these populations. Moreover, naturally people tend to carry their Smartphones in different orientations and locations (hand, pocket, bag, etc.). This makes inference very erroneous. Wrist-worn device, on the other hand, seem to put less amount of burdens on these populations. They can be very light and they can be un-seemingly worn for a long time in the same location. This makes them ideal choice for chronic, elderly and frail patients. Moreover, for a lot of (Activities of Daily Living) ADLs which involve hand motions, they provide a better inference capability compared to Smartphones. In addition to all these advantages, when it comes to research potentials, another fact makes wrist-worn sensing very interesting. Wrist-worn sensing has been around for much less time compared to phone-based sensing and this makes the investigation of their challenges and benefits more exciting and at the same time more rewarding in comparison.

1.3 Activity State

Among all applications of wearable sensing, this dissertation focuses on activity recognition which by itself is a window toward a lot of health insight. Information about ADLs is a significant piece of data well suited for determining the general well-being of a patients. The amount of ADL a person is able to fulfill on a daily basis is correlated with the stage and severity of chronic disease he or she is in [15]. The type and extent of exercise regime a person is going through can be an important indicator of his relative risk (RR) of non-insulin-dependent diabetes mellitus (NIDDM) [16]. Cancer patients' chemotherapy prescription is determined by a metric called ECOG in which ADL plays a significant role [17]. A list of important ADLs to look for in chronic patients is provided in many articles, but the time a person is spending sitting, standing, lying and moving and his ability to perform bathing and using the appliances at home are amongst the most important ones [18]. From the ADLs that can be detected using a wrist-worn device, we are interested in sit, stand and lie positions (posture) as well as the gait quality in this dissertation. The reason for this is two-fold. First, the information about the posture and gait provides an incredible insight about patients' capability in following their daily routines to address their basic needs (how up and about they are). For example, the percentage of the time during the day that a patient is bed-bound or sitting still is a significant indicator for clinicians to determine how severe a chronic disease is [19]. Secondly, there are many serious challenges in detecting these ADLs when it comes to wrist-worn sensing systems especially when posture and gait quality is targeted, which makes the problem rather complicated but interesting as a PhD dissertation. We will talk about these challenges in the next Chapter but just to get a sense of the extent of the challenge, you can imagine the range of different noise activities (not to be detected) that can be done using hands while performing these ADLs. This confuses the inference machine and increases false positive rate.

The combination of the aforementioned ADLs (stand, sit, lie and walking) is what

we call "Activity State" in this dissertation. The word "state" is used considering the fact that at each single timestamp, a person is either in standing, sitting, lying or moving states. Moving state includes walking, jogging, running, etc. Having this concept in mind, the content of this dissertation is divided into two main parts in terms of types of activities. In the first part we look into Posture (including sitting, standing and lying) and the second part investigates gait analysis. An important step toward analyzing detection of these ADLs is to look into their significance in different applications of health.

1.4 Why Posture and Gait

We talked about the importance of the amount of ADL a person is capable of performing in previous section. There are various, sometimes contradictory arguments on determining which ADLs are more important. At the end of the day, the application and population selection determines which ADLs to look for. A number of recent articles on detecting ADLs for different health applications will be provided later in this Chapter. An interesting observation from these works is that, detecting main three postures (sit, stand, lie) together with walking is common in most of them. This indicates the significance of these four activities in assessment of general well-being of patients and even healthy subjects.

Quality of gait is another piece of information that gives a great insight about the wellness of risky and vulnerable patients: Applications include geriatrics, Alzheimer patients and patients with neurological disorders [20, 21], etc. A very common tool to assess cardiopulmonary patients is called 6-minute walking test (6MWT- measuring the distance taken in 6 minutes) [22] which is a standard test to detect the functional exercise capacity of elderly patients. Similarly, the average walking velocity in 30-minute walking test (30-mWT) is a reliable tool to assess the functionality of chronic obstructive pulmonary disease (COPD) patients [23]. Gait symmetry is another signif-

icant gait parameter which is increasingly being reported for people with neurological disorders, particularly after stroke. In addition, gait symmetry is a strong indicator of some negative clinical health issues such as risk of musculoskeletal injury, loss of bone mass density and spinal cord disorders. Patterson et al. in [24] has provided a detailed comparison of the current methods for gait symmetry evaluation. Gait velocity is also another key human metric which is a substantial indicator of health status of the people. An extensive study shows that there is a strong correlation between walking speed and 10 year survival rate [25]. They observed that 70 years olds with $1.4m/s$ walking speed aged 6 years more than 70 years olds with $1.0m/s$ walking speed on average. A similar study with the goal of predicting survival rate showed that, from the list of all the metrics they investigated, only "increase in usual gait speed" over a 1-year period was significantly associated with subsequent mortality [26]. In a totally different study in terms of subject scale, it was shown that there is high correlation between GDP of a country and the average walking speed of its people [27].

1.5 Purpose of the Study

With all that we mentioned about preference of wrist-worn sensing over phone-based in activity recognition, there needs to happen a deep investigation of the benefits and challenges come with them to evaluate their applicability for activity recognition. This dissertation is an endeavor to provide this information. In the second chapter, we will go more into details of these benefits and challenges and we will provide a thorough overview of the recent related works. Chapter III introduces a proof of concept wrist-worn sensing system, built in our lab to show the feasibility of posture tracking using wrist data and provide a comparison with the peer phone-based sensing system. Although in the proposed system, wrist-worn sensing is shown to be feasible for posture recognition, the accuracy is very susceptible to unwanted hand motions when it comes to in-field experimenting of the system. This leads to high rate of false-positives and

false-negatives which limits the accuracy. Context information is employed in Chapter IV as a mean to improve this limitation in accuracy as well as the limitation in battery lifetime of the wrist-worn sensing systems. In chapter V, we will investigate the viability of wrist-worn sensing in gait assessment. The issues and challenges of wrist-worn devices in gait quality assessment will be discussed and solutions to mitigate them will be provided. Post-processing of the classified activity states is proposed as a technique to boost the yet-to-be-improved accuracy values of the mentioned four activities in Chapter VI. Chapter VII provides investigation of wrist-worn sensing systems beyond activity state recognition application and eventually the summary of contributions of the work as well as the future directions will be given in Chapter VIII.

CHAPTER 2

Wrist Worn Activity Recognition

2.1 Why Wrist-Worn Sensing

Healthcare systems have been struggling with aging populations and wide expansion of chronic disease worldwide. Therefore researchers have been actively pursuing new solutions to accurately and unobtrusively monitor these populations for the purpose of prediction and intervention. With miniaturization of integrated circuits and advancements in fabrication of sensors and their analog front-end circuits, wearable devices have shown to be decent candidates for non-invasive monitoring of health metrics. A wearable medical device can be described as an autonomous, non-invasive system that performs a specific medical function such as monitoring,educating, intervention and support [28]. Wearable devices have been used for a wide range of health applications. Non-invasive ECG sensors have been employed to continuously monitor patients with cardiac abnormalities [29]. Foot-worn accelerometers have been used to assess gait quality of patients with neurological disorders and to give hint about their progress in post-surgery rehab [30]. Belt-worn devices have given a profound knowledge about the general activity level of patients and consequently their overall well-being [31]. An inclusive survey on wearable sensor-based systems for health monitoring and prognosis is given in [32].

Among all the different devices that can be worn by human, perhaps the one with the most penetration within all different populations is Smartphone. Smartphone has been the dominant wearable device for health tracking over the past decade due to its

prevalence among all the different layers of society. Market penetration of Smartphones in United States has risen from 20 in 2010 to 68.9 percent in 2017 [33]. Moreover, studies have shown that Smartphone users spend about 90% of their time in close proximity of their phones [34]. With Smartphones consistently improving in computing, networking and battery performance, it is no surprise that their applications cover a dominant portion of our lives. In addition, considering how integrated Smartphones are in the life of human being and how essential being unobtrusive and unnoticeable is for a wearable device, Smartphones can easily be considered as the single perfect candidate. A key aspect of Smartphone which made it one of the leaders in the area of health tracking, is the advancement of sensing, both, in variety and precision of sensors. Smartphones are now equipped with abundant variety of sensors including inertial sensors, barometer, heart rate sensor, humidity and temperature sensors and even in some Cases SpO2 and UV sensors. This has enabled their employment for many remote health monitoring applications such as cardiovascular and cancer disease management, elderly care, sleep and stress assessment, etc. Nemati et. al in [35] provides a precise survey on different sensing modalities of Smartphones and their applications in health and environmental tracking.

Although smartphones are becoming more and more predominant, they suffer from a couple of limitations when it comes to clinical tracking. Although they seem to be very much integrated in human daily life, they are not the most convenient wearable to carry all the time. They can be bulky and noticeable, especially when elderly and frail patients are targeted. Also, Smartphones are barely worn by their users in the night time. Moreover, even though Smartphone is the most prevalent wearable, users don't necessarily carry it in the same way and the same location all the time. Smartphones can be in a pocket or purse, on a table or mounted in a car. While phones present ample opportunity to track users, studies have shown that, while close to the user, the Smartphone often is not actually worn by the user [19]. This puts a big question mark on all the works that try to utilize Smartphones for continuous remote activity or health

tracking. Another limitation with Smartphone is that, it is fundamentally not built for continuous sensing of vital signs such as heart rate. The front and back camera of the phones have been used to predict the heart-rate and SpO2 [36], but at best they provide information only when participation from the user is involved.

Wrist-worn devices are relatively young compared to the other wearables and they still occupy a much smaller portion of the consumer electronics market compared to Smartphones. The number of people who own Smartwatch in United States has grown from 3% in 2015 to 12% in 2016, and fitness band owners have grown from 12% to 22% for these years [market]. With advancement in technology, more and more sensors are embedded in wrist-worn devices. Moreover, they are now able to provide fairly high processing power and battery lifetime. In addition to inertial measurement unit (IMU), wrist-worn devices are now equipped with heart rate, PPG, light and pressure sensors and sometimes SpO2 and galvanic skin response sensing modalities. Therefore, wrist-worn devices are capable of continuously monitoring a wide range of vital signs without interfering the daily life of the wearer due to their proximity to the skin (Reeder et al. has provided a good review of these applications [37]).

In addition to providing this opportunistic sensing platform, wrist-worn devices are being worn in a standard location by the user, which perhaps is the most important factor differentiating them from Smartphones in the stand point of activity recognition. They are more comfortable to wear and they are worn by the user most of the time, even in the night-time while sleeping. They don't need to be carried like Smartphones, therefore intense activities and sports can be done while wearing them which is a huge benefit when it comes to sport analytics applications. From all the applications of wrist-worn devices, this dissertation focuses on the activity state recognition with the zooming lens being put on elderly and chronic populations. We will go over some of the wrist-worn sensing systems designed for activity recognition in Section 2.2 of this Chapter and then some of the limitations of wrist sensing are provided in 2.3.

2.2 A Survey on Wrist-Worn Sensing Systems for Activity Recognition

With advancement in technology, Smartwatches and smart bands are now capable of combining sensory information such as accelerometers, gyroscopes, compasses, and heart rate, with global positioning satellite (GPS) data. This is particularly promising in applications that require continuous physical activity monitoring to identify unexpected changes in activity patterns and provide alarm upon the given localized area. Alarms and messages can also be more easily observed than those sent to Smartphones, as phones are not worn all the time while individuals can receive and observe vibrations, text, and sounds all the time on a wrist-worn platform.

2.2.1 Wrist-Worn Devices in mHealth

Emergence of wrist-worn devices started the era of wrist-based health monitoring. However, what triggered the exponential growth in health applications was when they got equipped with vital sign sensors. Applications of wrist sensing nowadays covers a wide range of health monitoring. A big portion of these applications are related to activity sensing (will be covered in details later in this Section). Chronic disease self-management is another big investment in the area of wrist sensing. Intervention in Parkinson patient's daily life has been done by Lopez et al. using auditory signals to help improving patient's gait [38]. Sharma et al. employed a Smartwatch to sense facial tremors, dysfunctional speech, and limb dyskinesia in addition to gait abnormalities [39]. Epilepsy was intervened by detecting tonic-clonic seizures using Smartwatch in a hospital setting while video surveillance and electroencephalogram (EEG) monitoring took place [40, 41]. Kalantarian et al. utilized Smartwatch for weight management by detecting chews and swallows using the built-in microphone of the watch to tackle the obesity [42]. Diabetes management was done using an app on the watch by Arsand et al., but they required participation from the user in terms of manually importing all

sorts of information including insulin, blood glucose, physical activity type and carbohydrates taken [43]. In another similar work, inertial sensors of the watch are used to detect the gestures of eating while camera of the watch detects the type of the food [44]. In Hosseini et al., a smartwatch application provided pediatrics suffering from asthma with risk levels of having an asthma attack through various physiological and environmental sensors including the heart rate sensor, accelerometer, gyroscope, and GPS to assess physical activity and location [41]. In cardiac management, Micallef et al used smartwatch as an exercise reminder for post-stroke therapy [45].

Wrist-worn devices have also been used in home or nursing care setup. Researchers evaluated sleep quality, patient's visits, mobility and activity level to provide beneficial intervention for patients with dementia [46, 41]. In healthcare education, Jeong et al. employed Smartwatch platform to teach and evaluate cardio-pulmonary resuscitations to healthcare professionals. In medication adherence, one study utilized the built-in accelerometer of the watch to detect opening up the pill [47] and another study proposed detection of the rise of the hand's palm as an indication of getting medication to the mouth [48]. Speech therapy has been done using the microphone of the Smartwatch proving that recordings were comparable to traditional recordings for primary speech quality metrics (SQMs) of loudness and fundamental frequency [49]. In another very interesting work, a Smartwatch-based system was used to estimate mental health by detecting the activity, motion, light, and heart rate of the subject as well as the user interactions from a web-based application [50].

2.2.2 Wrist-Worn Devices for Activity Recognition

Inertial sensors have been the core of activity recognition for decades, although they have been used in different platforms and architectures. Wrist-worn devices are introduced to the market mainly with the goal of activity tracking using these sensors. Inertial sensors being mounted on the wrist has enabled detection of a lot of activities and gestures that involves hand motions. And in a lot of these activities the final goal

was not the physical activity itself. For example, hand gestures were used to determine the eating events [44], smoking sessions [51], medication adherence [47, 48], fall detection [52] and many more health-related applications. In this dissertation, we are interested mainly in the physical activities that a person is doing or should be doing on a daily basis. Perhaps the closest term to this concept is ADL. This includes sitting, standing, walking, washing the dishes, vacuuming, cleaning, etc. As we discussed in the previous chapter, detecting the type, intensity and duration of these activities carries significant information about the general well-being of the patients. Recently, there has been numerous research efforts to use wrist-worn devices for detecting ADLs, most of which with the hope of fulfilling the dream of having a completely unobtrusive activity tracking system.

2.2.2.1 Literature on ADL and Posture Recognition

Medical scientists have been trying to find correlations between ADL and different health metrics. These metrics for example can be how much a chronic disease has been advanced in a patient or what is the effect of a drug/therapy on a patient's treatment journey. With wrist-worn devices there comes a lot of challenges in sensing many activities. Hand-motion based activities could perhaps be easily detected while other activities like sitting that does not involve hand motion might be more difficult to detect. Duclos et al in [53] uses a wrist-worn device for distinguishing between sedentary and active behavior and provides an energy expenditure estimation. In a similar work by ahanathapilla et al. activity level and step count is detected from the amplitude of ACC signal and the peak in ACC's FFT signal respectively [54]. In [55] by Jovanov et al., the built-in sensors of the Smartwatch was evaluated by comparing them to two standard monitors, Zephyr bioharness and polysmnographic monitor SOMNOscreen+ during sleep. It was shown in this work that Smartwatch technology provides sufficient information for longitudinal monitoring of these health metrics [55].

There have been some studies comparing the results of activity sensing in Smart-

watch and other body sensors. Trost et al. compared the results of activity recognition of seven ADLs with a wrist-worn and a hip-worn sensor using logistic regression [56]. It turned out that wrist have high potentials for activity detection when it is compared to hip-worn inertial sensors. In a similar study, 9 activities including sitting, standing, walking, running, cycling and stair and elevator assent and descent were compared between a Smartphone and Smartwatch which showed that results are comparable [57]. Similar comparison of Smartphone and Smartwatch is done by weiss et al. which proved that Smartwatch is very efficient in detecting some of the activities which are hand-based while not very efficient for other activities [58]. For example, "drinking" activity was detected with 93% accuracy with Smartwatch while it was 77% with Smartphone.

In all of these comparison studies, no fusion of sensors were done to show how combination of Smartwatch and other sensors will improve the results. This was done by Haescher et al. in which three sensor nodes were incorporated: Head, using a smart glasses, wrist, using a Smartwatch and hip, using a Smartphone [59]. Majority voting was used to fuse the result of the classification of each of the sensors which resulted into descent classification between activities of resting, being active, walking, running, jumping, cycling and office work. Similarly faye et al. showed that adding a Smartwatch to a phone-based system improves the accuracy of ADL classification using multimodal metrics as advanced feature sets for SVM model [60]. ADL classification was also done by solely relying on the wrist data, presenting promising results within the scope of activity recognition for a variety of ADLs including sit, stand, walk, run, cycling, sleeping, etc [61, 62].

2.2.2.2 Literature on Gait Assessment

Most of the previous works on gait assessment have focused on implementing algorithms for either foot, chest or back-mounted sensors. None of these works are really applicable for long-term ambulatory remote health monitoring. This is because a lot

of these sensing systems require bulky and uncomfortable devices being attached to the user and that imposes a lot of inconvenience. This eventually results into non-compliance causing user rejection, data loss and eventually patient drop. This is especially true for patients within the categories of elderly and frail. Smartphone has provided a more convenient platform for gait assessment, as the subjects would normally carry it. Therefore, Smartphone-based gait quality estimation systems have been recently under a lot of attention. With all that, still a lot of elderly and frail subjects are not willing to wear a bulky phone all the time. These patients unfortunately happen to be the category with the most need for monitoring. With the emergence of Smartwatches with inertial sensors embedded in them in the past decade, a great deal of attention and effort has been put in building up wrist-worn gait assessment systems to addresses sensing for these categories of patients. In most of them, a correlation between stride length and some features of the inertial sensors is detected. Vertical displacement was used in [63] and an empirical relation between that and step length was identifies. [64] included the step duration, range of vertical acceleration and number of sample in each step in designing their step length estimator as well to improve the accuracy. Most of the hand-mounted gait assessment systems though, have been focusing on dominant step frequency as the most correlated feature. The correlation between hand frequency and step frequency has been estimated in [65] and then step length and velocity is estimated from there. This required having different models for different positions of the sensor (in-pocket, in-hand and carrying in bag). Accuracy was improved in a similar system in [66] by including GPS calibration while the subject is outdoor. Step length has also been estimated using the abstraction model generated from hand motion frequency and height of subjects in [67]. They showed an error of 5% for short range but this work offers a hand-held system (not hand-mounted).

2.2.3 In-Lab vs. In-Field Activity Recognition

In all of the aforementioned ADL classification works, the results are coming from the testing of in-lab data (not in-field data). In all of these works, a classification among some specific activities is done. Even though the results of the classification for those in-lab measured activities can be high, the story could be dramatically different when the system is introduced to an activity which is not seen by the classifier in the in-lab training session. Even if the observed in-field activity is among the activities of in-lab training, it might not be detected properly due to changes in the condition, user and context. There is no research on the challenges that the wrist-worn sensing system might face when it is used outside the lab environment or when the system is recording some activities which were not initially in the training set. We are going to talk about these issues and challenges of wrist-worn sensing in Section 2.3. As a quick preview, a major issue in wrist sensing is unwanted hand motion that makes the recognition rather difficult if not impossible. This issue intensely imposes itself when it comes to in-field, not-very-clean data. This drastically degrades the accuracy of the activity inference. In a similar vision for most of the aforementioned gait assessment works using hand-held or wrist-worn systems, the biggest challenge comes from the fact that arm swing causes addition of the noise in distance and velocity estimation which causes under-counting or over-counting of steps. This concept seems to be not investigated thoroughly in the previous related works. We will talk about the issue of unwanted hand noise and other issues of wrist-worn sensing in the next section of this chapter. Rest of the chapters are efforts in introducing methods to tackle these issues and to provide accuracy and power performance improvement techniques.

2.3 Challenges and Limitation of Wrist-Worn Sensing in Activity Recognition

Wrist-worn devices have recently been introduced to the market. Therefore, there has not been enough investigation on their capabilities for different applications. Especially when it comes to health applications, there is not enough evidence of comparison of their performance to clinical measures. So the disadvantages of using wrist-worn sensing systems are not quite clear yet. Although during past few years of working on these systems, we came to know some of these disadvantageous and challenges for the purpose of activity recognition.

The main challenge in wrist-worn activity tracking systems is the poor accuracy. Some of the activities and movements to be detected do not involve any hand motion. This makes them impossible to capture, if only inertial sensors on the wrist are to be employed. Even for the activities that contain hand motion, the motion from other body parts cannot be captured. This is in general true for any system with limited location sensors such as in a phone-based sensing system. However, Smartphone is worn closer to the center of mass which makes the inference of many activities easier. The problem with wrist-worn activity sensing is even worse than this. Even when the motion to be detected is purely a hand-based motion, the accuracy can be still low due to the fact that people generally tend to use their hand for a lot of other things. A lot of these unwanted motions could be captured as the targeted activity which causes false positive. Also, when a person is doing an activity, a sudden unwanted hand motion can interfere the inference of that activity. For example while standing, a person might use his hand for something else and this might be inferred as walking which causes false negative.

Another limitation of a wrist-worn device compared to a Smartphone is its small screen size which restricts the feasibility of the system when user intervention is part of the procedure of activity detection. Online learning, active learning and opportunistic learning are some of these methods. Not to mention that having s smaller screen size

limits wrist-based systems in functionality as well. Giving feedback to patients from clinicians, and asking for participation from the user are some of these functionalities.

In addition to accuracy, battery lifetime is another limitation that wrist-worn devices are dealing with due to small fill-factor that is designed for battery placement. However, this is more of an issue in Smartwatches. Smart bands such as Fitbit and Jabone often do not provide screen and complicated entertainment capabilities (which are power hungry) and are essentially designed to record contextual data and transmit them, rather than interaction-based functionalities. Smartwatches are more power-hungry and sustain power only less than a day at best for a normal wearer. This power issue becomes more critical when part of the data processing and learning needs to be done on the watch (when a cloud or communication to cloud is not provided).

Processing and memory capacity of watches is also lower than Smartphones but this is only an issue in applications where a huge load of data has to be stored on the watch or complex data processing algorithms need to be run on them. In the modern RHM models, where cloud is an essential part of the system (as mentioned in Chapter I), wrist-worn device is only and purely a data collection and transmission module with some very preliminary data processing algorithms (such as a low-pass filters or a down-sampler). Therefore, the limitation in processing and memory capabilities of the wrist-worn devices is usually irrelevant [68].

This dissertation realizes these challenges in wrist-worn activity sensing systems and tries to provide different techniques to resolve them. A novel system is proposed in Chapter III, which act as a proof of feasibility of posture tracking for wrist-worn systems. In Chapter IV, contextual information is utilized to improve the accuracy of the recognition and battery performance of the system for posture tracking. Chapter V goes over the main limitations in the recognition of gait parameter which takes place due to unwanted hand motion and chapter VI provides a two-level classification architecture using "Random Forest" and "Majority Voting" to improve the precision of "Activity State" recognition when it comes to in-field data collection.

CHAPTER 3

Posture Recognition using Wrist-Worn Devices

3.1 Introduction

As previously mentioned in Chapter II, Smartwatches have many constraints that may limit their effectiveness, including screen size, weaker hardware for sensing and computing and limited battery and storage capacity. This work investigates whether the Smartwatch can effectively track user activity and posture without the aid of a Smartphone, to then potentially serve as the base platform for a remote health monitoring system for elderly oncology patients.

Elderly patients with cancer are a group that stand to benefit tremendously from remote sensing: they are prone to unwitnessed decline and hospitalization between clinic visits, resulting in high morbidity, mortality and cost. According to the most recent American Cancer Society statistics, 60% of cancers and 70% of cancer deaths occur in adults aged 65 and over. Physicians must make ”snap” decisions regarding treatment intensity and follow-up, but the tools physicians currently use to classify elderly patients as ”frail” or ”robust” are faulty at best; more than 20% of elderly patients' cancer doctors classified as fit for therapy are classified as ”frail” by geriatric specialists [25]. A full assessment for frailty in an elderly subject can require 45 min or more, which is an impractical time requirement for busy cancer clinics. However, to fully track the posture of these patients, the sensing technology must first be developed and validated for the necessary tracking, on any individuals, before any systems can be developed for actual clinical trials.

This work will investigate the ability of Smartwatches to provide the necessary tools to assist in wrist-worn posture tracking in a laboratory setting, as a proof-of-concept study for the use of such a system for clinical assessment. The system will need to track and record the necessary activities and activity levels of users from the wrist rather than the traditional hip locations. In particular, being up and about, sitting or lying in bed is very important for identifying posture and activity in each posture state. However, where Smartphones have an advantage of tracking such posture from the hip, a Smartwatch should see significant activity in all three phases of posture as a user might move her/his arm while sitting. This Chapter develops such a Smartwatch system, to test whether Smartwatches can replace Smartphones for posture tracking, rather than simply augment them. This system will need to record activity all day (a goal of about 18 h of battery life) and accurately report patient activity levels. Prior analysis in [26] showed energy consumption in continuous sensing and trade-offs with model accuracy. Indeed, by reducing the sampling rate, storing results on the watch and transferring via USB cable rather than via a wireless network and computing results on a host computer, improved battery life should be achievable. The work in [69] then presents the challenge of using Smartwatches, after turning off wireless communication and other processes, as the challenge of reducing the sampling rate while maintaining accuracy.

We will analyze the classification accuracy of such a system and provide evidence that a Smartwatch, alone, can properly identify the necessary movements to identify human posture without needing a Smartphone or other such hip-worn sensor and at a low enough sampling rate to last without needing constant battery recharges or data uploads that might hamper the use of this platform.

3.2 Smartwatch-Based Activity Tracking Systems

Activity monitoring with Smartphones and devices with these phones have been well studied. Monitoring activities of daily living through wearable sensors or Smartphones seem to be fairly accurate [9, 70]. In particular, the work in [71] looks at activity tracking for a clinical environment and how to guarantee that users are performing the desired activity. This work intends to follow the same model of activity recognition presented there. In particular, by identifying the transitions between sitting, standing and lying and appropriately identifying (and ignoring) all other wrist movements, this work approaches the classification of user posture similarly to the anti-cheating developed in [72]. By showing the same levels of accuracy, this Chapter will show that Smartwatches are capable of replacing Smartphones.

This Chapter extends the methods presented in [29, 73], by first finding the appropriate features for proper posture tracking of users with a Smartwatch and, second, by doing so with reduced sensing rates to extend the battery life, if possible. The work in [74] presents methods by which continuous measurement on Smartwatches can be performed in an energy-efficient manner. While this work does not intend to do an intensive energy-expenditure calculation such as the one done in [74], the selection of data and the context of the current state of the user could be used in a similar fashion. For this reason, it is believed that the method presented, along with the reduced sampling rate, would result in the improved battery life of the device. Further analysis of energy expenditure, such as in [74], is left for the limitations and future work discussion in Section 5.2.

3.2.1 Methodology

The system developed here was a pervasive sensing system that could be worn by the user at all times, tracking the activity while also prompting questions as needed, seen in Figure 3.1. The goal of the system was to accurately track activity levels, as well as

Figure 3.1: User wearing the Smartwatch on the left hand.

to provide an interface for important questions necessary for future assessment status, though the interface. This system needed to be able to record and track data for large periods of time in order to provide a more informed classification of a user's entire day. Further, by identifying the three key posture states of sitting, standing and lying, a classification algorithm is presented that can appropriately identify transition movements of these postures versus other activity movements.

3.2.2 Hardware Platform and Data Collection

The Samsung Galaxy Gear Smartwatch was used for experimentation, as it employed a ± 2 g triaxle accelerometer and a 300° per second gyroscope sensors, while further providing a software environment for interactive applications and 4 GB of internal storage. Given that the movements recorded are for posture tracking only and the transitions between states tend not to be violent actions, the 2-g accelerometer was not considered a limitation. Data were stored on the Smartwatch in internal memory, which provided ample storage for the duration of the collection desired. All extraneous applications and

wireless communication are turned off, and the screen timeout was set to the shortest time possible. Further, the data are uploaded to the host computer via a wired USB cable at the end of each day, and this computer communicates and computes, as necessary. When looking at the watch on the left wrist, the y-axis points to the hand, the x-axis directly up, while the z-axis comes out orthogonal to the watch face. In order to appropriately compare against smartphones, a Samsung Galaxy S4 was used, worn in the pants pocket of the user on the same side that the watch was worn (left) during data collection to simulate hip-worn sensors. The Galaxy S4 smartphone came with a $\pm$2-g triaxial accelerometer and $\pm 300^{\circ}$ per second gyroscope sensors, as well, and 2 GB of internal storage data were collected from a group of 20 volunteers within the age bracket of 19 to 30 years in a supervised study, in order to validate the ability of such a watch to accurately identify such movements. The age group was selected as part of an Institutional Review Board (IRB) approved pilot trial (UCLA IRB #14-000176) to demonstrate the feasibility of such a sensor system. Each of the participants performed multiple activities while wearing a Smartwatch placed on the participant's left wrist and Smartphone in their left pocket (though data can easily be transformed to use the right hand, if needed). Data were sampled at a rate of 100 Hz. The data collection application was developed to annotate the data while collecting it, as seen in Figure 3.2. In order to assist the users and to prevent unrealistic motions of moving the watch to press the buttons, one of the authors supervised the data collection trial and pushed the appropriate buttons for annotation while the users were conducting the collection trial. This was done in an effort to minimize error in the annotation times, as well as to prevent excess movement by the users to begin and end annotations of movements. The annotations were then applied to the Smartphone data, as well.

Each subject was then asked to perform a set routine of activities meant to train an algorithm to classify sitting, standing and lying. For each activity, users were asked to repeat each action 10 times. Table 3.1 shows the list of movements captured. The data were captured in three phases. The first labeled transitions, tracked transitions between

Figure 3.2: Screenshot of the data-recording application running on the Smartwatch.

sitting in a chair, standing up and lying on a bed (of varying heights depending on the location of the data collection) with little to no extraneous movement. These were the clean movements that the system needed to identify. However, potential trouble in identifying the transitions from a wrist-mounted sensor include the similarity between certain transition movements and certain activities of daily living that can look similar to these transitions. As a result, the second phase of data collection, shown in Table 3.1 as activities of daily living, was run. Finally, the third phase was run to identify steps for a pedometer-like application. After the data collection was run, the system recorded the user removing the device and plugging it in to the charging environment to properly mark the start and end of a day of recording. Since the movements were annotated, a start and end point for each transition was determined and the mean window size across all users and all moves selected (5 s or 500 points at 100 Hz). Data were saved in the internal storage of both the Smartwatch and Smartphone. At the end of each day of the trial, data were uploaded manually to a desktop computer for the recognition algorithm, via a USB cable.

3.2.3 Feature Extraction and Selection

The data collected and annotated were then processed for feature extraction. The first step was to low-pass filter the data for noise. For filtering purposes and to potentially coincide with a future real-time recognition system, a moving average window was

Table 3.1: Movements Captured

Phase	**Movement State**	**Activity Description**
Transitions	Sit - Stand	Minimal Movement Transition
	Stand - Sit	
	Sit - Lie	
	Lie - Sit	
	Stand - Lie	
	Lie - Stand	
Activities of Daily Living	Standing	Using Phone (10 sec) Brushing Teeth (10 sec) Lifting Cup (10 times) Swinging Arms(10 times) Walk (10 sec) Open Door (10 times) Look at Watch (10 times) Clean with broom (10 sec)
	Sitting	Typing (10 sec) Reading Book (10 sec) Brushing Teeth (10 sec) Look at Watch (10 times) Bicep Curl (10 times) Use TV Remote (10 sec)
	Lying	Adjust Pillow (10 sec) Text with phone (10 sec) Adjust in Bed (10 sec) Reading Book (10 sec) Adjust blanket (10 sec)
Walk	Step Forward Step Backward	10 times 10 times

used. Since the average movement length was 5 s, a movement window of 1 s (100 points) was used, found heuristically to be the best filter. Next, the feature extraction was run. While there are several features that are common in smartphone platforms, including max, min, mean, sum, standard deviation, kurtosis, skewness and energy over a window, because this work incorporated a gyroscope and a different position on the body, a wider range of features were developed from which to be selected. The 25 features, listed in Table 3.2, were collected for each axis, as well as for the magnitude of acceleration, resulting in 175 total features. These features were selected due to their strengths in various recognition techniques, including activity monitoring, handwriting recognition and wrist-worn tracking [16, 17, 34–36] [8, 9, 75, 76, 77].

Once the features were extracted, a selection algorithm was run using Weka's [78] Information Gain Feature Selection algorithm, with a ranker to provide the top 30 features. The top 30 features were selected to avoid overfitting the model to the training set. In fact, [79] stated that linear support vector machines (SVM) should only have a ratio of 10:1 for features to data samples. In the case of this work, 20 users repeated each of seven actions (six transitions and a no-movement class). Each repetition of these movements would pollute the 10:1 ratio, so they were not considered in the calculation. As a result, 140 unique data samples were considered, which indicated that 14 features should be the maximum in a linear setting. As this work employed a more advanced kernel, double those features were considered to adhere to the same principal, while accounting for a more advanced kernel and multiclass setting. Once the subset of features was selected, the model was tested in cross-validation for its prediction strength. In particular, it was important to achieve high precision and recall to appropriately identify the transitions between states when performing activities and to avoid identifying false transitions.

Table 3.2: Features Extracted per Axis

Feature	**Description (domain)**
Minimum	Minimum value obtained over the movement window (time)
Maximum	Maximum value obtained over the movement window (time)
Sum	Sum of values obtained over the movement window (time)
Mean	Mean value obtained over the movement window (time)
Standard Deviation	Standard Deviation of values obtained over the movement window (time)
Kurtosis	Peakedness of the distribution (time)
Skewness	Asymmetry of the distribution (time)
Energy	Calculation of the energy (sum of the absolute value of the fft components) (frequency)
Variance	Variance of values obtained over the movement window (time)
Median	Median value obtained over the movement window (time)
Root Mean Square (RMS)	Root mean square of values over the movement window (time)
Average Difference	Average difference of values (pairwise) in window (time)
Interquartile Range	Dispersion of data and elimination of outlier points (time)
Zero Crossing Rate	Rate of sign changes in signal (time)
Mean Crossing Rate	Rate of crossing the mean value of signal (time)
Eigenvalues of Dominant Directions	Corresponds to dominant direction of movement (time)
CAGH	Correlation coefficient of acceleration between gravity and heading directions (time)
Average Mean Intensity	Mean Intensity of Signal (time)
Average Rotation Angles	Calculates rotation based upon gravity (time)
Dominant Frequency	Dominant frequency in transform (frequency)
Peak Difference	Peak difference of frequencies (frequency)
Peak RMS	Root Mean Square of peak frequencies (frequency)
Root Sum of Squares	root sum squares of frequencies (frequency)
First Peak (Energy)	First peak found in energy (frequency)
Second Peak (Energy)	Second peak found in energy (frequency)

3.2.4 Training the Algorithm

In order to classify the motions accurately, Weka's implementation of a support vector machine (SVM) was used, using the Pearson Universal Kernel (PUK), which is based on the Pearson VII function adapted to a universal kernel. As explained in [80], this kernel function has a remarkable ability to model data well represented by each other commonly found SVM kernel and, as a result, can be considered a universal kernel for learning algorithms. In particular, with enough data, the PUK kernel can be modified, through its optimization of hyperparameters, to look like any other kernel for SVM. The work in [81] applied this kernel to activity recognition, showing higher accuracy than more commonly-used kernels and methods. The parameters were left as default, with the exception of the complexity, which is raised to a value of 100, to further penalize mistakes of the classifier in its optimization routine. The SVM was supplied with training data labeled with eight labels, the labels being the six transition movements, one label for no movement and one encompassing label for all other movements to reduce false positives of the first six labels. The model was tested at 100 Hz, 50 Hz and 10 Hz and compared to the phone in the pocket, as well as combined with the phone to determine the strongest results.

3.2.5 Testing the Algorithm

The recognition algorithm was then validated to ensure the proper development of a system to accurately track the posture of users. While the activity level was presented as a general magnitude of acceleration, the state of the user provided context to the level of activity achieved and the duration of those activities. As a result, the algorithm needed to be strongest at determining the posture of a user. A leave-one-subject-out cross-validation (LOSOCV) was used to determine the model's effectiveness over user populations. This was chosen over a commonly-used 10-fold cross-validation because of the potential for the pollution of the results in training and testing on the same user.

In this manner, it became possible to interpret results as they extend to new users not in the training system. Each move of the test subject was feature extracted and tested. For each movement, a label is known for the ground truth transition state. If the algorithm appropriately classifies the movement with the appropriate class, then this is considered a true positive result. If not, it is considered a false negative result. For example, if the user is standing and sits in a chair, this should be a stand-to-sit transition. If this movement is appropriately classified as a stand-to-sit, it is considered a match and a true positive. If, however, the system calculates this movement as stand-to-lie, then this movement counts as a false negative for stand-to-sit and a false positive for stand-to-lie. From these true positive, true negative, false positive and false negative results, precision and recall are derived, per class. We then average these results for the precision and recall of the system. This micro-averaging result does not bias toward a specific movement, since the quantities of each label are equal. Further explanation of this can be found in [82]. The results for this study were presented by reporting the F-score of each test subject and then averaging those F-scores. The F-score, sometimes referred to as the micro f1 score, is:

$$F = 2 \times \frac{P \times R}{P + R} \tag{3.1}$$

where P is the precision of the system and R is the recall (also known as the sensitivity). Thus, the F-score is an indication of how well the system can identify the transition movements. The F-score is used as a measurement to better indicate the ability of an algorithm to detect all movements and to reduce false positives at the same time, often a more reliable measurement of performance than accuracy.

3.3 Results

A leave-one-subject-out cross-validation was run on all subjects in the training set. The first step was the feature extraction, then the validation that the Smartwatch can ac-

curately classify the movements necessary at only 10 Hz. Then, these results were compared to 50 Hz and 100 Hz in order to compare the differences, along with comparing the phone in the pocket, and using both datasets together. Further, battery usage was compared, as well. In order to compare the battery life of each system, the data collection platform was run until the watch died, with timestamps of the outputted data providing durations. The 10-Hz Smartwatch collected, on average, about 19 h of data, while the 50-Hz version lasted only 9 h and the 100-Hz version only about four hours. The large discrepancy is due likely not only to the sensor usage, but power associated with the storage of larger files of more data points. Data were logged and stored on the Smartwatch and were under the 4 GB of internal storage per day. For the purposes of this work, this validates the use of only 10-Hz data and that it can provide the necessary duration and store the necessary data for offline communication and computation. Further energy analysis in actual use is left for future work. The PUK kernel was also compared against a radial basis function (RBF) kernel, which was more commonly found in activity recognition systems, to validate the selection of the chosen kernel, as well as a commonly-used method with that kernel used for recognition of activities of daily living (ADL) [8, 9].

Figure 3.3 shows a summary view of the data collected by the system over six days for one of the user's from the collected IRB trial. Figure 3.3a show the daily breakdown, while Figure 3.3b shows the total for a week. The accuracy of this view is dependent on the accuracy of each individual movement recognized, discussed below.

3.3.1 Feature Selection Results

The top features for the method run at 10 Hz are presented in Table 3.3. The reason only 10 Hz is shown is because of its success at saving battery life and accurately determining the user state, though, for the watch, the 50-Hz and 100-Hz methods result in similar feature sets. Incidentally, the comparison to the Smartwatch and smartphone data used shows that the combination uses primarily watch features (only four phone

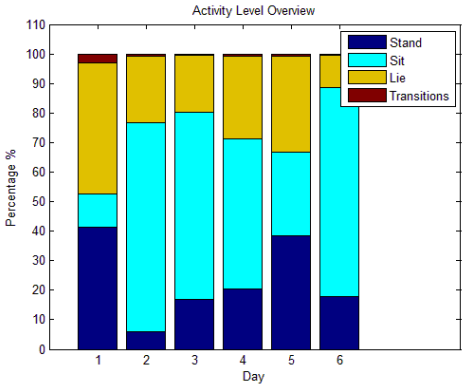

(a) Daily state information of a user from the trial

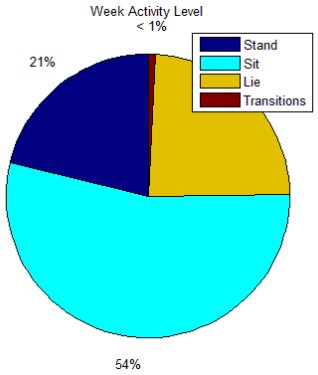

(b) summary of the week

Figure 3.3: Clinician summary view of weekly activity of a user from the trial

features at 10 Hz).

3.3.2 Cross-Validation Results

The cross-validation was run in three cases, using data from the watch only, using data from the phone only and using the data from both the watch and phone together, and at the three sampling rates, as discussed: 10, 50 and 100 Hz. Results are plotted in Figure 3.5. For the 10-Hz case, the algorithm using only data from the watch achieves a mean F-score of 0.93, using data only from the phone a mean F-score of 0.82 and using data from the watch and phone a mean F-score of 0.94. For the 50-Hz case, the algorithm using only data from the watch achieves a mean F-score of 0.93, using data only from the phone a mean F-score of 0.80 and using data from the watch and phone a mean F-score of 0.94. For the 100-Hz case, the algorithm using only data from the watch achieves a mean F-score of 0.93, using data only from the phone a mean F-score of 0.80 and using data from the watch and phone a mean F-score of 0.94. Finally, when selecting a subset of features by rank, Figure 3.4 showed a high mean F-score with only the top 15 features.

Table 3.3: Top 30 Features Selected for Smartwach at 10Hz (and axis)

Features 1-10	**11-20**	**21-30**
Average Difference (a_x)	Mean (g_y)	Mean (a_x)
Average Difference (a_z)	Sum (g_y)	Sum (a_x)
Median of Intensity of Gyroscope ($\|\|g\|\|$)	Eigenvalues (a_x)	Dominant Frequency (g_x)
Mean (g_z)	Root Mean Square (a_x)	Energy (g_x)
Sum (g_z)	Energy (a_x)	Root Mean Square(g_x)
Dominant Frequency (g_z)	Root Sum of Squares (a_x)	Root Sum of Squares (g_x)
Energy (g_z)	Standard Deviation (g_z)	Peak Difference (g_y)
Root Sum of Squares (g_z)	Variance (g_z)	Peak Difference (g_x)
Root Mean Square (g_z)	Variance (g_x)	Dominant Frequency (g_y)
Peak Difference (g_z)	Standard Deviation (g_x)	First Peak (g_z)

3.3.3 Method Comparison

The algorithm, using data sampled at 10 Hz, was compared against the same method using an RBF kernel instead, as well as the ADL algorithm using an RBF kernel. The ADL algorithm used the three-axis accelerometer attached to the hip and extracted features over a 5-s window of the mean, standard deviation, energy and correlation of each axis of the accelerometer [9]. This same algorithm was also extended to use the gyroscope. The phone version was labeled pADL and was also run on the watch data, labeled wADL. Results for all of the methods are in Table 3.4.

3.4 Discussion and Conclusion

The results of the experiments show promise in using the Smartwatch as the platform of choice for future remote health monitoring applications. The first important finding is that the watch, on its own, can accurately detect posture and transitions between postures. The watch alone provides strong results, with an F-score of 0.930 at only 10 Hz compared to 0.932 at 100 Hz. This indicates that the system can, in fact, provide strong

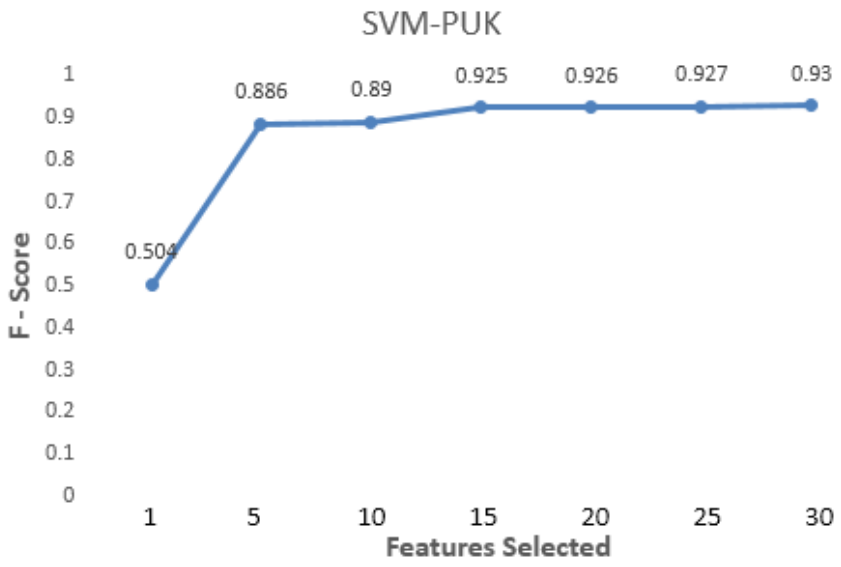

Figure 3.4: F-score Per Features used for Smartwatch at 10Hz with SVM with a PUK Kernel

classifications of the transition movements and, as a result, determine the state of the user at all times, while also using minimal internal storage and minimal battery life. Further, the watch, in fact, outperforms the phone in this particular method. The reasoning for this seems to be because the phone does a poor job at identifying the general activities, since the hip is relatively still during those, and versus no movement at all. In regards to the 10-Hz watch method, the sensor is particularly suited for this application. Referring once again to Table 3.3, notice the strength of the gyroscope features, indicating its importance in such systems. Further, the response to the algorithm and the features is shown in Figure 3.4. The maximum comes at 30 features, but if the strict 14 features of the linear SVM are desired, the system still produces an F-score of 0.925. Finally, such platforms must come with independent machine learning algorithms tailored to their usage. When examining the results in Table 3.4, it becomes clear that generally, strong methods of recognition for activities of daily living do not perform as well when tailored to specific applications. Note, in fact, that the ADL algorithm was extended to the watch and with the gyroscope and provides an F-score of 0.91, which is

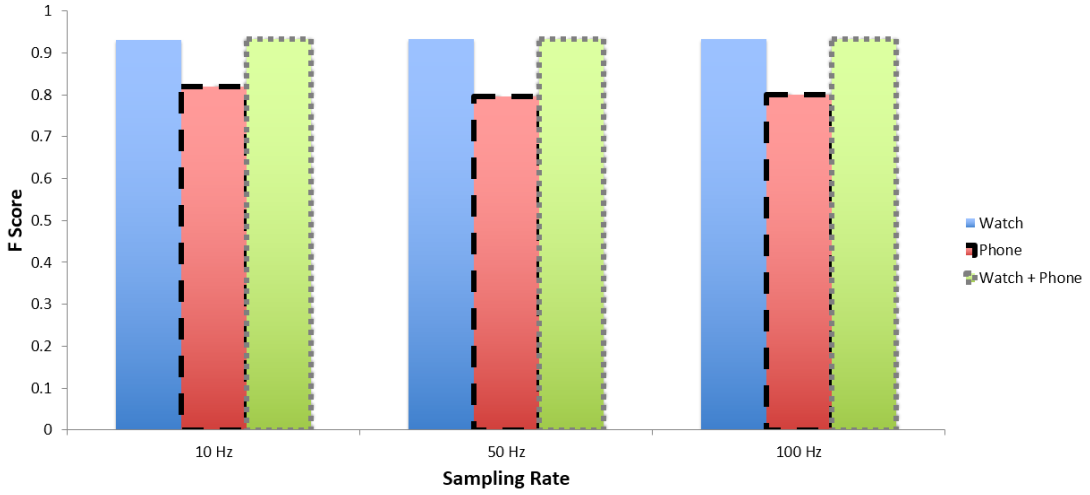

Figure 3.5: F-Scores at three sampling rates for watch, phone, and watch + phone

quite good, but can be improved when picking specific features trained for the specific dataset and movements required.

In summary, this work introduced a Smartwatch-based system to assist in tracking the posture of users wearing a wrist-worn platform instead of a hip-worn platform. In this Chapter, we investigated the feasibility of developing such a system to be worn all day (removed only for charging at night). A platform was developed based on the Samsung Galaxy Gear, which allows activity tracking and the execution of custom Android applications. This system allowed for the collection of a week of activity to track the posture of the user. In fact, the recognition results of an F-score of 0.930 for the watch running at only 10 Hz is a promising result for a watch-only system to monitor human posture. Further, the features selected were presented to guide the future development of Smartwatch applications, an emerging field with the advent of ever-increasingly powerful wrist-wearable devices. The work presented shows the capabilities of such a device in tracking human posture, enabling future development and trials in more complex environments and with varied user populations.

Table 3.4: F-Scores of SVM with PUK, SVM with RBF, Activity of Daily Living (ADL) Algorithm, with and without gyroscope (all at 10 Hz) (phone then watch)

Algorithm	**F-Score**
SVM (PUK)	.930
SVM (RBF)	.812
pADL (Accel Only)	.702
pADL (Accel + Gyro)	.783
wADL (Accel Only)	.814
wADL (Accel + Gyro)	.908

CHAPTER 4

Wrist-Worn Context-Aware Posture Tracking

4.1 Why Context Information

Although RHMS have shown promises in reducing healthcare costs and improving quality of care, effective analysis of the data collected by these systems and the potential benefits of utilizing such analysis is by large an open problem. One of the key demands in such an assistive environment is to promptly and accurately determine the state and activities of an inhabitant subject. There have been a number of studies on utilizing machine learning algorithms to monitor the activities of daily living such as [83] and [84] but most of these works have been ignorant or insufficient in analyzing and addressing the challenges that are mentioned in Chapter II, both in accuracy and power performance. In this Chapter, we propose a novel context-aware data analytics framework to classify the physical activity based on the signals received from a wearable sensor (e.g. SmartWatch) and the contextual information including the ”location” of the subject and its ”current state” using advanced machine learning algorithms. The location of a patient can provide important prior information that can be used to better classify the physical activity. We hypothesize that the location information of the human subject can get involved in classifier decision making as a prior probability distribution to improve the accuracy of activity recognition. In other word, we take into account the location of the subject as contextual information to improve the accuracy of the activity classification. A similar effort is also done employing the ”current state” contextual information. The results demonstrate improvements in accuracy and performance of the classifier when applying the proposed method compared to typical

classifications. In addition to improving the accuracy, a dynamic switching algorithm is proposed to switch in between data sources to increase the battery lifetime of the wrist-worn device.

4.2 Context-Aware Framework

The context-aware framework is feeding from two main sources. These sources are signals received from embedded accelerometer and gyroscope of a SmartWatch and the contextual information received from other external devices or systems. This contextual information can be anything such as location, time, temperature, etc. Although this chapter provides a general solution which works for any type of context, the context examples that are used as proofs of concept are location and current state. In this manner, we propose a context-aware technique by taking into account the location or current state as prior contextual information that can modify the classifier model, and consequently provide more accurate results for activity recognition. The activity recognition module includes feature extraction, feature selection, and context-aware classification submodules as described in the following. The activities to be recognized and the wrist-worn data collection module is exactly the same as in Chapter III. The data collection protocol is also the same as in Chapter III. Aside from the classification algorithm, the only differences in this chapter are first the presence of another data source (to provide contextual information) and second the selected feature set.

4.2.1 Feature Extraction and Feature Selection

A total number of 150 features are extracted from accelerometer and gyroscope signals. Statistical and morphological features are the most common features used for data analytics. Theses features are extracted for each one of the three axes of the accelerometer and gyroscope. A complete list of implemented features can be found in Table 3.2.

Once the features are extracted, a dimensionality reduction algorithm is applied to

select the most prominent features and reduce the redundancy. The conventional feature selection algorithms usually focus on specific metrics to quantify the relevance and redundancy of each feature with the goal of finding the smallest subset of features that provides the maximum amount of useful information for prediction. Thus, the main goal of feature selection algorithms is to eliminate redundant or irrelevant features in a given feature set. Applying an effective feature selection algorithm not only decreases the computational complexity of the system by reducing the dimensionality and eliminating the redundancy, but also increases the performance of the classifier by removing irrelevant features. In this Chapter, we tried both wrapper and filter methods; the two well-known feature selection categories. Wrapper methods usually utilize a classifier to evaluate feature subsets in an iterative manner according to their predictive power. A new feature subset is used to train a predictive model that will later be evaluated on a testing dataset to assess the relative usefulness of subsets of features [85]. Figure 4.1 (a) provides an illustration of the wrapper feature selection method. Filter methods use a specific metric to score each individual feature (or a subset of features together). The most popular metrics used in filter methods include correlation coefficient, mutual information, Fisher score, chi-square parameters, entropy and consistency. Filter methods are very popular (especially for large datasets) since they are usually very fast and much less computationally intensive than wrapper methods. Figure 4.1 (b) illustrates the steps involved in the filter feature selection method.

In this study, after trying several filter and wrapper methods, we finally chose only 5 features to keep the computational complexity low on the device. The selected features includes: minimum of acceleration axis x (min ax), average acceleration axis z (avg az), eigenvalue acceleration axis z (eigen az), correlation between acceleration axis x and y (cor axy), sum gyro axis z (sum gz).

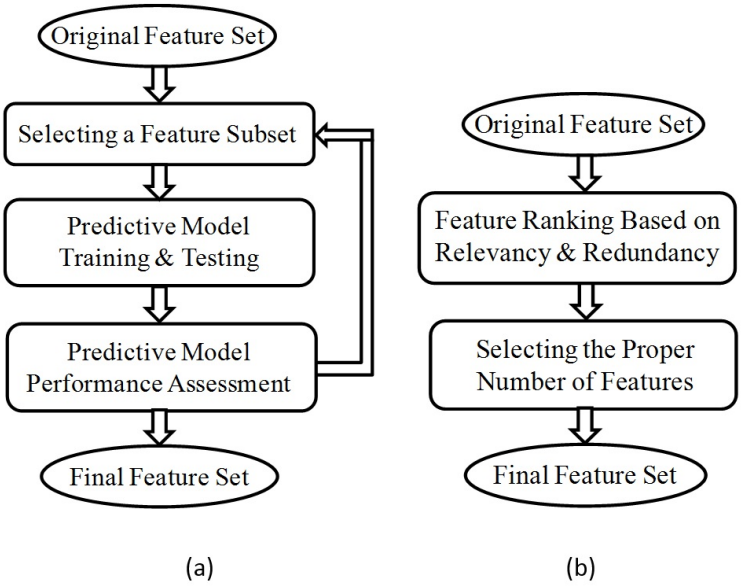

Figure 4.1: Feature Selection: (a) Wrapper method, (b) Filter method.

4.2.2 Conventional Classification

Once the subset of features is selected, a machine learning based classifier is applied to classify the motions. In this research, we tried various classification algorithms such as SVM, Random Forest, BayesNet, and Artificial Neural Net (ANN) as the predictor. According to our results, a Random Forest classifier with 100 trees provided fast and accurate prediction results for our dataset. Random Forest is an ensemble learning classification method comprising of a collection of decision tree predictors operating based on i.i.d random vectors. In this process, each tree casts a unit vote for the most popular class [86]. The classifier was supplied with training data labeled with 6 labels being the six transition movements (sit_to_lie, sit_to_stand, stand_to_sit, stand_to_lie, lie_to_sit, lie_to_stand). The recognition algorithm must then be validated to ensure the proper development of a system to accurately track the state of subjects.

4.2.3 Context-Awareness

As we mentioned before, context information can be anything, but for simplicity, without sacrificing on the generality of the problem, let's consider the indoor location as the context. The indoor location of a patient (received from indoor localization and tracking module) can provide significant prior information about the possible physical activity. For example, when we know that the patient is in the kitchen, the probability of standing is much higher than lying, consequently, the labels are not uniformly distributed anymore. Thus, by knowing the approximate position of the patient, we will have better understanding about the possible activities that the patient can have. We hypothesize that the location information can get involved in classifier decision making as a prior probability distribution to help improve the accuracy of activity recognition module. Assume that $F_1, ..., F_N$ are the classifier input features and C represents the classifier labels. Then, the classifier probability model can be expressed as a conditional probability $p(C|F_1, ..., F_N)$ (known as Posterior Probability) that can be formulated using the Bayes' Theorem as following [87].

$$p(C|F_1, ..., F_N) = \frac{p(C, F_1, ..., F_N)}{p(F_1, ..., F_N)} \tag{4.1}$$

The joint probability in the numerator can be reformulated as:

$$\begin{aligned} p(C, F_1, ..., F_N) &= p(C)p(F_1, ..., F_N|C) \\ &= p(C)p(F_1|C)p(F_2, ..., F_N|C, F_1) \\ &= p(C)p(F_1|C)p(F_2|C, F_1)...p(F_N|C, F_1, ..., F_N) \end{aligned} \tag{4.2}$$

A "Maximum A Posteriori" (MAP) decision making rule can be applied as following to pick the most probable class label:

$$classify(f_1, ..., f_N) = arg\max_c p(C = c)p(f_1, ..., f_N|C = c) \tag{4.3}$$

The term $p(F_1,...,F_N|C)$ (called likelihood) is usually determined in the training stage. For the case of simplicity (e.g. in Naive Bayes classifier), the features can be assumed to be conditionally independent. In this case, the equation 4.3 can be simplified to:

$$classify(f_1,...,f_N) = arg\max_c p(C=c)\prod_{i=1}^{N} p(F_i=f_i|C=c) \tag{4.4}$$

In traditional classification, a uniform distribution is used for Prior Probability $p(C)$. However, in our approach, we hypothesize that the patient's position can provide some information about the distribution of the prior probability $p(C)$. Thus, we can write $p(C)$ as:

$$p(C=c) = \sum_i p(C=c,L=1_i) = \sum_i p(L=l_i)p(C=c|L=l_i) \tag{4.5}$$

where $p(C,L)$ is the joint probability distribution of location and activity label. Thus, when the location is known, the uniformly distributed Prior Probability $p(C)$ will be replaced by the conditional probability $p(C|L=l_i)$ and consequently, the equation 4.4 provides more accurate model for activity recognition.

An equation similar to 4.5 can be written for any other contextual information, such as current state:

$$p(C=c) = \sum_{j=1}^{M} p(C=c,S=s_j) = \sum_{j=1}^{M} p(S=s_j)p(C=c|S=s_j) \tag{4.6}$$

where M is the number of states.

4.3 Activity Recognition Accuracy Improvement

The improvement in the accuracy is due employment of contextual data in the prior probability of the classification algorithm. This novel technique is tested using both lo-

cation and current state information. The collected inertial sensor data and the protocol is exactly the same as the ones mentioned in Chapter III (data of the transition between sit, lie and stand states).

4.3.1 Location as the context

Table 4.1 shows the F-Score results for the activity recognition using only 5 features in two different cases:

- Using conventional classification without considering the location information
- Context-aware activity recognition knowing and taking into account the location information

As we see, for example in the kitchen, we achieve 7% improvement (using 5 features) since knowing the location of the subject provides significant information about the activity. However, in the living room, we achieve 3% improvement, and it totally makes sense, because the likelihoods of sitting, lying, and standing in the living room are almost similar, and consequently the prior probability distribution is closer to the uniform distribution which is the pre-assumption for conventional activity recognition too.

Figure 4.2 and 4.3 shows the F-Score versus the number of selected features for conventional and context-aware analytics in the kitchen and living room. Again, as we expected, the accuracy improvement by using context-aware approach is higher in the kitchen compared to the living room because the probability distribution of various activities in the living room is closer to uniform distribution.

4.3.2 Current State as the Context

To investigate the possibility of activity classification accuracy improvement using current state, we analyzed the precision of classification for both smartphone and smart-

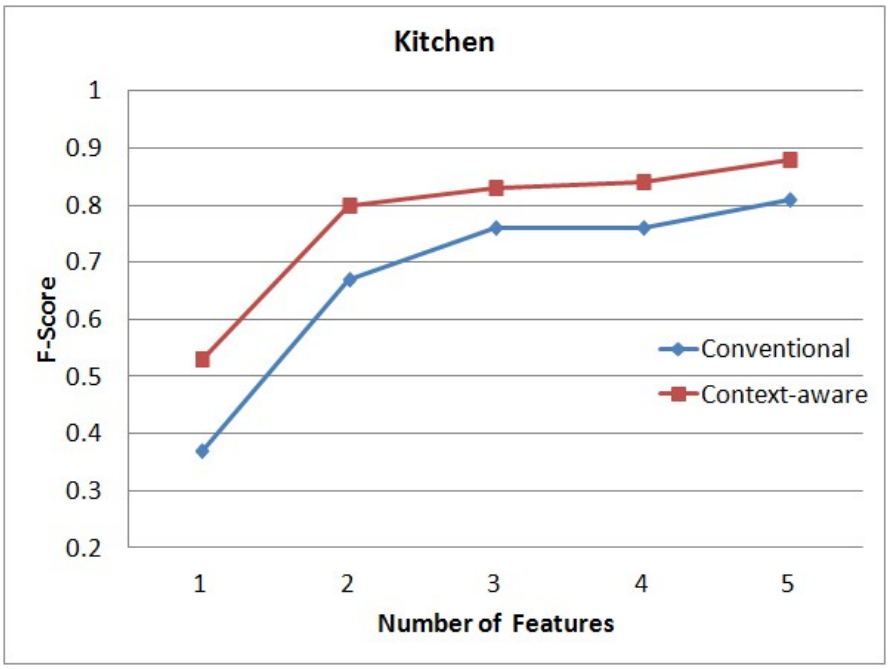

Figure 4.2: F-Score versus the number of selected features for conventional and context-aware activity recognition in kitchen.

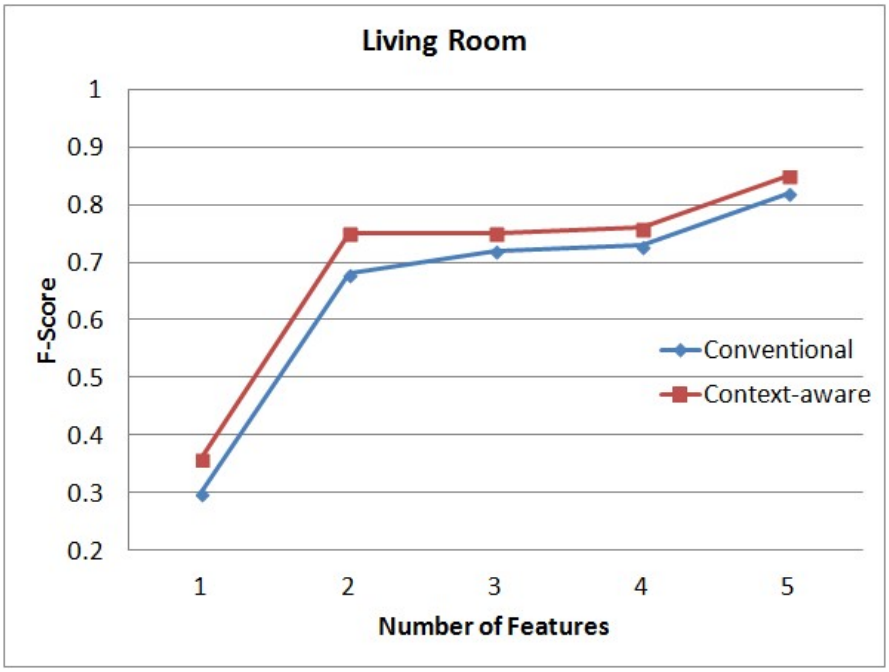

Figure 4.3: F-Score versus the number of selected features for conventional and context-aware activity recognition in the living room..

Table 4.1: F-Score For Regular And Context-Aware Analytics Using Only 5 Features

Location	**Conventional Classification**	**Context-Aware Classification**
Kitchen	0.81	0.88
Living Room	0.82	0.85
Bedroom	0.80	0.84

Table 4.2: Detailed Classification Precision Results

Current State	**Next State**	**Phone Precision**	**Watch Precision**	**Phone Average Precision**	**Watch Average Precision**
Stand	*Sit*	88.1	84.3	**83**	**78**
	Lie	77.9	71.7		
Sit	*Stand*	61	51.3	**69.7**	**46.1**
	Lie	78.4	40.9		
Lie	*Sit*	41.4	82.2	**58.75**	**80.9**
	Stand	76.1	79.6		

watch and for all the different combinations of ”current states” and ”next states”. Table 4.2 shows the result for this using PUK kernel of SVM algorithm (which we had previously shown to have the best result) in WEKA and by employing the top 5 features.

As can be seen from Table 4.2, the average precision of sit-to-stand and sit-to-lie transitions is better if the phone is picked as the data collection module rather than watch. In that case using phone instead even improves the overall precision. On the other hand, when the current state is ”lie”, watch seems to be the better option to go with. As can be seen from Table 4.2, in the ”stand” state, the difference is not that significant, so the approach in this ”current state” would be to keep the either of the phone or watch that was employed in the previous state as the data collection module.

This method of using current state involves switching data source in between smartphone and smartwatch, which means the data should be collected using both of these devices. This might appear to be contradictory to the main purpose of this work: ”replacing phone with watch for convenience and the fact that the targeted patients are not very inclined to carry the phone all the time”. However, this dynamic switching of the data source will only be enabled when the phone is worn by the subjects and only if the ”current state” predicts the phone to be the more accurate device for classification. So with no enforcement of carrying the phone, we show that battery lifetime and classification accuracy can be improved.

Using equation 4.7 and the values of Table 4.2, improved precision based on the current state information can be calculated:

$$Prec_{imp_j} = P_{CP}[P(S_j = sit).(Prec_{phone|sit} - Prec_{watch|sit}) + P(S_j = stand|S_{j-1} = sit).(Prec_{phone|stand} - Prec_{watch|stand})] \quad (4.7)$$

This means that depending on the ”current state” information the model will be changes and so the precision for classification and the improved precision will be the precision overhead based on this model switching. Assuming the phone is worn by the subjects 50% of the time:

$$Prec_{imp_j} = 0.5 \times [1/3 \times (69.7 - 46.1) + 1/6 \times (86 - 78)] = 4.35 \quad (4.8)$$

In general, it has been shown that 90% of the time people are in close proximity (same room) of their phone [88].

4.4 Battery Lifetime Improvement

The power saving due to turning off the wrist-worn device can be large depending on the percentage of the time in which the phone is a better source for classification (which

can be found from Table 4.2). As a result, the probability that the data collection on the watch is OFF (P_{DO}) can be estimated:

$$P_{DO} = P_{PW}.[p(S_j = sit) + p(S_j = stand|S_{j-1} = sit)] \tag{4.9}$$

P_{PW} is the percentage of the time in which the phone is being worn by the subject. S_j represents the current state and S_{j-1} is the previous state. Therefore, the data collection on the watch becomes OFF only when the phone is worn by the subject and also when the ”current state” is ”sit” in which the phone has better prediction capability. Also when the current state is ”stand”, if the previous state is ”sit” then the phone has already been selected in previous state and therefore stays as the data collector module. Improved battery life can be found from this probability:

$$T_{ext} = P_{DO} \times (T_{DO} - T_{DC}) \tag{4.10}$$

Where T_{ext} is the extended time and T_{DO} and T_{DC} are respectively the battery life time when data collection is OFF and ON. That means the total battery lifetime after the improvement is:

$$T_{ext} = T_{DC} + T_{ext} \tag{4.11}$$

Using the same assumption we had in Section 4.2 (phone is worn 50% of the time), P_{DO} can be found from equation 4.12:

$$P_{DO} = 0.5 \times (1/3 + 1/2 \times 1/3) = 0.25 \tag{4.12}$$

and this leads to:

$$T_{ext} = 0.25 \times (T_{DO} - T_{DC}) \tag{4.13}$$

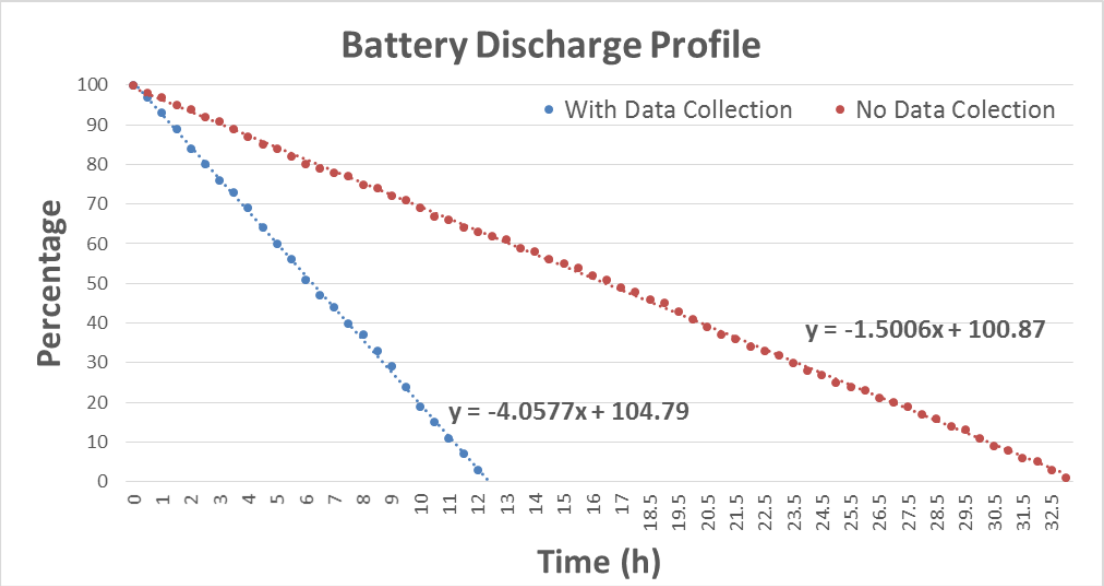

Figure 4.4: Watch battery discharge profile.

T_{DO} and T_{DC} can is found by looking the watch power profile for both situation of data collection being ON and OFF, Figure 4.4 shows this measured power profile for Samsung Galaxy Gear (which was used in the data collection).

As can be seen from Figure 4.4, the measurement values are 33 and 13 hours for T_{DO} and T_{DC}, which leads to 5 hours if we use equation 4.13.

4.5 Discussion and Conclusion

In this chapter, the same data from the pilot trial in Chapter III was used which contains 1200 data samples collected from 20 subjects. Unlike conventional classification, a context-aware classification is proposed in this Chapter. In the proposed method, context information is used to adjust the prior probability by giving different costs to each class based on the ”location” and the ”current state”. Table 4.1 shows the F-Score results for the activity classification using only 5 features for 3 different locations. As can be seen, for example in the kitchen, we achieve 7% improvement. This is because knowing the location of the subject provides significant information about the activ-

ity. However, in the living room, we achieve 3% improvement, and it totally makes sense, because the likelihoods of sitting, lying, and standing in the living room are almost similar, and consequently the prior probability distribution is closer to the uniform distribution which is the pre-assumption for conventional activity recognition too.

In a similar manner, improvement in the classification of accuracy was achieved using the ”current state” as the contextual information. The dynamic source selection algorithm was proposed which puts some of the burden of data collection on the phone but only if that does not penalize the overall precision of the classification. In fact, it was shown in this chapter that for some particular activities and states, the phone can be the superior module in terms of classification accuracy compared to the watch. We have shown in this work that this novel scheme can improve the overall classification precision by 5% and extends the battery lifetime of the Smartwatch by almost 5 hours or 40%. Future work can be conducted to test the algorithm in long-term situations and on real patients.

CHAPTER 5

Robust Gait Assessment for Wrist-Worn Devices

5.1 Introduction

Due to high level of comfort that Smartwatch delivers, frail patients are able to use Smartwatches as a mobile wearable technology to remotely log their health status metrics. These metrics range from physical activity [68], heart health [29], blood pressure [89], etc. One very significant health-related metric that has a great potential to be revisited by this technology is human gait. We have talked about the different applications of human gait in Chapter I and the significant research works in this area in Chapter II. In this chapter, we try to provide an overview of different gait monitoring techniques through wearable devices, ruling out any expensive, high-tech or high-burden systems. Then we introduce our novel gait assessment tool, which is an effort to overcome the accuracy challenge of wrist-worn sensing (which we discussed in Chapter II). The proposed method will be backed up with the experiment results and system verification and eventually we will provide conclusion and future directions at the end of this chapter.

5.2 Gait Measurement Techniques

Step detection and walking analysis using inertial sensors has been done through many different techniques. Usually these techniques are very dependent on the location of the inertial sensor on the body. Walking can be sensed by mounting inertial sensors on almost any locations of the body, however two locations among all seem to be giving the most promising accuracy results: waist (which is close to center of mass-COM)

and foot which is the most involved organ in walking. One simple approach for both foot-mounted and waist-mounted sensors is to detect the walking distance through determining the number of peaks or zeros in the vertical component of the accelerometer signal over the walking period. After detecting number of steps, the distance is calculated by multiplying it to a constant. That constant needs to be estimated based on the subject physical parameters such as height. This method for walking distance estimation is simple and low-cost, although it has two major issues. First is that, the length of the step varies over time and over different people which enforces frequent calibration. In addition, over-counting and under-counting of one single step results into a big noise estimating the distance as well as velocity. Another very common method in measuring the gait distance and velocity is to apply a Fast Fourier Transform (FFT) on the accelerometer signal and find the dominant frequency component of it. This frequency is shown to be highly correlated to the step length [67, 71]. This correlation can be determined using both analytical and data-driven methods [90]. The same approach was applied for a sensor carried in the pocket as well [71]. This approach provides relatively high accuracy if the subject goes through calibration phases before testing (resulting in a user-tailored model).

Mostly used in foot or ankle-mounted sensors systems, one can calculate the stride velocity and length by single and double integrating the horizontal acceleration respectively [91]. The issue in this approach is error accumulation due to integration, which is called ”sensor drift”. ”Error zeroing” has been used to resolve this issue by periodically zeroing the accumulated error when the foot touches the ground (detected using the angular velocity data [92]). This methods is has been known to be called ”zero velocity updating” (ZVU) technique. Double integration has also been used for chest and waist-mounted sensors as well but on the vertical acceleration. This vertical displacement does not give the estimated stride length but it is correlated with it. [93] and [73] have designed estimators to calculate the step length from both the vertical displacement as well as physiological parameters such as height and weight of the subjects.

Another popular technique is finding the gait parameters based on the physical modeling of the movement of the center of mass (COM) as the inverted pendulum [94]. When one leg is on the stance mode, the other one swings like an inverse pendulum. Using the properties of isosceles triangle where each leg was modeled as one single segment [95] has modeled the gait movement. This was done taking into account the fact that at heel strike, legs and the distance between them form an isosceles triangle. Using this biomechanical modeling as well as machine learning techniques horizontal displacement of the COM can be estimated based on the change in the orientation of the sensor and horizontal displacement.

With the advancement in machine learning and data mining tools and algorithms, another gait assessment technique that has been recently widely used is data-driven gait modeling. In this method, by collecting the training walking data from a set of subjects and by including their sensory data as well as their physiological data in the training, gait model is generated in data-driven manner. These parameters can include their height, accelerometer and gyro min, max and mean, etc. as well as the frequency domain parameters. Dominant frequency component of accelerometer data is shown to be highly correlated with the stride length and the gait distance and velocity [67].

While most of the previous works have been focused on implementing algorithms for either foot, chest or back-mounted sensors, none were much applicable in ambulatory remote health monitoring. This is because a lot of these sensing systems require bulky and uncomfortable devices attached to the user which imposes a lot of inconvenience for the subject. This eventually results into non-compliance in long-term which causes user rejection and data loss. This is especially true for patients within the categories of elderly and frail.

Smartphone has provided a more convenient platform for gait assessment, as the subject would normally carry it. Therefore, Smartphone-based walking speed and distance estimation systems have been recently under a lot of attention. Still, from our experience, a lot of elderly and risk subjects are not willing to carry a bulky phone all

the time. These patients unfortunately happen to be the category which is in the most need for monitoring. With the emergence of Smartwatches with inertial sensors embedded in them in the past decade, a great deal of attention and effort has been put in building up wrist-worn gait assessment systems which definitely addresses those categories of patients. In most of these works, a correlation between stride length and some features of the inertial sensors is detected. Vertical displacement was used in [63] and an empirical relation between that and step length was identified. [64] included the step duration, range of vertical acceleration and number of sample in each step in designing their step length estimator as well, to improve the accuracy. Most of the hand-mounted gait assessment systems though, have been focusing on dominant step frequency as the most correlated feature. The correlation between hand frequency and step frequency has been estimated in [65] and then step length and velocity is estimated from there. This required having different models for different positions of the sensor (in-pocket, in-hand and carrying in bag). Accuracy was improved in a similar system in [66] by including GPS calibration while the subject is outdoor. Step length has also been estimated using the abstraction model generated from hand motion frequency and height of subjects in [67]. They showed an error of 5% for short range but this work offers a handheld-based system (not hand-mounted).

In most of these handheld or wrist-worn systems, the biggest challenge comes from the fact that arm swing causes addition to the noise in distance and velocity estimation which causes undercounting or over-counting of steps. This concept seems to be not investigated thoroughly in the previous related works. We have introduced this issue and proposed a solution to address it in [96] and [97]. This work is a follow-up on those works that provides a detailed investigation of this challenge while a more comprehensive analysis is provided. Next section will introduce the methodology that is proposed which contains the novel peak detection algorithm that accurately detects the steps by applying sensible constraints between times and values of the consecutive peaks. Then the idea of using Kalman filter to recover the missing peaks due arm swing is thor-

oughly investigated. Then, significant gait parameters such as distance, velocity and symmetry are estimated using the linear regression while self-calibration methods are used to improve the estimation accuracy.

5.3 Methodology

Human walking is a complicated motion involving several body parts. These motions affect output of an inertial sensor unit on the wrist. In this section, major motions affecting the inertial sensor output are described, which is derived based on a simplified walking model. This relationship between walking and sensor output helps to identify walking steps from the sensor output. In this section we will first describe the inertial sensors' signals of the wrist-worn device while walking in sub-section 5.3.1. The rest of this section will be on the proposed algorithm to detect the walking behavior. Figure 5.1 shows the block diagram of the whole system with all the algorithm modules.

5.3.1 Inertial Sensors During Walking

Two coordinate frames are used for the explanation (see Figure 5.2). One is the reference coordinate frame, which is fixed on the earth. The z axis of the reference coordinate frame is assumed to coincide with the local gravity direction (upward direction). The choice of x and y axes is not important. The other coordinate frame is the sensor coordinate system, where the three axes coincide with the three axes inertial sensor unit. We use a symbol $[p]_R$ or $[p]_S$ to denote that a vector $p \in R^3$ is expressed in the reference or sensor coordinate frame.

Firstly, we investigate the accelerometer output during walking. There are mainly three acceleration sources during walking: Earth's gravity, inverted pendulum motion of a stance leg and arm swing. Earth's gravity is in the direction of reference coordinate frame z axis:

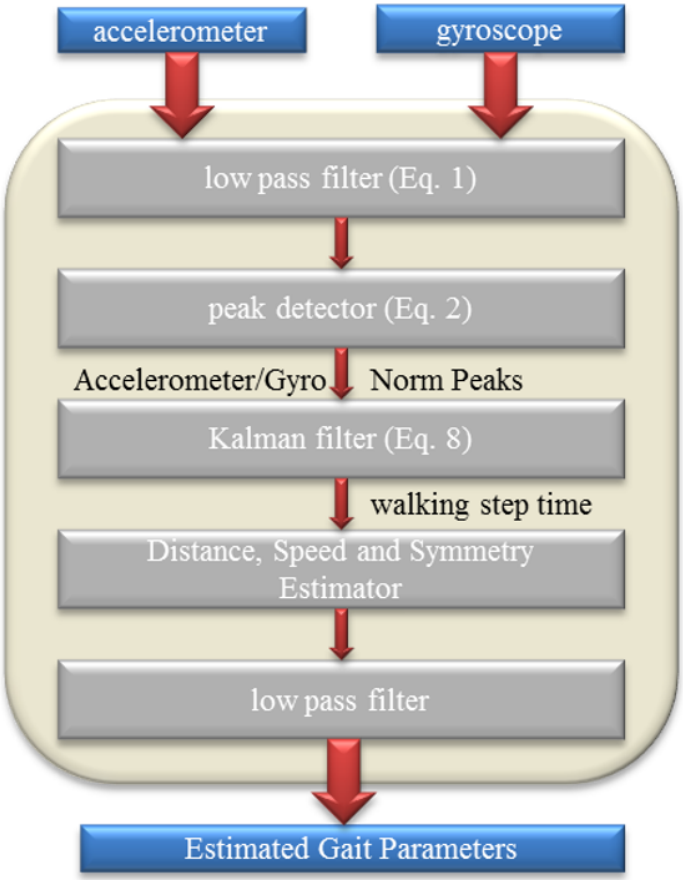

Figure 5.1: Block diagram of the proposed gait assessment algorithm

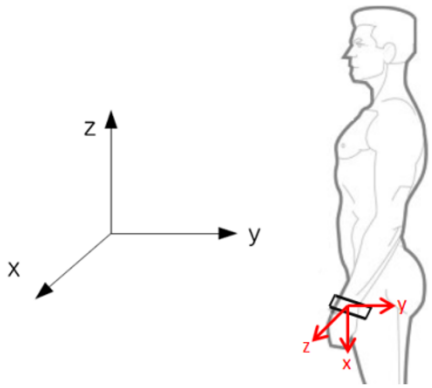

Figure 5.2: Two coordinate frames: Reference coordinate systems (left), Sensor coordinate system (right).

$$\left[y_{a,gravity}\right]_R = \begin{bmatrix} 0 \\ 0 \\ g \end{bmatrix} \tag{5.1}$$

where g is the magnitude of the local gravitational acceleration. The measured gravity is an quantity expressed in the sensor coordinate frame. For example, suppose a person is standing still while the x axis of the sensor coordinate frame is in the same direction of $-z$ axis of the reference coordinate frame (see Figure 5.2). Then the output of accelerometer is given by:

$$\left[y_{a,gravity}\right]_S = \begin{bmatrix} -g \\ 0 \\ 0 \end{bmatrix} \tag{5.2}$$

Two other major motions generating acceleration is leg movement and arm swing. To focus on the leg movement first, suppose a person is walking without arm swing in the direction of x axis (reference coordinate frame). If we assume a person is walking with constant speed, the x axis acceleration (in the reference coordinate frame) is 0. Since there is no motion in the y axis, the y axis acceleration is also 0. Thus during walking without arm swing, z axis acceleration (in the reference coordinate frame) is dominant.

There are many mathematical models describing walking motion [98, 99]. One of the simplest model is an inverted pendulum motion of a stance leg [98]. In Figure 5.3, during the interval (a) - (c), the right leg can be modeled as an inverted pendulum. The z axis position (reference coordinate frame) of a upper body is the highest at (b) period and lowest at (a) and (c) periods. Similarly, the left leg can be modeled as an inverted pendulum during the interval (c) - (e), where the highest z position is at (d) period. Thus during walking, z position value is almost sinusoidal. By taking double derivatives of z position value, we can see z axis acceleration is also almost sinusoidal in Figure 5.3.

In summary, the acceleration due to leg motion is almost sinusoidal when there is no arm swing and thus can be modeled as follows:

$$\left[y_{a,leg}\right]_R = \begin{bmatrix} 0 \\ 0 \\ A_1 \cos(\frac{2\pi}{T}t) \end{bmatrix} \tag{5.3}$$

where T is one step walking time and A_1 is a parameter depending mainly on the leg length. Now suppose a person is walking with arm swing. If we model arm swing as a pendulum motion around the z axis of the sensor coordinate frame, the acceleration due to arm swing is given by:

$$\left[y_{a,arm}\right]_S = \begin{bmatrix} -A_2\dot{\theta}^2 \\ A_2\ddot{\theta} \\ 0 \end{bmatrix} \tag{5.4}$$

where A_2 is a parameter depending on the arm length. The first element is related to centripetal acceleration and the second element is related to Coriolis acceleration [100]. Unlike $y_{a,gravity}$ and $y_{a,leg}$, this acceleration is represented in the sensor coordinate frame. Let $[y_a]_S$ be the acceleration measured by an accelerometer during arm swing walking. Since $y_{a,gravity}$ and $y_{a,leg}$ are given in the reference coordinate frame, they should be transformed to the sensor coordinate frame. Let θ be the angle between the reference and sensor coordinate frames (see Figure 5.4 for the θ angle definition), then the rotation matrix from the reference coordinate frame to the sensor coordinate frame is given by:

$$C_R^S(\theta) = \begin{bmatrix} 0 & \sin\theta & -\cos\theta \\ 0 & \cos\theta & \sin\theta \\ 1 & 0 & 0 \end{bmatrix} \tag{5.5}$$

Using this rotation matrix, $[y_a]_S$ is given by:

$$\left[y_a\right]_S = \left[y_{a,arm}\right]_S + C_R^S(\theta)\Big(\left[y_{a,gravity}\right]_R + \left[y_{a,leg}\right]_R\Big) \tag{5.6}$$

During walking, arm swing frequency is the same as walking frequency and the arm swing angular velocity can be modeled as:

$$\dot{\theta}(t) = A_3 \sin(\frac{\pi}{T}(t+\phi)) \tag{5.7}$$

where A_3 is a parameter depending on maximum forward and backward arm swing angles and ϕ is phase difference between leg movement and arm swing. Let θ_f and θ_b be the absolute maximum angles of arm forward swing and backward swing, respectively. Then from the relationship:

$$\int_0^T \dot{\theta}(r)dr = \theta_f + \theta_b \tag{5.8}$$

We have:

$$A_3 = \frac{\pi}{2T}(\theta_f + \theta_b) \tag{5.9}$$

In Figure 5.5 (no arm swing) and Figure 5.6 (with arm swing), simulated accelerometer and gyroscope norm plots during walking are given. In Figure 5.6, the data are generated with $\theta_f = 40^\circ$, $\theta_b = ang15$ and $\phi = 0.05$. When there is no arm swing (Figure 5.5), walking step can be easily identified using the maximum peaks of the accelerometer norm. We denote the maximum peak occurrence time by $p_{a,i}$. When there is arm swing, the accelerometer norm plot is different but walking step can be still identified using $p_{a,i}$. The walking step also can be identified using gyroscope norm minimum peak time, which are denoted by $p_{g,i}$. Note that $p_{a,i}$ and $p_{g,i}$ are not the peak values but the peak occurrence times.

The accelerometer norm plot with arm swing can be significantly different depending on parameters (θ_f , θ_b and ϕ). For example, the simulated accelerometer and

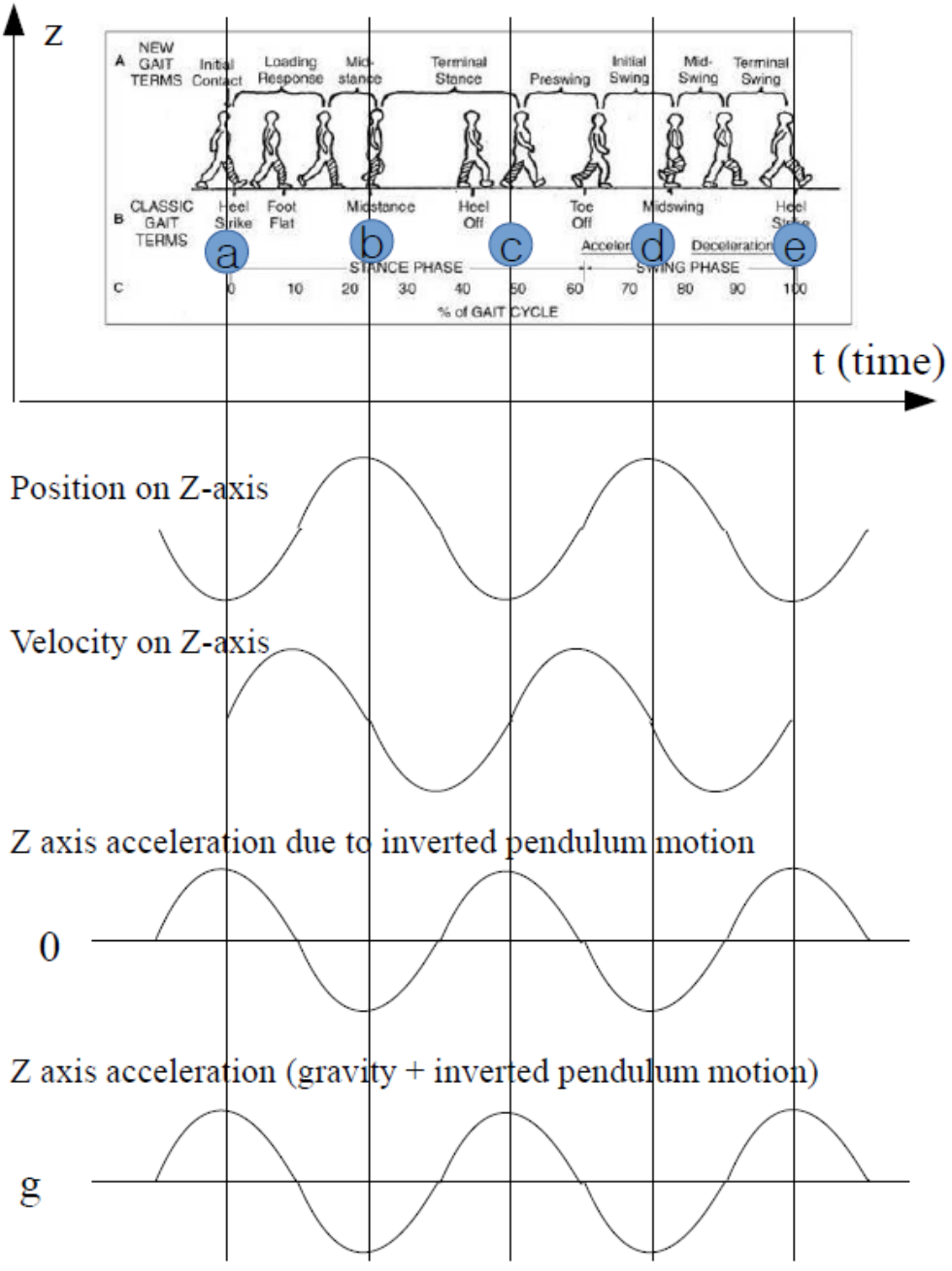

Figure 5.3: Gait cycles and reference frame z-axis acceleration

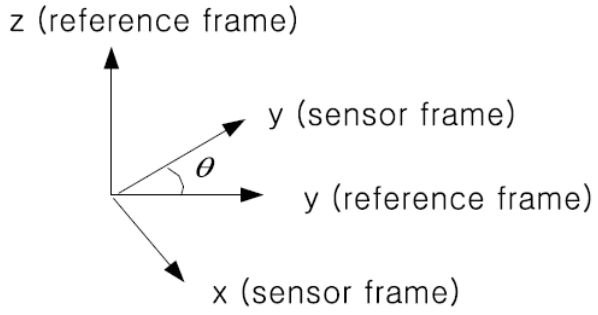

Figure 5.4: Rotation between reference and sensor coordinate frames.

gyroscope norm plots with $\theta_f = 40^\circ$, $theta_b = 20^\circ$ and $\phi = 0.02$ is given in Figure 5.7. It can be seen that the accelerometer plot is quite different even with the slight change of parameters. Also, in this case, less conspicuous peaks ($p_{a,1}$ and $p_{a,3}$) may not be detected if there is small nose or other terms in the accelerometer output.

5.3.2 Preliminary peak detection algorithm

The first step after high-frequency noise removal using a low-pass filter is a preliminary peak detection of the inertial sensors' signals to identify the step events. This initial step event detection algorithm is simply a 5 data points peak detection algorithm. Let $y_i \in R$ be a signal (either the norm of accelerometer output or the norm of gyroscope output) and i be the discrete time index. y_i is the low-pass filtered output of y_i:

$$\overline{y_i} = \alpha_1 y_{i-1} + (1 - 2\alpha_1) y_i + \alpha_1 y_{i+1} \tag{5.10}$$

where α_1 is the weighting factor for the low pass filter. Then after this low-pass filtering the signal is searched for significant maximum or minimum peaks using these three conditions:

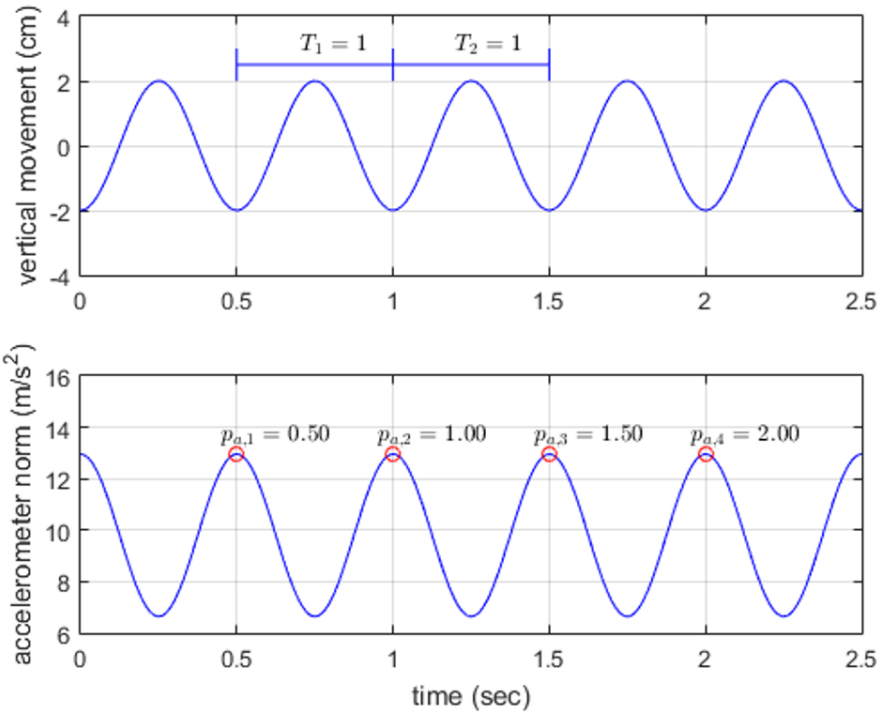

Figure 5.5: Simulated accelerometer norm during walking without arm swing.

$$
\begin{aligned}
(a) : (\bar{y}_{i-2} < \bar{y}_i) \ \textit{and} \ (\bar{y}_{i-1} < \bar{y}_i) \ \textit{and} \ (\bar{y}_i > \bar{y}_{i+1}) \ \textit{and} \ (\bar{y}_i > \bar{y}_{i+2}) \ \textit{and} \\
(\bar{y}_i - \max(\bar{y}_{i-2}, \bar{y}_{i-1}, \bar{y}_{i+1}, \bar{y}_{i+2}) > \alpha_2) \\
(b) : (\bar{y}_{i-3} < \bar{y}_{i-2}) \ \textit{and} \ (\bar{y}_{i-2} < \bar{y}_{i-1}) \ \textit{and} \ (\bar{y}_{i-1} < \bar{y}_i) \ \textit{and} \ (\bar{y}_i > \bar{y}_{i+1}) \ \textit{and} \\
(\bar{y}_i - \max(\bar{y}_{i-3}, \bar{y}_{i-2}, \bar{y}_{i-1}, \bar{y}_{i+1}) > \alpha_2) \\
(c) : (\bar{y}_{i-1} < \bar{y}_i) \ \textit{and} \ (\bar{y}_i > \bar{y}_{i+1}) \ \textit{and} \ (\bar{y}_{i+1} > \bar{y}_{i+2}) \ \textit{and} \ (\bar{y}_{i+2} > \bar{y}_{i+3}) \ \textit{and} \\
(\bar{y}_i - \max(\bar{y}_{i-1}, \bar{y}_{i+1}, \bar{y}_{i+2}, \bar{y}_{i+3}) > \alpha_2) \qquad (5.11)
\end{aligned}
$$

where α_2 is a parameter that defines the selectiveness of the peak detection algorithm. If α_2 is chosen to be a big value, only conspicuous peaks are detected and any small peaks are ignored. Although, this increases the probability of missing a real peak. This can be observed in Figure 5.8 where only 3 peaks are detected with $\alpha_2 = 1$ and 2nd peak is ignored. Each detected peak satisfies at least one of the three conditions in (2): peak 1 (a,b,c), peak 2 (a,c) and peak 3 (a,c). The condition 5.11 can be easily

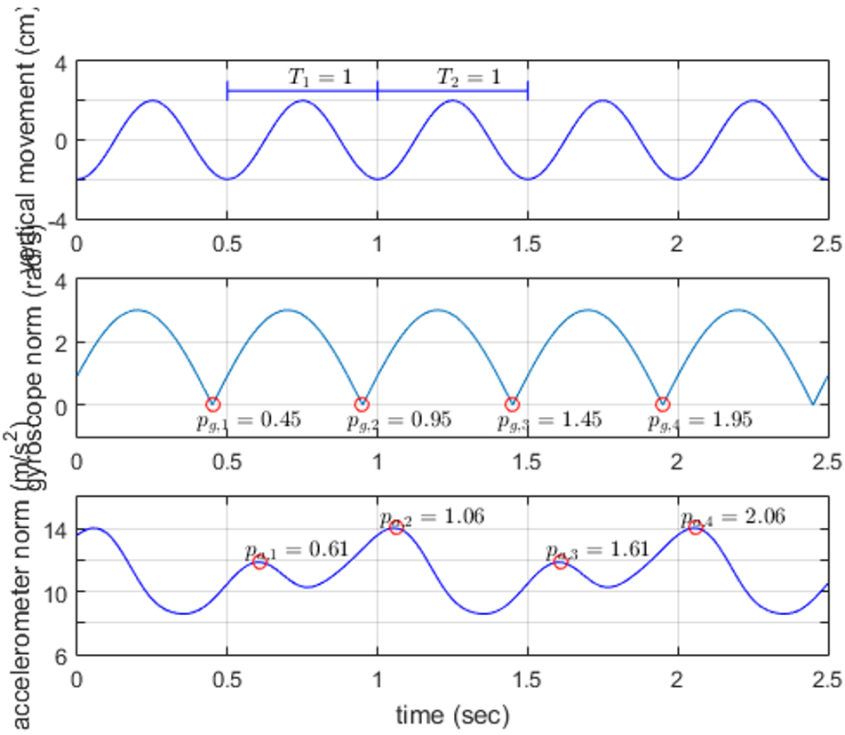

Figure 5.6: Simulated accelerometer norm during walking with arm swing ($\theta_f = 40^\circ, \theta_b = 15^\circ, \phi = 0.05$).

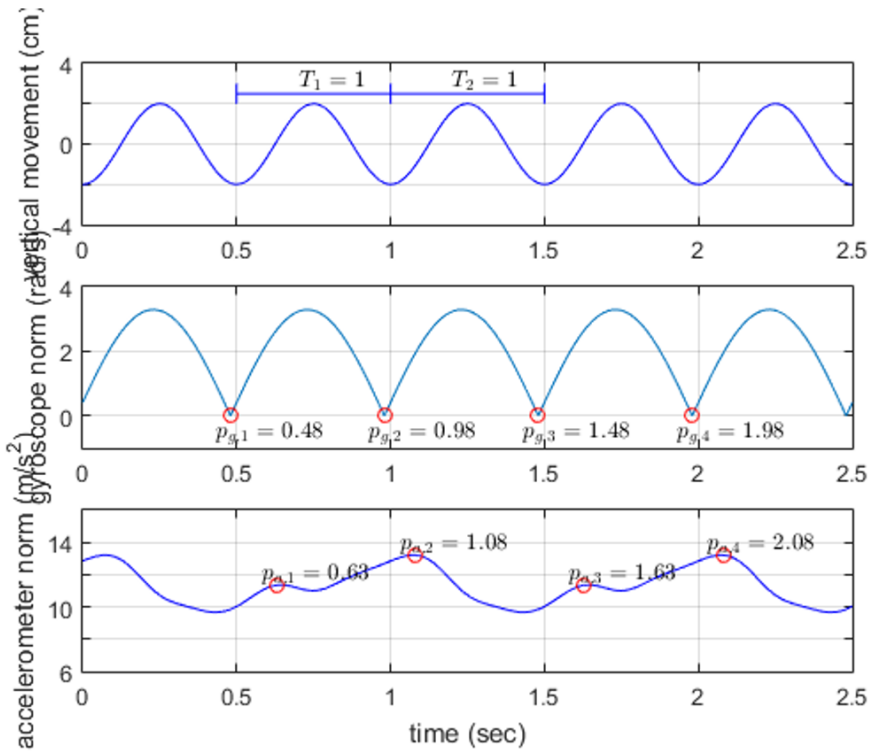

Figure 5.7: Simulated accelerometer norm during walking with arm swing ($\theta_f = 40^\circ, \theta_b = 20^\circ, \phi = 0.02$).

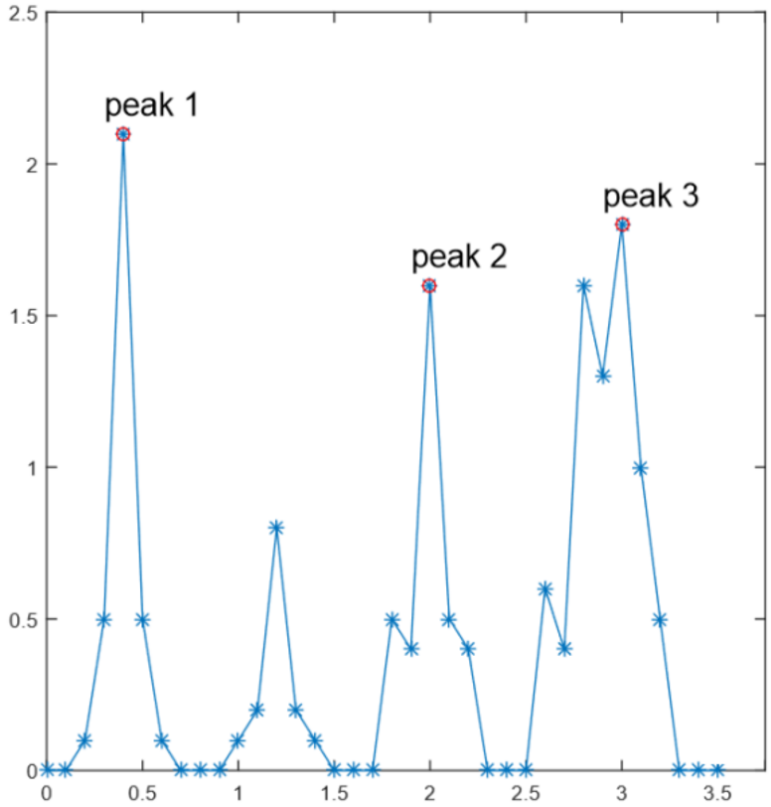

Figure 5.8: Maximum Peak detection using condition (2).

modified to detect the minimum peaks.

5.3.3 Walking mode detection

As we mentioned earlier, even with small values of α_2 there happened to be some true step event peaks which are not detected. These missing peaks can be detected using a Kalman Filter. We are taking advantage of the fact that walking is happening if the detected peaks occur periodically. A scalar variable m_k is used to represent whether a person is walking or not. m_k can take only 0, 0.5 and 1 values. If $m_k = 0$, it means a person is not walking. If $m_k = 1$, it means walking is happening and if $m_k = 0.5$, a person is considered to be walking if $m_{k+1} = 1$ and not to be walking if $m_{k+1} = 0$. This is best represented by the state diagram in Figure 5.9.

Defined by the state diagram in Figure 5.9, suppose $m_k = 0$ and we encounter a

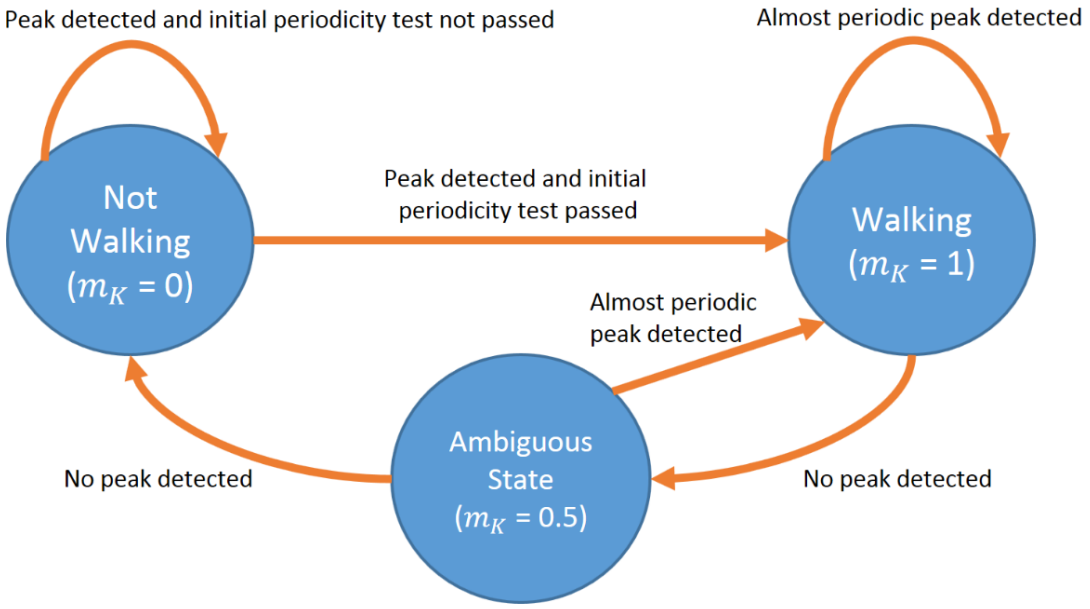

Figure 5.9: Walking/Not Walking state diagram.

peak $z_{a,i}$. Since there is no way to know this is due to walking or other actions, we wait until $z_{a,i} + \alpha_3$ time to determine whether the peak occurrence is periodic: that is, the interval $[z_{a,i}, z_{p,i} + \alpha_3]$ data are used to check periodicity. If the parameter α_3 is large, we can determine periodicity more robustly. However, short walking events could be ignored.

The initial periodicity check is done as follows. Let $z_{a,i}, \ldots, z_{a,i+1}$ be the peak times belonging to the interval $[z_{a,i}\ , z_{a,i} + \alpha_3]$. Let $T_{init,j} (1 \leq j \leq l)$ be defined by:

$$T_{init,j} \triangleq z_{p,i+j} - z_{p,i+j-1} \tag{5.12}$$

If peaks are almost periodic, $T_{init,j}$ values should be similar except for the first walking step time $T_{init,1}$, which could be quite different from other steps since the walking speed is slower in the beginning of walking. To reflect this fact, we compute a weighted average value of $T_{init,j}$ by minimizing:

$$J(T) \triangleq \alpha_4 (T_{init,1} - T)^2 + \sum_{j=2}^{l} (T_{init,j} - T)^2 \tag{5.13}$$

where $\alpha_4 < 1$ is a weighting factor to allow large deviation of T from $T_{init,1}$. Let T_{ave} be the minimizing solution to 5.13. From [101], T_{ave} is given by:

$$T_{ave} = \frac{1}{\alpha_4 + (l-1)} (\alpha_4 T_{init,1} + \sum_{j=2}^{l} T_{init,j}) \tag{5.14}$$

We determine $T_{init,j}$ is almost periodic if:

$$\frac{J(T_{ave})}{l} < \alpha_5 \tag{5.15}$$

If we chose very small value of parameter α_5, all $T_{init,j}$ should be the same to pass the periodicity test. If larger α_5 is used, more variance of $T_{init,j}$ is allowed. As an additional fail-safe measure, the three axes accelerometer value at the peak time is also investigated. During walking, the acceleration direction at the peak time is almost similar. Let $U_{init,j}$ be defined by:

$$U_{init,j} = \frac{y'_{a,z_{p,i+j}} y_{a,z_{p,i+j-1}}}{\left\| y_{a,z_{p,i+j}} \right\| \left\| y_{a,z_{p,i+j-1}} \right\|} \tag{5.16}$$

where $y_{a,i} \in R^3$ is three axes accelerometer sensor value at the discrete time i. The angle between the accelerometer vectors at the two consecutive peaks is $cos^1 U_{init,j}$. We determine the acceleration directions at the peaks are similar if the following is satisfied:

$$\frac{\sum_{j=1}^{l} U_{init,j}}{l} > \alpha_6 \tag{5.17}$$

If conditions 5.15 and 5.17 are satisfied, m_k is changed to 1.

5.3.4 Walking step time detection using Kalman Filter

Now while the state of the subject is walking (measured by the previous sub-section or $m_k = 1$), Kalman Filter will be used to estimate the walking step time. The state of a Kalman filter is defined by:

$$x_k = \begin{bmatrix} p_k \\ T_k \end{bmatrix}$$

where P_k is the accelerometer norm peak time and T_k is the walking step time. The state dynamic equation is given by:

$$x_{k+1} = Ax_k + w_k \tag{5.18}$$

The noise term w_k is a zero-mean Gaussian noise used to represent the step-to-step variation of walking step time. Matrix A and the covariance of the noise are defined as:

$$A \triangleq \begin{bmatrix} 1 & 1 \\ 0 & 1 \end{bmatrix}$$

$$E\left\{w_k w_k'\right\} = \begin{bmatrix} 0 & 0 \\ 0 & q \end{bmatrix} \in R^{2\times 2} \tag{5.19}$$

The variance q represents step-to-step variation of step time.

The detected accelerometer norm peak time $z_{a,i}$ is used as a measurement in the Kalman filter. Since the measurement equation $z_{a,i}$ and the dynamic equation 5.18 are not synchronized, we use a simple method to match $z_{a,i}$ and x_k. Let $\hat{x}_{k-1}$ be the posterior Kalman filter estimated value of $x_{(k-1)}$ and $P_{(k-1)}$ be the corresponding estimation error covariance. From the standard Kalman filter equation [102], the prior (before measurement) estimated value $\hat{x}_{\bar{k}}$ and corresponding estimation error covariance $P_{\bar{k}}$ at the step k can be computed as:

$$\begin{aligned} \hat{x}_{\bar{k}} &= A\hat{x}_{k-1} \\ P_{\bar{k}} &= AP_{k-1}A' + Q \end{aligned} \tag{5.20}$$

Since the peak time is almost periodic during normal walking, a peak should be near $H_a\hat{x}_{\bar{k}}$ where $H_a = [10]$. If $z_{a,i}$ is near $H_a\hat{x}_{\bar{k}}$, a standard measurement update is done. If a peak is not near $H_a\hat{x}_{\bar{k}}$, there are two possibilities. One case is that a peak is not detected due to arm swing. In this case, T_k can be measured from the arm swing period (gyroscope norm minimum peak time difference). The other case is that a person stops walking. In this case, no measurement update is done. In both cases, m_k value is decreased by 0.5. If two consecutive peaks are missing, the walking mode is changed to 0 (not waking mode). The above explained measurement update equations are summarized as follows:

- If there is a $z_{a,i}$ satisfying the following condition:

$$|z_{a,i} - H\hat{x}_{\bar{k}}| < \alpha_7\sqrt{P_{\bar{k}}(1,1)} \tag{5.21}$$

  $z_{a,i}$ is used as the measurement update where: $z_{a,i} = H_a x_k + v_{a,i}$.

- If there is no $z_{a,i}$ satisfying 5.21 but there is one satisfying the following condition:

$$\begin{aligned} z_{g,i} \leq H_a\hat{x}_{\bar{k}} < z_{g,i+1} \\ z_{g,i+1} - z_{g,i} < \alpha_8\sqrt{P_{\bar{k}}(2,2)} \end{aligned} \tag{5.22}$$

  $z_{g,i}$ is used in the measurement update where: $z_{a,i} = H_g x_k + v_{g,i}$ and $H_g = [\ 0\ 1\ ]$. Also m_k is decreased by 0.5.

Table 5.1: Parameters for Kalman Filter

Symbol	Value	Purpose
$\alpha_{1,a}$	0.2	*low pass filter parameter for the accelerometer (1)*
$\alpha_{1,g}$	0.2	*low pass filter for the gyroscope (1)*
$\alpha_{2,a}$	1	*significant accelerometer peak detection (2)*
$\alpha_{2,g}$	0.3	*significant gyroscope peak detection (2)*
α_3	4	*initial periodicity check*
α_4	0.2	*initial periodicity check (3)*
α_4	1.5^2	*initial periodicity check (5)*
α_4	0.9	*initial periodicity check (7)*
α_4	1	*next peak time estimation (11)*
α_4	1	*next peak time estimation (12)*
q	1.5^2	*process noise covariance (9)*
R_a	2^2	*measurement noise covariance of* $v_{a,i}$
R_g	2^2	*measurement noise covariance of* $v_{g,i}$

- If none of the above conditions are satisfied, then again, m_k is decreased by 0.5:

Where $P_k(i,i)$ is the (i,i)th element of the matrix. In this way, Kalman filter compensates for the missing accelerometer peaks due to arm swing. The parameters used in the Kalman Filter are given in Table 5.1.

5.3.5 Distance and Velocity Models

Let L_k be one step walking length for the $k-th$ walking step. If we can estimate one step walking length, the walking distance can be computed by summing up L_k. It is known that walking length is inversely proportional to walking step time during normal walking. When we walk fast, the walking step time tends to be small and the walking length tends to be large. Thus the estimated walking length $\hat{L}_k$ is given by:

$$\hat{L}_k = a\frac{1}{T_k} + b \tag{5.23}$$

where a and b are person-dependent parameters, which should be calibrated from experiments. As walking length is inversely proportional to walking step time, it could be inferred that walking velocity (speed) is inversely proportional to the square of T_k. Thus the estimated walking velocity $\hat{V}_k$ is given by:

$$\hat{V}_k = c\frac{1}{T_k^2} + d\frac{1}{T_k} \tag{5.24}$$

During normal walking, walking speed is almost constant or slightly changing. To reflect this fact, the estimated velocity $\hat{V}_k$ is low pass filtered. The low pass filtered speed is denoted by $\overline{V}_k$.

5.3.6 Symmetry Models

We talked about the importance of gait symmetry as a key health indicator in numerous applications. There are many different models for gait symmetry such as these four: Ratio Index (RI), Symmetry Index (SI), Gait Asymmetry (GA) and Symmetry Angle (SA). Each of these models provide a comparison between some parameters of right and left leg. This parameter could be step length, step duration, stance phase, etc. The work in [103] has provided a great comparison between all the different symmetry models and verified that SI is perhaps the best of the four. Symmetry index of gait is defined as:

$$SI = \frac{|X_L - X_R|}{0.5\,(X_L + X_R)} \tag{5.25}$$

X_R and X_L could be any parameters belonging to right and left foot respectively. In this work, we will use the step duration (which is estimated using the Kalman filter) for left and right legs as the parameters to form the SI. So the estimated symmetry in this

work will be:

$$SI = \frac{|\bar{T}_L - \bar{T}_R|}{0.5\,(\bar{T}_L + \bar{T}_R)} \tag{5.26}$$

where $\overline{T_L}$ and $\overline{T_R}$ are the average of the step duration (T_K) for all the left and right steps respectively.

5.3.7 Parameter Calibration

The calibration of model parameters is similar for both distance and velocity parameters estimation. For example, for the calibration of a and b (distance parameters), a person needs to walk M times (straight line with known distance D). For each walking (index i is used), let N_i be the number of walking steps and $T_{(i,j)}(1 \leq i \leq M, 1 \leq j \leq N_i)$ be one step walking time. For i-th walking, we have the following equation:

$$D = \sum_{j=1}^{N_i} \left(a\frac{1}{T_{i,j}} + b \right) = a \sum_{j=1}^{N_i} \left(\frac{1}{T_{i,j}} \right) + bN_i \tag{5.27}$$

In the matrix form, 5.27 can be re-written as $B_p = b$, where:

$$B = \begin{bmatrix} \sum_{j=1}^{N_1} \left(\frac{1}{T_{1,j}} \right) & N_1 \\ \vdots & \vdots \\ \sum_{j=1}^{N_M} \left(\frac{1}{T_{M,j}} \right) & N_M \end{bmatrix} \in R^{M\times 2},\ p = \begin{bmatrix} a \\ b \end{bmatrix} \in R^{2\times 1},\ b = \begin{bmatrix} D \\ \vdots \\ D \end{bmatrix} \in R^{M\times 1} \tag{5.28}$$

The solution for p which is the parameter matrix is the solution to the following minimization problem:

$$\min_p \left\| B_p - b \right\|_2^2 \tag{5.29}$$

which is given by:

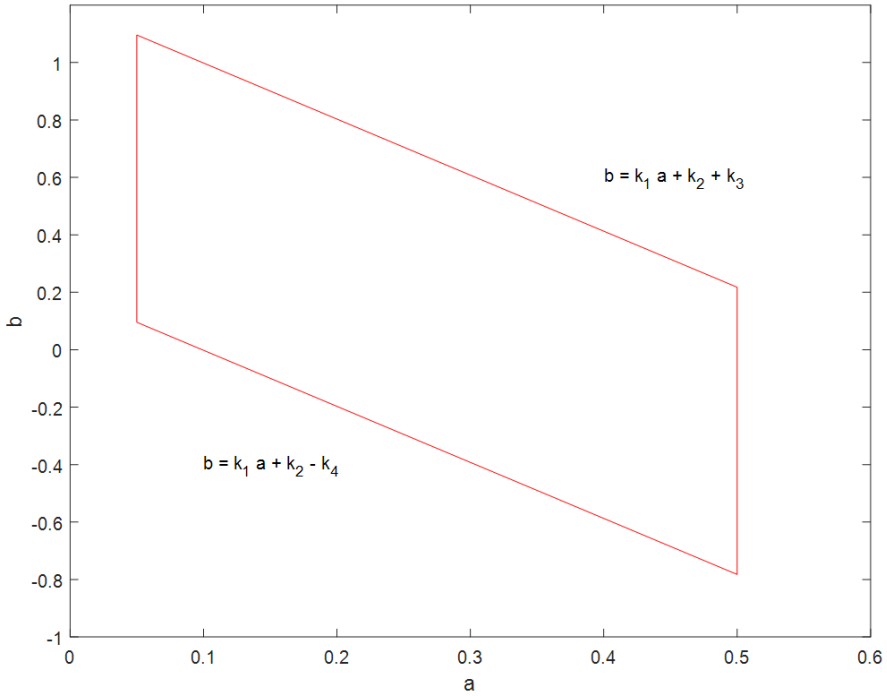

Figure 5.10: Constrained a and b relationship.

$$p = \left(B'B\right)^{-1} B'b \tag{5.30}$$

Since the number of parameters is 2 (that is, a and b), at least two sets of walking data are required to solve 5.30 (that is, M should be equal to or larger than 2). However, when M is small, the optimization problem becomes sensitive to noises and thus the estimated parameters may not be accurate. From experiments, we have found that possible combinations of a and b are rather constrained. We have found that a and b combinations can only exist inside the quadrilateral region in Figure 5.10, where k_1 to k_4 are parameters computed from experiments. The constraint in Figure 5.10 can be stated in the following equations:

$$\begin{aligned} a_{\min} \leq a \leq a_{\max} \\ k_1 a + k_2 - k_4 \leq b \leq k_1 a + k_2 + k_3 \end{aligned} \tag{5.31}$$

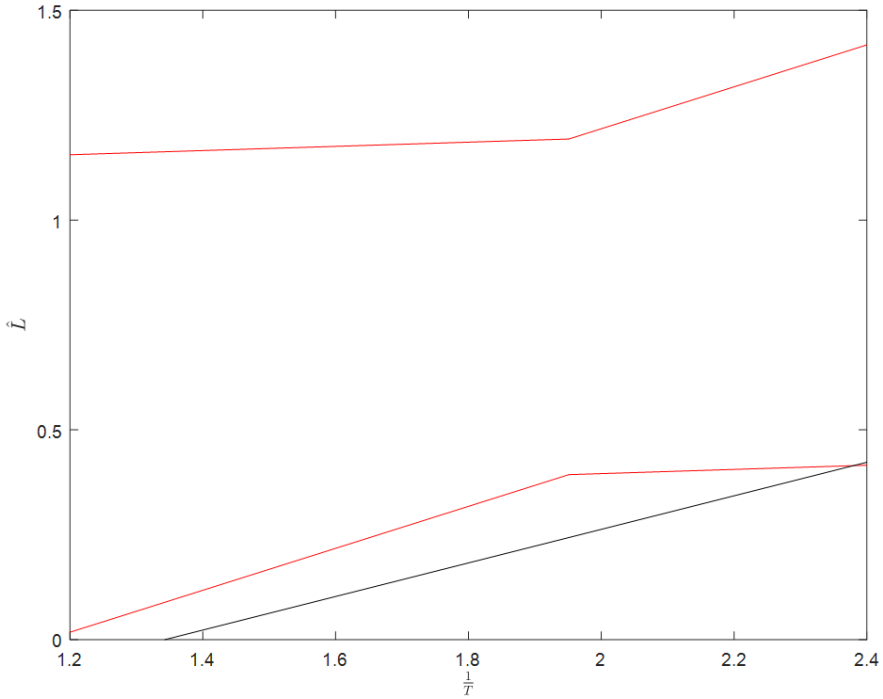

Figure 5.11: Boundaries of the linear relationship in 5.23 (red line) and example of a linear relationship violating it (black line).

The constraint in 5.10 makes the linear relationship 5.23 only exists inside two boundaries which is shown as the red lines of Figure 5.11. The black line shows an example of a linear relationship which does not satisfy the constraint imposed by the red lines. This kind of linear relationship should be rejected during the calibration process. We propose a constrained optimization problem for the calibration by minimizing 5.29 subject to the constraint 5.31. This problem is a standard constrained quadratic optimization problem and can be solved easily [101].

5.4 Experiments

To experiment the gait quality using the proposed algorithm, the Samsung Galaxy Gear Smartwatch was used as the hardware platform (same system that was utilized in Section III). The watch was worn on the left hand of the subjects. Similar to Chapter

Table 5.2: 25 Subjects' Information

	Age	**Weight**	**Height(cm)**
Range	18 – 40	46 – 100	153 – 186
Mean	26	65.1	168.1
Standard Deviation	4	12.4	7.5

III, data was sampled at a rate of 100 Hz to make sure no high frequency information on the gait is lost. Although, low-pass filter is used later in the algorithm to remove the unwanted noise. The data was manually annotated by a supervisor during training collection process.

5.4.1 Experiment Design

The experiment designed based on the gait performance of 25 participants. The information about the subjects which included 4 females and 21 males are given in Table 5.2. Each subject was asked to walk a fixed distance of 50 meters with a self-paced constant velocity. The velocity information and the start and stop times are recorded. At the same time, one Xsens inertial sensor is attached on the left foot with sampling frequency of 100 Hz which estimates the walking distance information with high accuracy (centimeter level error) using the inertial navigation algorithm [104, 105]. The experiment was conducted with six different types of walking with different modes and velocities which can be observed in 5.3. The modes include: four times of normal speed walking, one time of slow speed walking and one time of fast speed walking. Among six walking data collections, a hand-held briefcase is carried for two of the times, which has an effect of suppressing arm swing.

Table 5.3: 6 Walking Patterns For Participants

Walking ID	Speed	Arm Swing)
1	*Normal*	*Arm is naturally swinging*
2	*Slow*	*Arm is naturally swinging*
3	*Fast*	*Arm is naturally swinging*
4	*Normal*	*Arm is naturally swinging*
5	*Normal*	*Carrying a briefcase*
6	*Normal*	*Carrying a briefcase*

5.4.2 Preliminary peak detection performance

The first step in the proposed algorithm is the preliminary 5-point peak detection which is described by 5.11. After low-pass filter is applied minimum and maximum peaks are detected. Figure 5.12 shows the detected peaks annotated by 'o' symbol for three different modes of walking: slow, normal and fast. In the first graph (person id = 1, walking id = 3), the gyroscope peaks are periodic, which means periodic arm swing. Still the accelerometer norm peaks are almost sinusoidal and thus we can easily determine walking step time from accelerometer peaks. Although, in the last two graphs, the arm swing is more dominant (see the magnitude of gyroscope norm). In normal arm swing, it can be observed that one accelerometer peak is missed at 11.5 seconds and in the extreme case (large arm swing), there are four peaks which have been missed if only the preliminary peak detection algorithm is used.

5.4.3 Kalman Filter peak recovery performance

The preliminary peak detection algorithm might suffice to detect the step events when foot-worn inertial sensors are used. But in the case of wrist-worn sensors, arm swing leads to large deviations in the accelerometer signal which results into missing some of the peaks. The Kalman filter that is described in 5.3.4 is used to recover those missing

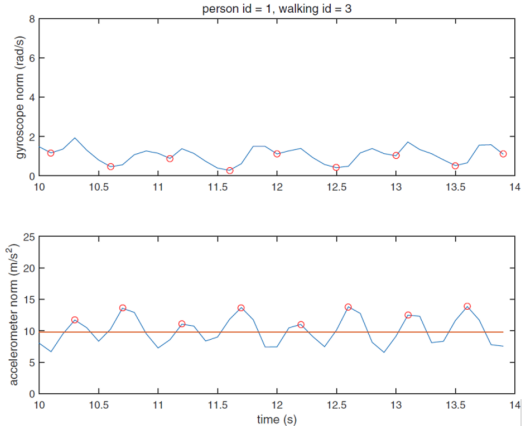

(a) slow arm swing

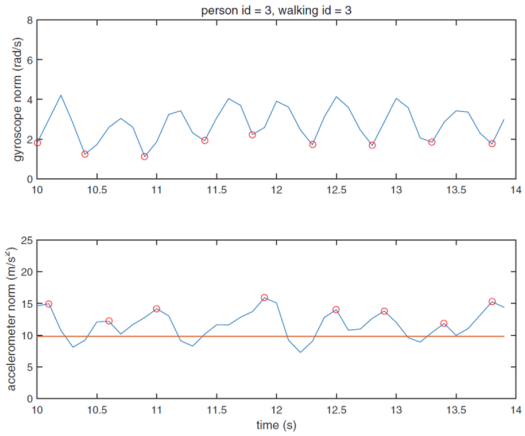

(b) medium arm swing

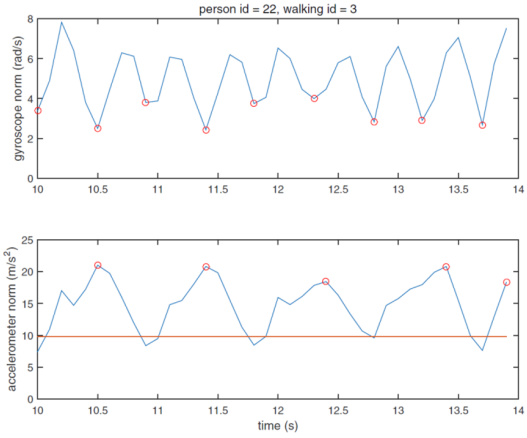

(c) large arm swing

Figure 5.12: Preliminary peak detection algorithm applied to low-pass filtered gyro and accelerometer norm signals.

Table 5.4: Estimated person-independent parameters

	a	**b**	**c**	**d**
Values	0.1569	0.3769	0.1572	0.3761

peaks which happen due to large arm swings. Figure 5.13 shows how Kalman filter recovers those peaks. The vertical lines in the figure represent the walking step times. It can be seen that the peaks are detected even if they are missed by the preliminary detection algorithm.

5.4.4 Distance and Velocity Estimation

The Kalman filter outputs the peak times during walking. These peak times are then used to estimate the distance and velocity using the models that is introduced in Sections 5.3.5 and 5.3.6. Using the training data collected from the 25 subjects (each walked 6 times), we generated 150 data sets for both velocity and distance. Each of the data sets includes N data point where N is the number of steps in each of the trials (Equation 5.25). Then the model parameters (a,b,c,d) were estimated using Equation 5.30. Walking distance for each step is measured using the foot-worn inertial sensors.

We computed the person-independent parameters from all the 25 subject walking data based on the step length (L), step duration (T) and measured average velocity for each trial. Figure 5.14 shows the correlation between L and inverse of T for all the collected data points. As mentioned in the methodology of this Chapter, the walking velocity has a correlation with the inverse of the step duration which is given by 5.24. Figure 5.15 shows this correlation for the given measured data points. For person-dependent parameter estimation, we will have a unique model for each of the subjects in which only the data from that subject is used to estimate a and b. Table 5.4 shows calculated person-independent parameters for both distance and velocity.

Using person-dependent and person-independent parameters, the walking distance

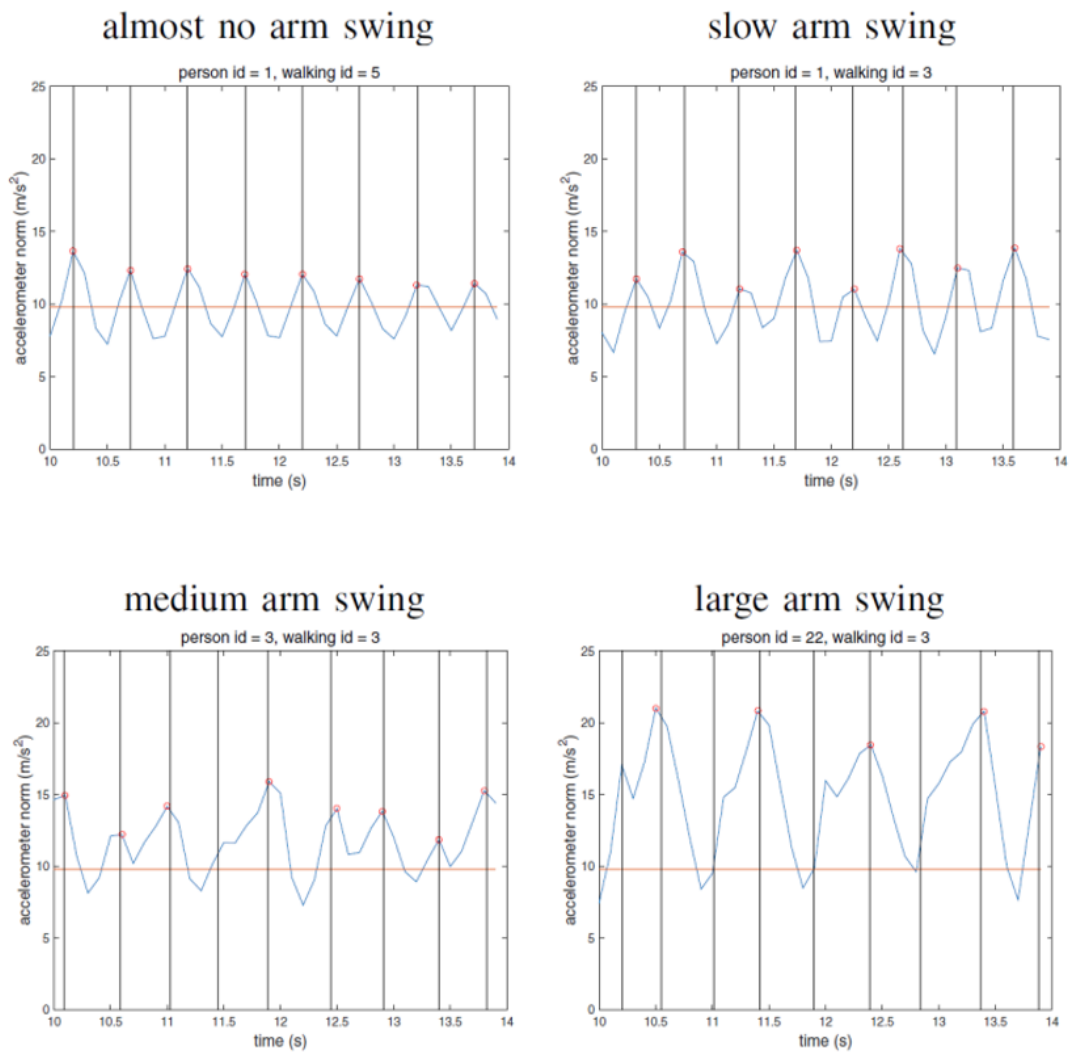

Figure 5.13: Walking step time estimation by the Kalman filter (vertical lines): the missing peaks are restored by the filter in large arm swings.

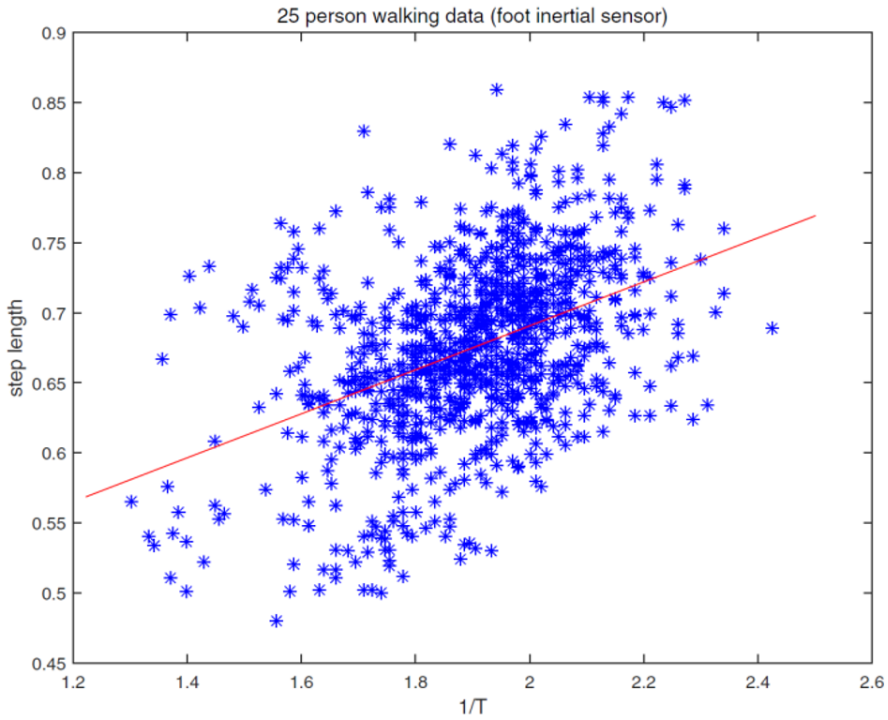

Figure 5.14: step length (L) and inverse of walking time ($1/T$) relationship: The curve parameters a and b are estimated to be 0.1569 and 0.3769 using the least square method.

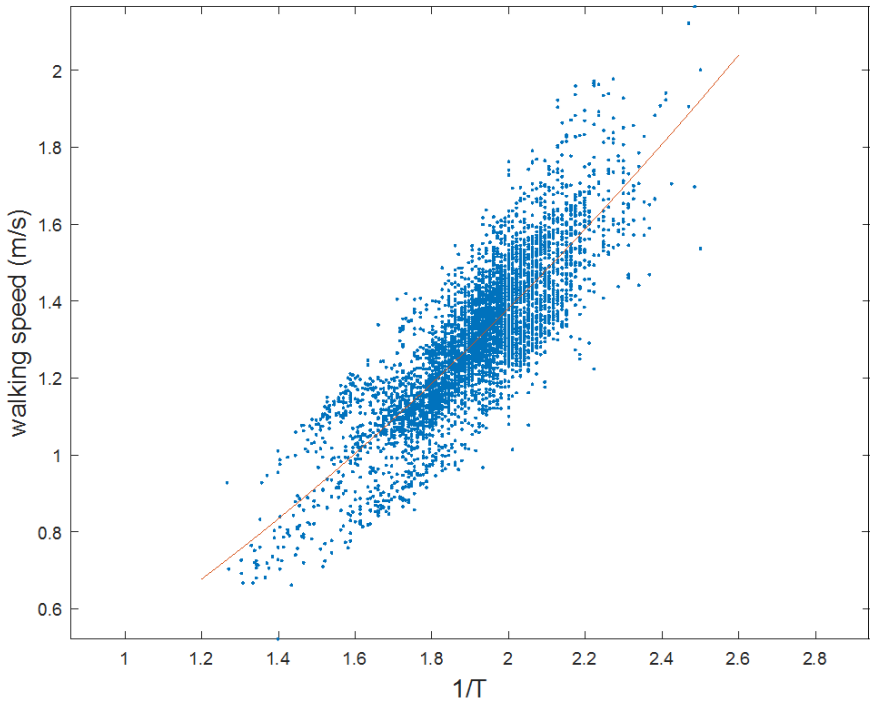

Figure 5.15: Walking velocity (V) and inverse of walking time ($1/T$) relationship: The curve parameters c and d are estimated to be 0.1572 and 0.3761 using the least square method.

Table 5.5: Walking Distance Estimation for all Walking Modes

	Person-Independent		**Person-Dependent**	
Walking ID	Mean	Standard Deviation	Mean	Standard Deviation
1	50.6	2.9	50.7	1.7
2	53.1	4.7	50.7	2.8
3	47.3	3.2	48.5	1.7
4	50.1	3.4	50.1	1.1
5	49.9	3.4	49.9	1.5
6	49.5	3.2	49.7	1.9
total	**50.1**	**3.9**	**49.9**	**1.9**

for all the subjects in different walking modes (given in Table 5.3) is estimated and given in Table ‘5.5. As you can see the standard deviation reduces from 3.9 to 1.9 over a 50 meter distance when we use the person-dependent parameters. Similar estimation was done for velocity using Equation 5.24 in which the person-independent and person-dependent walking velocity standard deviations are calculated to be 0.1009 and $0.0630 m/s$ respectively.

The model was generated based on the training data collected from the 20 subjects. For the testing, we asked 10 subjects outside the training set to perform a velocity test. The subjects are first asked to walk a 66 meters distance with their normal (preferred) speed uniformly. Then they were asked to walk with a speed that they consider slow and on the third run with a fast pace. Table 5.6 shows the results for the estimated velocity and the precision for each of the speed scenarios. The reported velocity values are the average over all the subjects for each speed scenarios, estimated and actual. As can be seen the average precision for all the scenarios is 91.7%.

Table 5.6: Walking Velocity Estimation Results

Walking Mode	Actual Velocity(m/s)	Estimated Velocity(m/s)	Precision
1-Normal	1.222	1.216	91.25
2-Fast	1.323	1.284	90.79
3-Slow	1.060	1.017	93.11

Table 5.7: Gait Symmetry Estimation Results

Walking ID	Mean	Standard Deviation	Min	Max
1	0.85	0.74	0.049	2.9
2	1.26	1.05	0.029	4.5
3	1.38	1.29	0.007	5.98
4	0.73	0.56	0.053	1.82
5	0.98	0.89	0.026	3.76
6	0.89	1.22	0.020	5.61
total	0.89	0.96	0.03	4.1

5.4.5 Gait Symmetry Estimation

As mentioned in part 5.4.6, symmetry index is calculated based on the step duration for left and right legs using Equation 5.26. Table 5.7 provides the symmetry estimation results for all the 6 different walking types over the 25 subjects.

As can be observed from Table 5.7, the symmetry index numbers are very small for all the different walking modes which is expected due to the fact that all subjects are healthy. However, the index is larger for slow and fast walking modes compared to the normal walking mode which accommodates with the fact that people are expected to walk more symmetric when they walk in their preferred walking speed. In addition, one can observe that walking symmetry is worse when the subject caries a briefcase (walking modes 5 and 6).

Table 5.8: Walking distance estimation using person-dependent parameters (Unconstrained Least Square)

Walking id	mean	Standard deviation	Maximum Error (m)	Minimum Error (m)	Calibration data (walking id)
6	49.7	1.9	52.6	42.6	[1 2 3 4 5]
	49.6	2.2	53.1	42.3	[1 2 3 4]
	49.5	2.9	53.8	41.2	[1 2 3]
	49.3	3.1	55.2	41.4	[1 2]
	49.9	2.8	53.2	41.3	[2 3]
	48.5	4.0	53.4	35.7	[1 3]
	51.9	8.7	82.8	46.4	[1 4]

5.4.6 Constrained Person-Independent Calibration

Since each person has different walking characteristics, it is not surprising to expect that person dependent parameters a and b would give more accurate walking distance estimation. For each person, a and b are estimated using the unconstrained least squares (Equation 5.29). In the calibration process, a and b are estimated for each person using some of walking data other than walking id 6. Then the calibrated person dependent a and b are tested on the walking id 6 data. The result is given in Table 5.8. The last column shows walking data used in the calibration process. In the second row, [1 2 3 4 5] means that walking data 1, 2, 3, 4 and 5 are used in the calibration of a and b. The standard deviation 1.9 is significantly lower than 3.2 (person-independent results in Table 5.5), which shows person dependent parameters give more accurate walking distance estimation. In Table 5.8, we can see inaccurate parameter estimation when too few walking data are used in the calibration. For example, in the calibration using walking data 1 and 4 (last row), the standard deviation of the walking distance estimation is $8.7m$, which means a and b are not accurately calibrated.

To avoid inaccurate parameter estimation, we applied the constrained quadratic op-

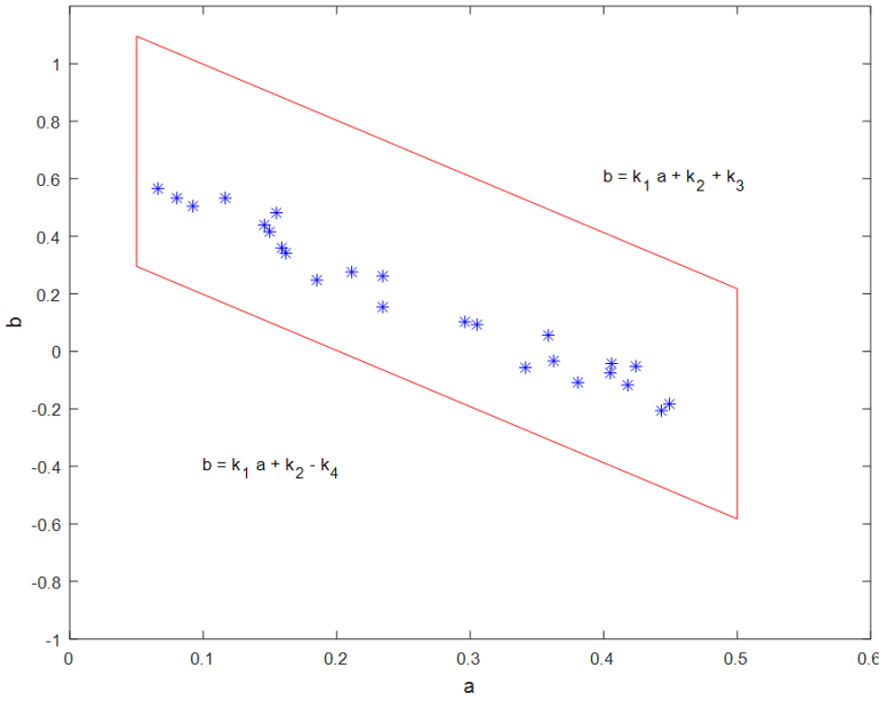

Figure 5.16: Person dependent a and b for 25 subjects computed using foot inertial sensor data.

timization (Equations 5.29 and 5.31) to find a and b. This algorithm is based on the observation that (a,b) pair can only exists inside the quadrilateral region in Figure 5.10. To show this, person dependent (a,b) parameters are computed using foot inertial sensor data for 25 subjects. The (a,b) pair for 25 subjects are plotted in Figure 5.16. We can see that (a,b) pair exists in the region defined by 5.31, where:

$$k_1 = -1.9512, k_2 = 0.6932, k_3 = 0.5, k_4 = 0.3, a_min = 0.05, a_max = 0.5.$$

The walking distance estimation result using the constrained quadratic optimization is given in Table 5.9. When five or four data are used for the parameter calibration, there is no improvement in the estimation accuracy. However, there is large improvement in the accuracy when fewer data are used. For example, the standard deviation is 2.1 for the last row while the standard deviation in Table 5.8 is 8.7.

In Figure 5.17, walking data used for the calibration are plotted, where each '*' symbol is walking data 1 to 5 obtained from a person with person id 23. The red circled

Table 5.9: Walking distance estimation using person-dependent parameters (constrained Least Square)

Walking id	mean	Standard deviation	Maximum Error (m)	Minimum Error (m)	Calibration data (walking id)
6	49.7	1.9	52.6	42.7	[1 2 3 4 5]
	49.6	2.2	53.1	42.4	[1 2 3 4]
	49.5	2.4	53.8	42.1	[1 2 3]
	49.1	2.8	55.2	41.4	[1 2]
	49.9	2.3	53.2	42.5	[2 3]
	49.4	2.5	53.4	42.5	[1 3]
	49.4	2.1	54.7	44.2	[1 4]

'*' symbols represent walking data 1 and 4. If we try to obtain a and b using the unconstrained least squares, the estimated parameters are not accurate as can be seen in Figure 5.17. With this parameter, the estimated walking distance (walking id) is 82.8m, which is the worst case in the last row of Table 5.8. When the constrained least squares method is applied, the estimated line is more accurate as indicated in Figure 5.17. With this parameter, the estimated walking distance (walking id) is 50.7m. Thus we can clearly see the benefit of the constrained optimization when the number of walking data is small.

Finally, the walking distance estimation results using person dependent parameters (constrained least squares) are given in Table 5.10. For each walking mode, the parameters are computed using the remaining data.

For example, walking id 2, 3, 4, 5, 6 data are used to compute the parameter and the distance estimation is tested on walking id 1 data. The total standard deviation is 1.9, which is significantly smaller than 3.9 (the person independent result in Table 5.5).

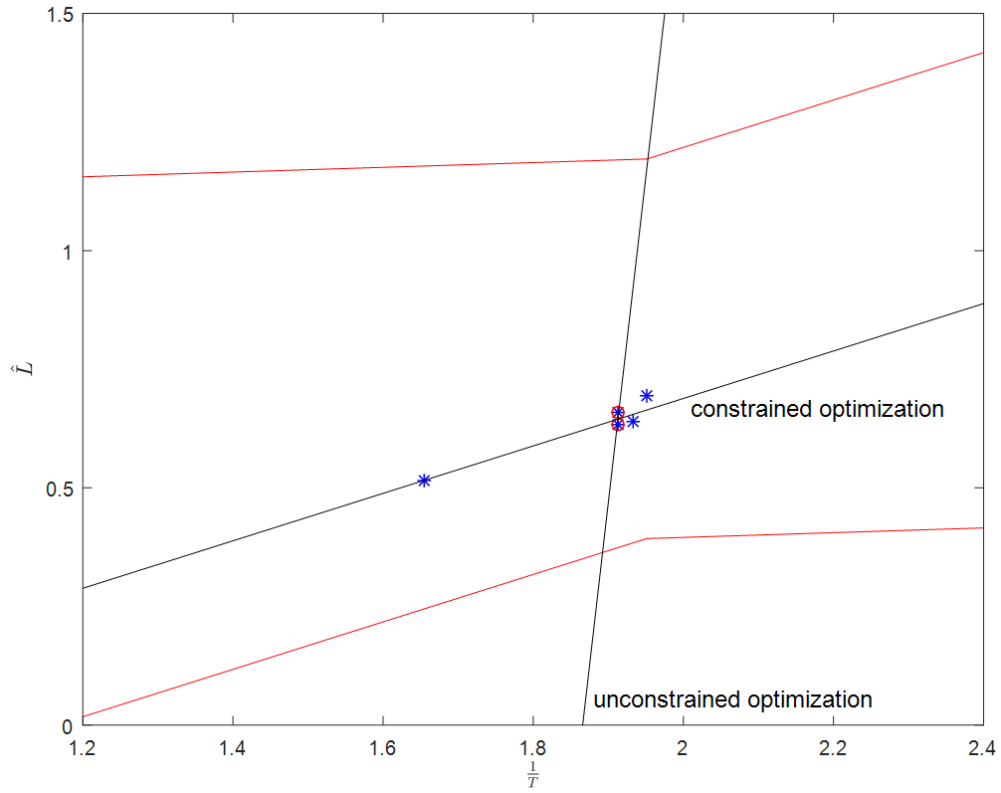

Figure 5.17: Calibration results of unconstrained and constrained optimization (persond id = 23, calibration data [1,4]).

Table 5.10: Walking distance estimation using person-dependent parameters (constrained)

Walking ID	Mean	Standard Deviation	Min	Max
1	50.7	1.7	47.2	54.0
2	50.7	2.8	44.7	49.5
3	48.5	1.7	43.7	51.4
4	50.1	1.1	47.3	52.2
5	49.9	1.5	46.2	52.5
6	49.7	1.9	42.7	52.6
total	49.9	1.9	42.7	59.5

5.5 Conclusion

This Chapter presents a robust gait quality estimation algorithm for wrist-worn platform. The algorithm analyzes the inertial sensor data (accelerometer and gyroscope) of a Smartwatch to determine the gait parameters from the complicated patterns of walking signal. A complete description of this complex pattern (which is due to combination of arm swing and leg movement) is given in this Chapter. The main contribution of the Chapter though, is the robust peak detection algorithm that identifies each step event and the step duration for each event. A combination of 5-point peak detection algorithm and a Kalman-filter-based peak restoring algorithm is employed to estimate the step duration. The Kalman filter performs based on the output of the defined state diagram which stores the current state of the mode of the walking. Gait parameters such as the gait distance, walking velocity and gait symmetry are then estimated based on their relationship with step duration. To identify this relationship, we collected walking data from 25 subjects, each performing 6 times of 50-meters walking tests for different walking modes and used least square error minimization algorithm. Unconstrained optimization resulted into promising distance estimation with standard deviation of $3.9m$

and $1.9m$ for person-independent and person-independent calibration. These numbers are found to be $0.1009m/s$ and $0.063m/s$ for velocity estimation. Walking symmetry is calculated for all the different walking modes using a symmetry index which found to the most informative. It was observed that walking symmetry is better in preferred walking speed mode compared to slow and fast walking. Moreover, the symmetry is poorer when a briefcase is carried. Constrained quadratic optimization was also used as well to minimize the walking distance estimation error. When the number of walking data is small, it is shown that the constrained optimization gives significantly better results (the estimation error standard deviation is less than a quarter of that of unconstrained optimization). It is interesting for the next step to apply the parallel asynchronous HMM or energy-based approaches to our raw sensor inputs and observe the accuracy results [106].

CHAPTER 6

Post Processing to Improve Activity State Recognition

6.1 Introduction

In Chapter III, we introduced a smartwatch-based system for tracking cancer and frail patients in order to prove the feasibility of this system for posture tracking published in [68]. There, we explained the power of a wrist-worn device in detecting the sit, stand and lie ADLs. As we discussed in Chapter I, another significant ADL is gait (including walking, running, jogging etc.) which was the focus of this dissertation in Chapter V. There we proposed using kalman filter to mitigate the arm swing noise issue. In Chapter IV, we investigated the usage of contextual information to improve the accuracy of posture detection. This chapter serves as another effort to improve the recognition accuracy of wrist-worn systems for both gait and posture when it comes to issue of unwanted hand motion.

In this chapter, we persuade using a two-layer classification. We intend to show the second level of algorithm can be effective to improve inference for long-duration activities such as sitting, standing, lying and moving which we named as activity state in this dissertation. Detecting these long-duration activities using classic machine learning algorithms is proven to depict a better results when longer sliding window size is selected. However, using large window size is not suitable when a mix of both short-duration and long-duration activities is to be considered. Shoaib et al tried to analyze 13 activities including repetitive ones (e.g. walking) and non-repetitive ones (e.g. smoking) and realized different activities require different window sizes in the sliding window algo-

rithm for optimal detection [107]. For example, for long-duration moves such as sit, stand and walk, F-score results were 90, 95 and 95% respectively using window size of 30 seconds. However, the score declines to 79%, 88% and 76% when a window size with 5 seconds duration is used. In a similar effort, Dey et al used logistic regression to infer sit, stand, lie, walk, run and dance activities and reported 88.4% overall accuracy for 10 second window size [56]. Similarly, in a recent work by Weiss et al, 10 second window size was picked and 85%, 96% and 80% accuracies for sit, stand and walk activities were achieved [58]. However, for short-duration activities, accuracy results were relatively poor and the overall accuracy was 70% for 18 activities. It is inferred that; long-duration activities will be better detected when a bigger sliding window size is used, but at the cost of reduced accuracy in detecting short-duration moves such as pointing, grabbing and transition moves. Having a dynamic window-size can resolve this challenge although this adds to the complexity of the system as the system needs to constantly search for a signature based upon which the window-size should change.

Another issue that makes the aforementioned results somewhat unreliable in practical situations is the fact that out-of-the-lab situations, usually bring a high amount of unwanted hand motions to the picture. These hand motions lead to misclassification of activities and degrade the accuracy when the model is only based on in-lab training data. In our previous work, where we investigated the feasibility of posture tracking (sit/stand/lie states) using Smartwatch, this issue was clearly observed [68]. The model was built using transition moves between the states. Model was generated from the in-lab collected data which led to 93% F-measure in cross-validation. However, the results were considerably worse when the model was tested in the field due to unwanted hand motions. This work uses [68] as baseline and tries to mitigate this issue by making the activity detection model robust for in-field testing using the same window-size as was used in [68] while applying a post-classification algorithm to improve the results.

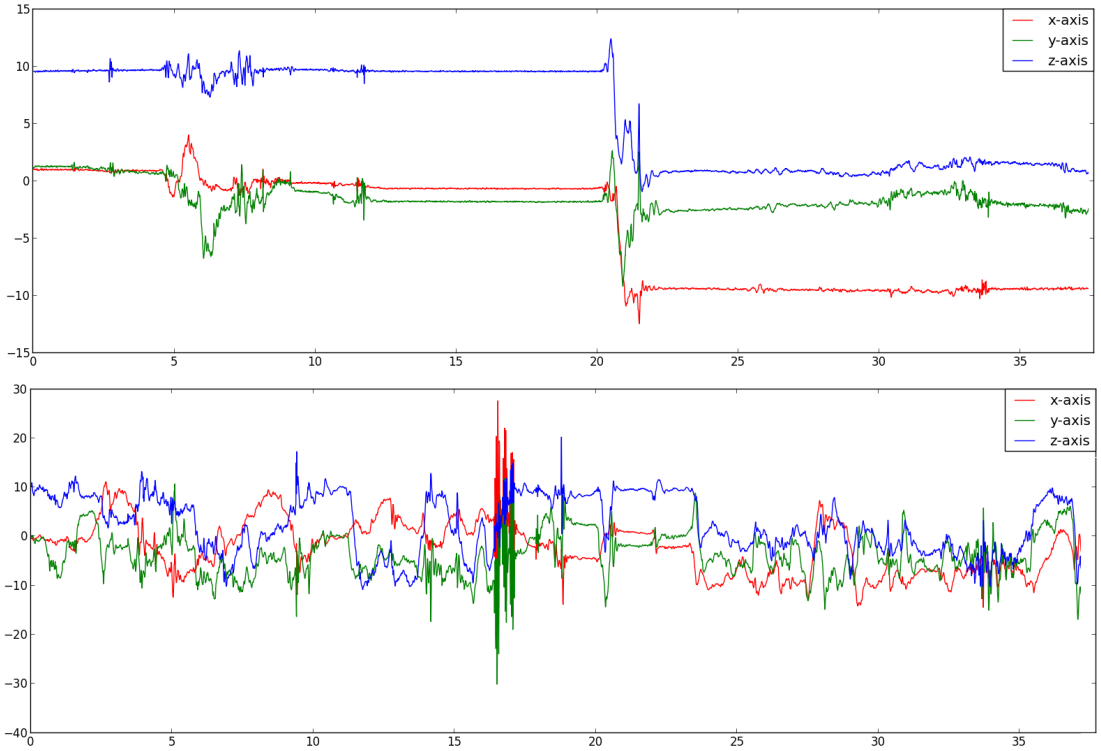

Figure 6.1: Unwanted hand motion effect on accelerometer data.

6.2 The Proposed Two-Level Algorithm

Hand orientation is very much possible to know using the acceleration vectors of a wrist-worn device. This is because acceleration signals carry the gravity information. So while standing or sitting still, the accelerometer data is good enough to distinguish the two. But when hand motion is added, accelerometer value changes dramatically, making sit versus stand distinction very hard. This is explained in Figure 6.1, where in the first 20 seconds, the subject is sitting still and then standing still in the next 20 seconds (top). In the bottom figure, subject does the same, but he uses his hand to perform motions that typically can happen while sitting and standing.

6.2.1 Two Level Algorithm Idea

The aforementioned issue makes the detection of these classes very challenging. A person who is sitting can produce the same hand motion as to when standing. Although in a larger time scale, the average orientation of the hand should be different for sitting and standing (unwanted hand motions could be ignored). Following this train of thought, we propose looking at the data in a longer period of time. However, this should not be done through increasing the window size as mentioned before. Instead we propose a two-level activity recognition scheme where we apply the classic machine learning algorithm on short duration windowed data in the first step. Then, we apply a second algorithm to correct for the misclassification occurred due to unwanted hand motions in the first layer.

6.2.2 Data Collection and System Design

In order to verify the proposed algorithm, we collected data from 20 healthy subjects. Samsung Gear S3 Smartwatche was used to collect the wrist Accelerometer and Gyroscope data with the sampling rate of 100 Hz. Subjects were asked to wear the Smartwatch on their left hand for consistency. The data collection protocol is as follows: 8 minutes of "Sitting", 8 minutes of "Standing", 8 minutes of "Moving" (including walking, ascending and descending stairs), 10 times of "Sit to Lie" and 10 times of "Lie to Sit" transitions. The transitions were collected to replace the state of "Lying". This is due to the fact that hand orientation in lying is subject to dramatic change based on subject's sleeping habits. At very best, lying data will look very similar to sitting data.

A very important fact in our data collection that distinguishes this work and our previous work in [68] (and so many other similar studies) is this: In this study, the subjects are suggested to use their hand occasionally to imitate all the hand motions that can happen in real-life situations while being in sit, stand and moving states. As we defined earlier in the first Chapter of this thesis, these activities are considered "activity

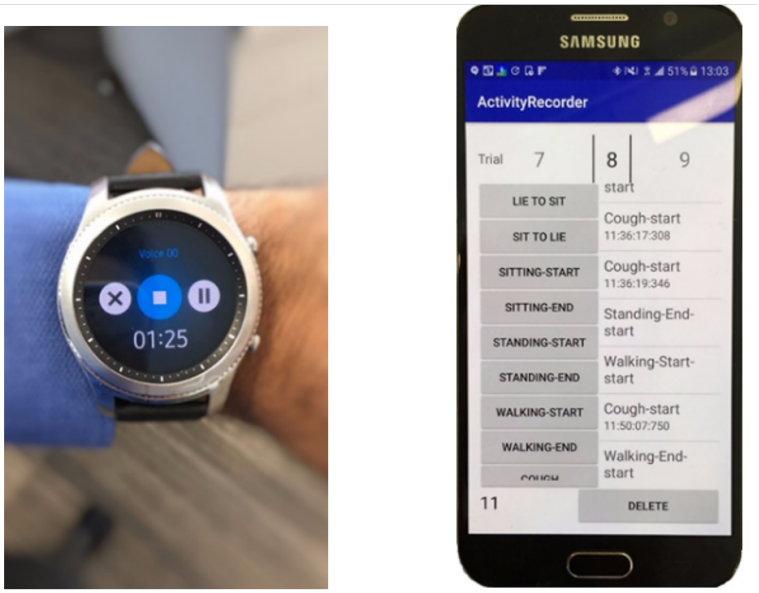

Figure 6.2: Samsung Gear S3 and Galaxy S6 for Data Collection and Annotation Respectively.

states" because they represent the state the person is in while other activities could take place within that state. For example, some of our subjects were moving their hand while talking in sit or stand modes while others occasionally used their phones. This provides us with a dataset which looks very similar to in-field data. A phone app was made for Samsung Galaxy S6 to annotate the start and end timestamps of each state. Figure 6.2 shows the phone and watch app user interface.

6.2.3 Data Pre-Processing

Accelerometer and gyroscope data are passed through a low-pass filter to remove high-frequency noise. A sliding window algorithm with window size of 4 seconds generates chunks of data to be processed. This window size was chosen to facilitate the transition moves which were 4 seconds on average. A total of 108 features were implemented for accelerometer and gyroscope data including both time and frequency domain features. More details on the features can be found in [68]. The features for all the data chunks

Table 6.1: Confusion Matrix for Unbalanced Data

Actual/Predicted	**Sit**	**Stand**	**Move**	**Sit to Lie**	**Lie to Sit**
Sit	4829	151	81	14	16
Stand	374	4193	222	2	6
Move	18	81	4540	0	1
Sit to Lie	61	19	30	85	10
Lie to Sit	42	19	37	14	95

are generated by the sliding window, forming a feature table that is imported to the learning machine to generate the model.

6.2.4 Random Forest as the First Level

Our data for transition moves is limited to 200 instances for each transition. But, the activity states' dataset can be considerably larger depending on how frequently we sample in the sliding window over the 8 minutes for each subject. For example, applying window size of 4 seconds with 50% overlap in the sliding window led to 14540 data points for sit, stand and move states. Applying random forest algorithm on this unbalanced dataset results into 91.8% overall precision for classification. Although this seems to be amazingly high, by looking at the confusion matrix (Table 6.1) we see that the overall precision is only high because of the high number of samples in activity states classes. So the model is biased toward those classes, resulting in low recall values for transition classes (41 and 46%) which is not desirable.

In order to make the model reliable, we applied random down-sampling which randomly samples down the data for sit, stand and move labels to make the dataset balanced for all the labels. Table 6.2 show the result of applying different machine learning algorithms on the balanced data. The classification algorithms were applied to the dataset after applying correlation-based feature selection algorithm (CFS) that was used

Table 6.2: Classification Results for Balanced Data From Selected Algorithm

	Precision	**Recall**	**F-measure**	**ROC Area**
Random Forest	**86.7**	**86.4**	**86.5**	**97.7**
SVM-PUK	86.1	85.7	85.5	94.3
Neural Net	82.8	82.7	82	95.8
Logistic Regression	82.8	82.7	82.8	96.5

Table 6.3: Confusion Matrix for Unbalanced Data

Actual/Predicted	**Sit**	**Stand**	**Move**	**Sit to Lie**	**Lie to Sit**
Sit	257	11	2	17	12
Stand	24	230	12	8	8
Move	0	4	259	6	7
Sit to Lie	13	1	1	177	13
Lie to Sit	10	3	6	14	174

to avoid overfitting. Total of 35 features were selected eventually to feed the algorithm.

As can be seen from this table, random forest provides us with the best result, although the precision is about 6% lower than for unbalanced dataset. Table 6.3 shows the confusion matrix for the balanced data. As it appears, the recall values for transition moves improved considerably (86.3 and 84.1%) which means the model is much more reliable, although the overall precision is worse comparing to unbalanced data.

6.2.5 Majority Voting as the Second Level

Although the results of the first level of the algorithm seems promising, it can still be misleading when the in-field data is used for testing. The activity state classes can carry a lot of unwanted hand motion noise which degrades the results. In order to avoid this decline, we propose applying a second level of algorithm to post-process the predicted

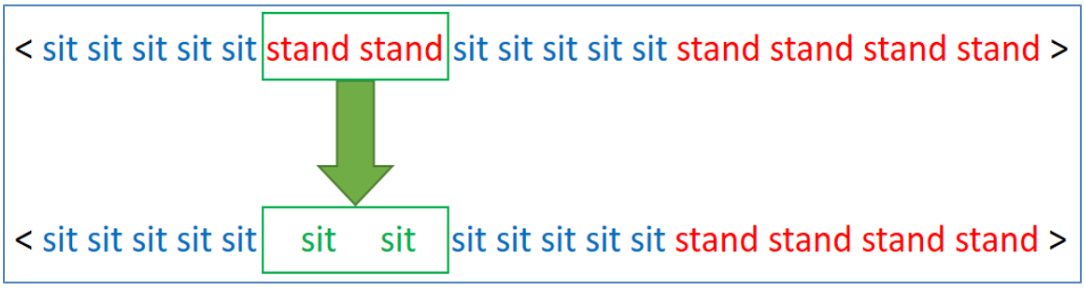

Figure 6.3: Majority Voting to recover misclassified labels.

labels generated by the first level. The theory behind the 2^{nd} level can be seen in Figure 6.3. If the first sequence in Figure 3 is the output of the level-one algorithm and the samples are not far apart (less than a second), then it is natural to consider the first two "stand" labels as misclassification due to hand motion. However, this cannot be said for the rest of the "stand" labels in the first sequence because perhaps the person stood up.

6.3 Recognition Improvement Due to Second Level Algorithm

To apply this concept, we implemented a sliding window that goes through the labels generated by the first algorithm and applies a majority vote on the labels within that window, only for activity state classes (the transition classes are not subject to modify). To verify this algorithm, we used the balanced-data model as training and a portion of data from activity state classes that is unseen by the model as test. This is because this idea of 2nd level is only reasonable for long-duration activities. Window size of 13 (consecetive instances) found to be optimal. Figure 6.4 shows the result of this post-processing. As can be seen, a lot of the glitches that happen because of misclassification due to unwanted hand motion can be suppressed. The numbers in y-axis represent sit, stand, move, sit-to-lie and lie-to-sit states respectively. Table 6.4 concludes the result of applying 2nd level algorithm on the data. Clearly classification results improve for sit, stand and move classes by applying the 2nd level (8% improvement in correctly classified samples). And this does not have any effect on the classification rates of

Table 6.4: Confusion Matrix for Unbalanced Data

	Precision	**Accuracy**	**F-Score**
Before Applying	92.7	86.7	89.9
After Applying	96	95.6	95.7

transition classes as they are not subjects for modification in the second layer.

6.4 Conclusion

General well-being of patients is a significant piece of information for clinicians dealing with elderly, cancer and frail patients. Amount of time they spend sitting, standing, lying and moving was assessed in this work to help provide that information. Smartwatch as the data collection module, provides convenience and robustness. Although, the task of inference is very challenging when it comes to in-field data due to unwanted hand motions issue. This work proposes a two-level classification architecture to resolve this issue. We show that using random forest combined with majority vote classifiers, the accuracy value improves from 87.6% to 95.6% (an 8% improvement) for the "activity state" classes (which are "sit", "stand" and "move" in this Chapter). This seems to be a reasonable solution to resolve low accuracy results of in-field data for a wrist-worn system in which data is polluted with unwanted hand motion.

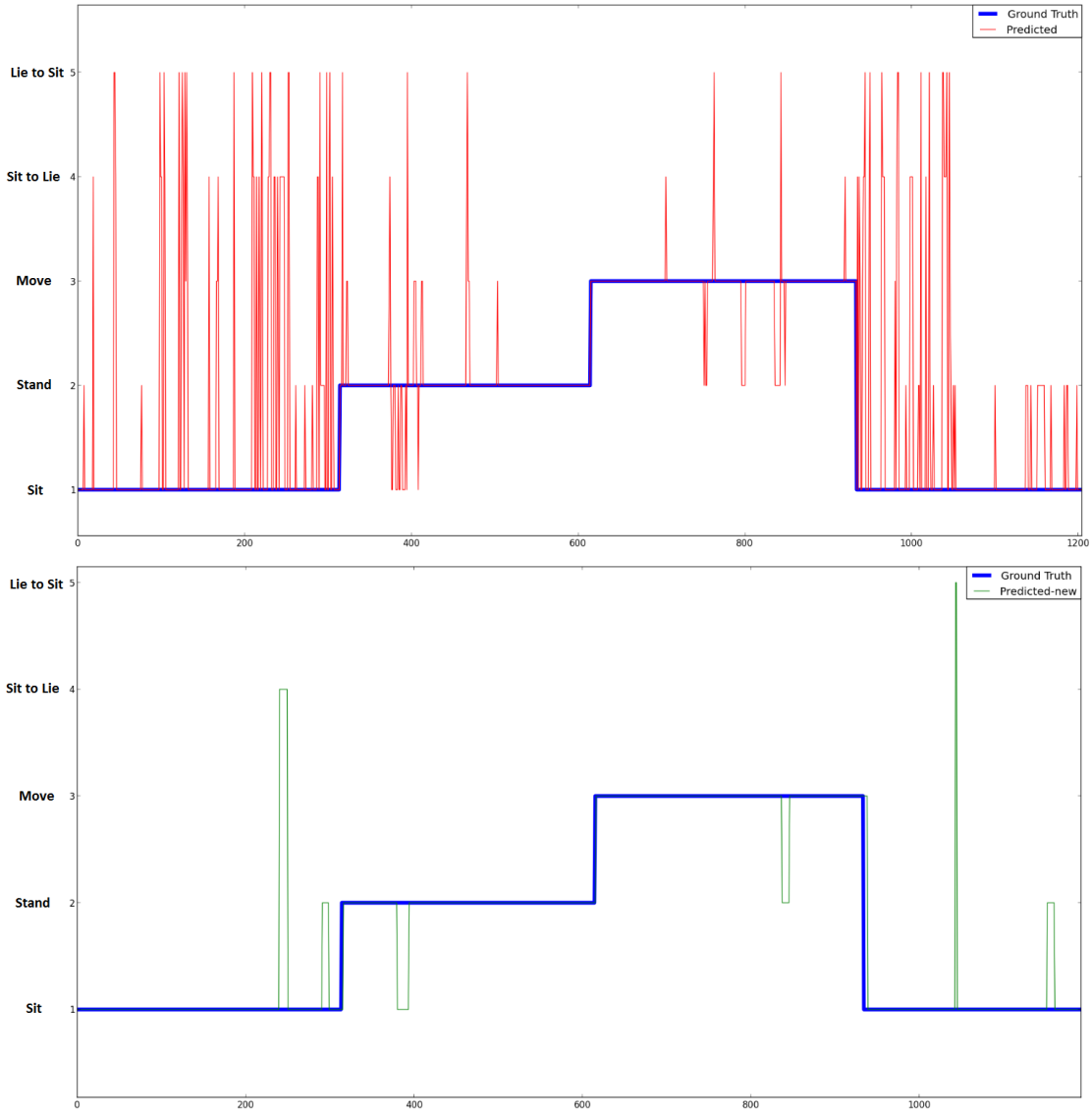

Figure 6.4: Predicted labels, before applying the second level (up) and after that (bottom).

CHAPTER 7

Beyond Activity State Recognition

With day-to-day advancement in fabrication technology, new sensors are added to the Smartwatch platform other than inertial sensors. This variety opens wrist-worn devices to be used for variety of applications, Also it enables improvement in learning from its data (due to increase in modalities of contextual information). In this chapter, we go over two of the important applications of Smartwatch: Medication Adherence and Blood Pressure estimation. Presence of inertial sensors on the wrist has enabled capturing hand motions which made researches thinking about implementing novel medication adherence algorithms. In first section of this chapter, we propose a novel adherence algorithm using the inertial sensors of the watch. Photoplethysmography (PPG) sensor of the watch has added a new piece of information to data that can be captured from them, enabling researchers to fantasize about predicting different vital signs from it. In the second part of this chapter, we propose a method to predict the continuous arterial blood pressure from the PPG data using deep recurrent neural network.

7.1 A Smartwatch-Based Medication Adherence System

7.1.1 Introduction

It is well established that poor adherence to prescription medication can limit the benefits of medical care and compromise assessments of treatment effectiveness. It has been estimated that lack of adherence causes approximately 125,000 deaths in the United States, and costs the health care system been $100 and $289 billion pear year [108].

A significant body of research has been conducted to improve adherence to prescription medications through various interventions. These techniques vary tremendously from reminder-based systems, simplified pill packaging, positive reinforcement, financial incentives, and counseling. However, these systems typically suffer from high complexity, user burden, and inaccurate estimations of adherence [109]. One survey of major interventions concluded that less than half of evaluated interventions were associated with statistically significant increases in adherence [110].

In recent years, a greater emphasis has been placed on the role of technology in detecting non-adherence to medications. However, these digital system suffer from several substantial limitations. Though they employ sensors to perform activity recognition, it is not always possible to accurately estimate adherence by recognizing a single action such as opening a pill bottle, or removing a capsule.

Recently, Smartwatches have become widely available on the commercial market. These devices contain a multitude of sensors including but not limited to: a microphone, camera, accelerometer, and gyroscope. Due to the ubiquity of watches, this technology can be used for various wireless health-monitoring applications discretely, with low user burden. Furthermore, from a user-acceptance standpoint, these systems have a clear advantage over other proposed solutions based on custom hardware such as the wrist-worn accelerometry proposed by Chen et al. in [111] or audio-based ingestion monitoring systems proposed by Sazonov et al. and Amft et al. in [112][113].

In this Section of this Chapter, we propose a system that estimates adherence of a user to gel-capsule-based medication using a custom Android application running on a Samsung Smartwatch. The activities that are detected are shown in Figure 7.2. Using on-board sensors, we can determine when a bottle is opened and a pill is retrieved. This is achieved through a combination of on-board peripherals including the tri-axial accelerometer and gyroscope. By employing several sensors to detect different actions, such as a system has the potential for higher accuracy than existing schemes, with no compromises on comfort and practicality. Furthermore, the proposed system can be

Figure 7.1: This figure shows the various ways in which a SmartWatch or similar wrist-worn device can be employed to detect medication intake and alert clinicians of low adherence.

used with any standard twist-cap prescription bottle, without requiring that each bottle to be equipped with sensors and wireless connectivity as in the case of the Vitality Glowcap [114].

This work is organized as follows. Section 7.1.2 outlines related work in electronic detection of adherence. Section 7.1.3 describes the major components of our proposed system. Section 7.1.4 describes the proposed algorithms. Section 7.1.5 presents the experimental setup, followed by results in Section 7.1.6 and concluding remarks in Section 7.1.7.

7.1.2 Related Work

7.1.2.1 Mobile-Phone Solutions

Several SmartPhone applications such as MyMedSchedule, MyMeds, and RxmindMe, provide advanced functionality for medication reminders. These applications issue reminders, allow users to manually enter their dosage information, and record when they

Figure 7.2: This figure shows the two motions associated with medication intake that are detected using the proposed SmartWatch-based system. In (A), the wrist motion necessary to twist the bottle cap open is detected using a tri-axial accelerometer. In (B), the act of turning the palm upward to pour medicine from the bottle is detected using a gyroscope.

have taken their medication[115]. Other works propose cell phone reminders and in-home technology to transmit reminder messages, but results are mixed [116].

7.1.2.2 Hardware Approaches

The work described in [109] describes a portable, wireless-enabled pillbox suitable for elderly and those suffering from dementia. Similar approaches for electronic detection and smart pill boxes have also been proposed [117][118][119]. These devices generally suffer from the same shortcoming: they cannot determine if the medication is ingested or simply removed and discarded. In another work, Valin et al. successfully identified medication adherence using a series of images and associated image processing algorithms [120]. Other works such as that by Huynh et al. [121] as well as Bilodeau et al. [122] propose camera-based systems for detecting medication adherence, with strong results. Very recent work by Chen et al. in [111] describes a system in which inertial sensors worn on the wrist are used for detection of gestures associated with medical

intake, based on a Dynamic Time Warping (DTW) algorithm.

The Vitality Glowcap is a wireless-enabled pill bottle that can report when medication is removed [114] using a cellular network, while a recent product from Amiko [123] is one of the few systems that can monitor the ingestion of medication directly, based on a smart-inhaler technology. Other notable technologies include the Smart Blister from Information Mediary Corporation [124], which can detect when medication is removed from a blister-packet. Lastly, our prior work in [125] explored the possibility of using inertial sensors on a necklace platform to detect medication swallows based on the movement in the lower throat during a swallow.

7.1.3 System Architecture

The SmartWatch application is capable of predicting if a pill has been swallowed using the on-board inertial sensors available on the Android SmartPhone. The application runs as a background service: data is collected and processed even while the user is interacting with other applications on the watch.

The hardware platform used is the Samsung Galaxy Gear SmartWatch running Android 4.2.1. Though the sample rate of the on-board sensors can be configured, a rate of 16.66 Hz was determined to be sufficient for activity recognition through experimentation.

7.1.4 Algorithm Design

In this section, we describe the algorithms running on the Android Service, which predict if medication has been ingested based on the recognition of two activities: (1) The bottle being opened while the SmartWatch is worn on the wrist by detecting the twisting motion of the bottle cap, and (2) the wrist being rotated for the palm to face upwards, in order to pour medicine capsules from the bottle into the secondary hand. Unless both of these actions are not detected within several seconds of each other, the

system considers that the medication has not been ingested. All results are based on data acquired from tri-axial accelerometer and gyroscope samples acquired at 16 MHz. Figure 7.2 shows the actions the proposed system was designed to identify.

7.1.4.1 Bottle Opening: Data Transformation

Figure 7.3 shows the waveforms acquired from the SmartWatch accelerometer for the X, Y, and Z-axis, which correspond with a bottle being opened nine times. Each bottle-opening event corresponds with a different peak, as shown in the figure. Successful identification of the event is dependent on analysis of the features of each peak in all three dimensions. Therefore, the data must be transformed to decouple the perturbations of the signal from the offset, and limit the effects of drift and noise. This new waveform, shown in Figure 7.5, provides a more objective representation of the features of a bottle opening event.

This signal transform is first achieved by generating a new waveform using a sliding-window average of the original data. The relevant equations for each axis are shown in Equation 7.1, in which β is defined as the window size. It was determined that 70 is an appropriate value of β, as significantly smaller values are too sensitive to minor fluctuations.

$$\begin{aligned} &\forall D \in \{X, Y, Z\}, \\ &\forall j \in D, \\ &\bar{D}(j) = \frac{1}{\beta} \sum_{i=j-\beta}^{j} D(j) \end{aligned} \tag{7.1}$$

After the moving-average representation of the data is generated, each point is then assigned a numerical value with respect to the average value in the previous window. This essentially removes the offset from the data and combats the effect of drift, while preserving the critical features of the original waveform. This is shown in Equation 7.2.

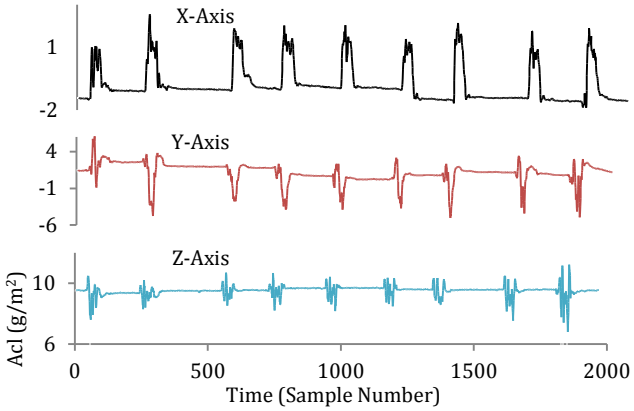

Figure 7.3: In Phase (1), the X, Y, and Z axis data is extracted from the accelerometer. This figure shows the accelerometer data that corresponds with an individual opening the pill bottle nine times, smoothed with a window size of 3 samples.

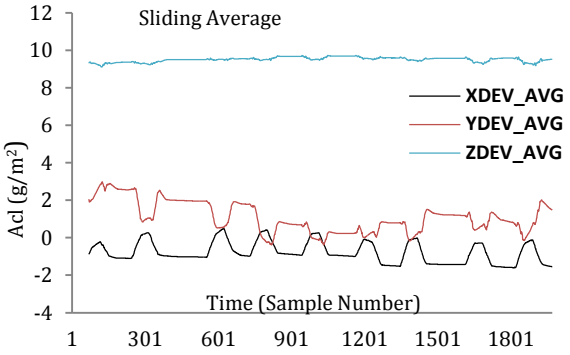

Figure 7.4: In Phase (2), the data corresponding with each axis of the accelerometer is converted to a sliding window representation, in which each point is the average of the 35 points that came before and after it. This step is necessary to remove the offset from the data and show relative changes in sensor data.

$$\begin{aligned} &\forall k \in D, \\ &\acute{D}(k) = |D(k) - \bar{D}(k)| \end{aligned} \tag{7.2}$$

The next transformation simply separates the continuous data into different peaks separated by spans in which the data is zero, based on a simple thresholding technique. This allows different instances to be more easily identified. The relevant equation is shown in Equation 7.3, and the corresponding waveform (with additional smoothing) is shown in Figure 7.6. The constant α refers to a predefined threshold for separating the different peaks. It was experimentally determined that an α value 0.5 g/m^2 of visually preserved the critical features of the waveform while removing noise during periods of inactivity.

$$\begin{aligned} &\forall n \in \acute{D}, \\ &\tilde{D}(n) = \begin{cases} 0, & \acute{D}(n) < \alpha \\ \acute{D}(n), & \acute{D}(n) \geq \alpha \end{cases} \end{aligned} \tag{7.3}$$

Subsequently, features from individual 'pulses' can be extracted, which each correspond with a different bottle opening episode. This is shown in Figure 7.7, which shows one individual pulse in the X axis. By performing a summation of each pulse, which is delimited by a value of zero as described in equation 7.3 as a result of the thresholding technique, a distinguishing feature can be extracted from each axis. The width of the pulse, once again delimited by zero, is a secondary feature that can used to improve classification accuracy.

7.1.4.2 Bottle Opening: Detection

Based on the previously collected features, we apply various constraints for the classification of each pulse, as shown in Equations 7.4. Figure 7.8 shows the distribution of

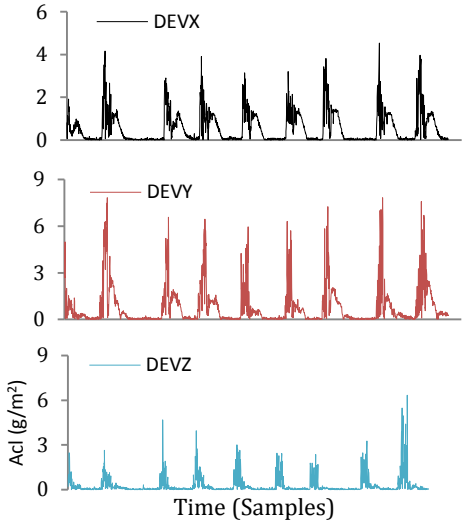

Figure 7.5: In Phase (3), the results from Phase (1) and Phase (2) are combined. The new waveforms show the variance of each data point relative to the sliding-window average obtained in Phase (2). This preserves the key features from the original waveform while removing the offset.

feature values such as pulse width for all three axes, and well as the area under the curve of each pulse, as users twisted the bottle cap during the initial phase of data collection. The observations that are made from the feature distribution associated with this activity are used to formulate the constraints for classifying an action as the opening of a bottle cap. Visually, it can be inferred that the data from the Y-axis of the accelerometer is weakly coupled with the act of twisting the bottle. However, the standard deviation of the X and Z axis data appears to show significantly less variation.

As Equation 7.4 shows, the first requirement is that the standard deviation of indices of the first nonzero values of the accelerometer data in each axis to be less than three, to reduce the effects of noise and drift. The remaining constraints are the widths of the X, Y, and Z pulses, which correspond with the overall duration of the bottle cap opening event. The bounds on the integral of acceleration (velocity) constrain the intensity of the motion based on what is typical for the action.

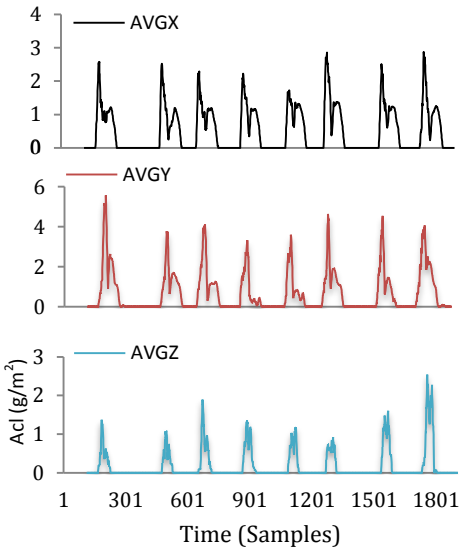

Figure 7.6: In Phase (4), data from Phase (3) is filtered to remove high frequency noise. Furthermore, values below a certain threshold are zeroed. This allows each bottle opening action to be a separate 'pulse', the width of which is a key feature indicative of the action being performed.

$$\begin{aligned} 30 < WidthX < 75 \\ 0 < WidthY < 80 \\ 10 < WidthZ < 80 \\ 60 < SumX < 1800 \\ 0 < SumY < 1200 \\ 20 < SumZ < 1600 \end{aligned} \tag{7.4}$$

Once it has been determined that the bottle has been opened with a high probability, the system makes a record of this event and begins detection of pill extraction.

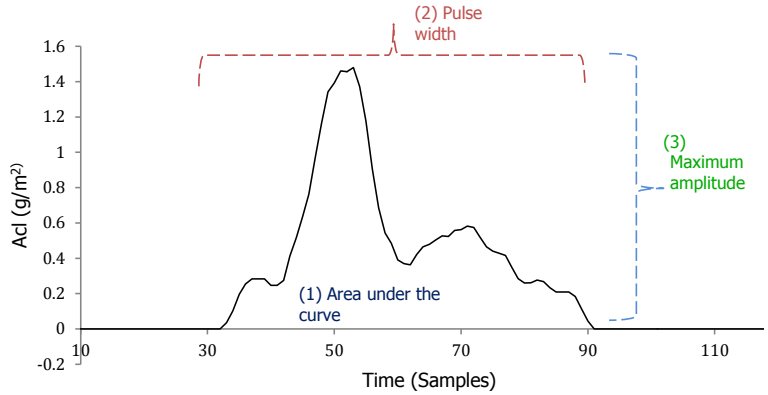

Figure 7.7: The output pulses from phase 4 can be analyzed based on several different features for activity recognition and classification.

7.1.4.3 Medicine Removal: Data Transformation

In the case of most twist-cap medication bottles, it is not possible to reach inside to retrieve the medication. Typically, once the bottle is opened, it is turned upside down and a medication capsule is emptied on the secondary hand. This requires that the individual turns their hand upside-down with their palm facing upwards for a brief period, as shown in Figure 7.2(B). If the SmartWatch is worn on the wrist of the secondary hand, this motion can be detected.

Data is acquired from the SmartWatch's built-in triaxial gyroscope at a rate of 16 Hz, which represent angular speed around the X, Y, and Z-axis in units of radians/second. The Android API provides output with built-in drift compensation algorithms, though raw data is also available. The gyroscope data can be integrated along each axis to provide an estimation of rotation in a given unit of time.

As in the case of the accelerometer processing used to estimate if the bottle cap is removed, the gyroscope data must be transformed for effective activity identification. Equation 7.5 shows the simple summation of the last β values acquired from the gyroscope. In this equation, x_n corresponds with the n_{th} sample of acquired data, and the same convention used for the Y and Z axis. The chosen value of β is 12 samples,

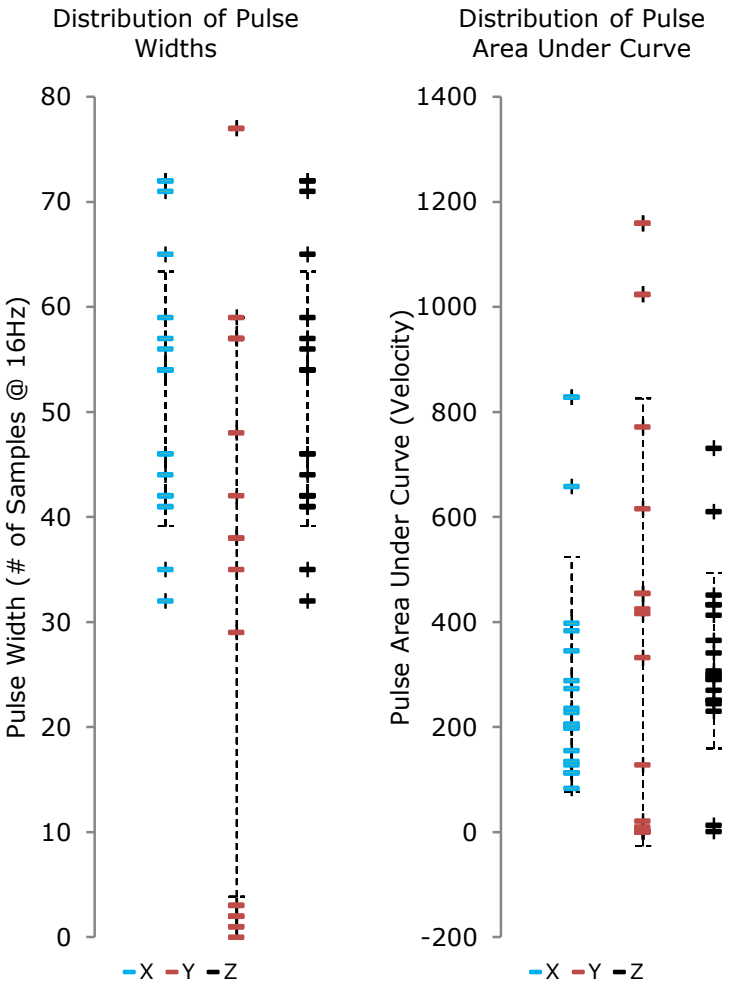

Figure 7.8: This figure shows the distribution of the collected features (pulse widths and area under the curve), based on collected data (twisting the bottle cap). An analysis of the clustering patterns for different features can be used to assign threshold values, in order to identify the action in question. The error bars correspond with one standard deviation. Larger standard deviations are typically associated with weaker features.

which corresponds with 750 ms of data at a 16 Hz sample rate. These values are selected based on the observation that most individuals will perform the hand motion in significantly under one second; longer sample rates would distort gyroscope data with extraneous movements and produce false positives.

$$\forall Sample_i \in \{Buffer\},$$
$$x_{sum} = \sum_{k=i-\beta}^{i} x_k$$
$$y_{sum} = \sum_{k=i-\beta}^{i} y_k \tag{7.5}$$
$$z_{sum} = \sum_{k=i-\beta}^{i} z_k$$

7.1.4.4 Removing the Medicine: Detection

Detecting that an individual has poured the medicine into his secondary hand is relatively simple, after the preprocessing shown in Equation 7.5. The detection of this movement does not imply that any medication was removed- simply that the palm was turned to face upward. The constraints on which this movement is detected are shown in Equation 7.6. First, some delta of time ΔT must have elapsed since the last recorded event, to prevent duplicate records of the same event. The absolute value of the movement in the y and z directions must also be less than some arbitrary threshold, to ensure that random hand movements are not considered. Lastly, x_{sum}, the movement around the x axis over the last 12 samples (16 Hz) in radians/second, must be less than the threshold of -28, or greater than 28, depending on which arm the watch is worn. Experimentally, it was determined that lower threshold values could not differentiate relatively minor turns of the wrist to the full action of turning the palm upward that is required to pour medication from the bottle into the hand.

$$\begin{aligned} \Delta T &> 1s \\ |y_{sum}| &< 5 \\ |z_{sum}| &< 5 \\ x_{sum} : &\begin{cases} < -28, & LeftHanded \\ > 28, & Right\ Handed \end{cases} \end{aligned} \tag{7.6}$$

7.1.5 Experimental Procedure

Training data was collected from five subjects between the ages of 21 and 25, all of which were left handed. The subjects wore the watch on their left hand in their preferred configuration, and were asked to open the pill bottle using the hand on which the watch is worn. The results were used to formulate the algorithm constraints, which were then tested on the remaining subjects.

7.1.5.1 Gesture Recognition

Twelve subjects were asked to perform several activities while wearing the SmartWatch including walking, opening a medicine bottle, and opening a bottle of water.

The data collection occurred in two separate sessions to increase the diversity in motion patterns. The medicine bottle used was a standard prescription variety containing empty gel capsules (Size 00). As in the case of most standard prescription bottles, opening the lid requires the application of downward pressure while twisting the cap in the counter-clockwise direction. However, the subjects used in the study were not given any instruction on how the bottle was to be opened, in order to avoid influencing activity patterns. After opening the pill cap, the subjects were asked to pause briefly for a period of three seconds, before pouring the medicine out of the bottle.

7.1.5.2 Survey of Habits

In order to design an appropriate activity recognition scheme, it is necessary to validate various assumptions about how people take their medication, as well as their opinion on Smartwatch devices. An online survey was conducted with a total of 221 responses, in which various questions were posed with respect to how individuals feel about wearing a Smartwatch, on what hand they would typically wear it, and how they retrieve and ingest a medication capsule.

7.1.6 Results

7.1.6.1 Gesture Recognition Results

The classification results are shown in Table 7.1 and 7.2. The results indicate that while accuracy of wrist rotation detection is very high as a result of the algorithm simplicity of the data processing, the false-positive rate of pill cap opening detection is very high. This design trade off is necessary to ensure that nearly all real pill opening events are detected; false positives will be filtered out in the second stage of the algorithm. Table 7.1 shows that despite very low precision across categories, the recall for the action of 'medicine bottle opened' is very high. The remaining false positives are filtered out in the next stage of the algorithm shown in Table 7.2 in which the precision of the 'other' category, which comprises the other four listed actions, is 100%.

7.1.6.2 Patterns in Medication Ingestion: Survey Results

From the survey based on responses from 221 individuals, 86% claimed to be right handed. A total of 76% of individuals claimed that they generally would wear a watch on their left hand, with an additional 19% who preferred to wear the watch on their right hand. The remaining 5% of those surveyed expressed no preference.

The next question in the survey asked subjects how they felt about watches in gen-

How would you open a typical twist-cap bottle?

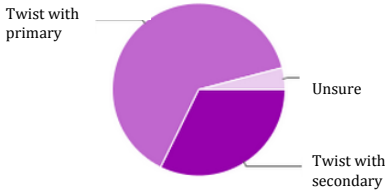

Steady bottle with primary hand, twisting with secondary.	32%
Steady bottle with secondary hand, twisting with primary.	63%
Unsure	4%

What would you typically do after removing the cap of the bottle?

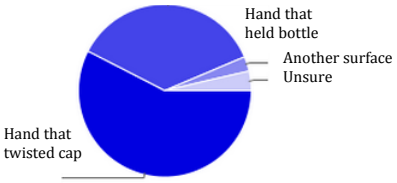

Pour medication into same hand that twisted cap.	57%
Pour medication into hand that originally held the bottle.	36%
Pour medication onto another surface (napkin, table, etc).	3%
Unsure or N/A	4%

Would you be willing to wear a watch or similar wrist-worn device on the opposite hand to which you are accustomed?

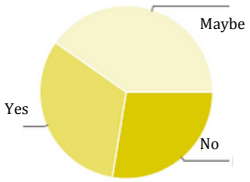

Maybe	40%
Yes	32%
No	28%

In what way would you open a medicine bottle?

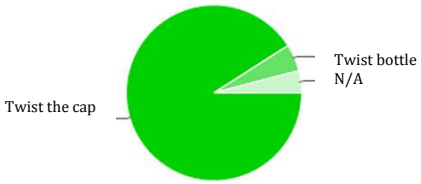

Hold the bottle steady while twisting the cap.	91%
Hold the cap steady while twisting the bottle.	11%
Unsure or N/A	4%

Figure 7.9: Partial survey results are shown above.

Table 7.1: Confusion Matrix using Accelerometer Data

	Predicted		
Actual	Med. Bottle Opened	Other	*Recall*
Med. bottle	21	3	87.5%
Raise Arm	14	6	30%
Walk	1	23	4.1%
Open door	14	10	41.6%
Water bottle	20	4	16.6%
Precision	30%	6.5%	

Table 7.2: Confusion Matrix using Gyroscope Data

	Predicted		
Actual	Palm Up	Other	*Recall*
Palm Up	24	0	100%
Raise Arm	2	22	91.6%
Walk	1	23	95.8%
Open door	2	22	91.6%
Water bottle	0	24	100%
Precision	82.7%	100%	

eral. 72% of responses were positive, as 38% claimed they always wear a watch, 14% preferred wearing a watch, and 53% stated that they would not mind. Subjects were then asked to estimate what percentage of the time they would remove medicine from the bottle and not consume the pill within the next minute. 12% answered that this would occur occasionally, 6% often, and 1% always. 76% of individuals stated that this would happen very rarely.

Figure 7.9 shows other relevant survey questions. The first question reveals that though most individuals open a bottle by twisting the bottle with the primary hand, a significant percentage (32%) preferred to steady the bottle with their primary hand, and twist with the secondary hand. Therefore, the bottle cap would more frequently be twisted by the opposite hand on which the watch is worn. This is confirmed by

another survey question, which established that only 11% of subjects opened the bottle by twisting the bottle base, rather than the cap.

The next question evaluated what happens after individuals open the pill bottle. As hypothesized, most individual's poured the medicine into the palm of their hand, as opposed to another surface such as a napkin or table. However, there was little homogeneity in responses, with 57% who stated that they would pour the medicine into the hand that twisted the cap, and 36% that originally held the bottle.

Generally speaking, the results suggest that some individuals will need to adapt their watch usage in order to recognize the motions suggested in this work. This can be partially mitigated by developing detection strategies for a broader range of motions and applying template matching, though this is left to a future work.

7.1.7 Conclusion

In this Section, a survey was conducted to understand how individuals take their medications from standard-sized twist-cap pill bottles in a normal environment. The results suggest that it is possible to use the Smartwatch as a platform for detection of medication adherence for many individuals. Using the tri-axial accelerometer and gyroscope on the Samsung Smartwatch, we are able to detect (1) the act of twisting the cap of a medicine bottle open, and (2) the removal of a tablet or pill by pouring the pill into the palm of the hand. Though the proposed system imposes some restrictions on how subjects should remove the pill bottle for successful recognition, the system nevertheless has much less human involvement compared to manual record keeping or phone calls from nurses and other forms of adherence detection. Future research will explore the integration fo the Smartwatch with existing smart-health systems, as well as detection of medication adherence with other forms of medication packaging.

7.2 Building Continuous Arterial Blood Pressure Prediction Models Using Recurrent Networks

This Section presents a methodology for developing highly-accurate, continuous Arterial Blood Pressure (ABP) models using only PPG. In contrast to prior approaches, we develop a system that exhibits dynamic temporal behavior which leads to increased accuracy in modeling ABP. We validate our approach using data from patients in the intensive care unit (ICU). We show that it is possible to build highly accurate, continuous blood pressure models using only finger work pulse oximeters. Our methodology achieves accurate systolic blood pressure estimation with a root mean square error 2.58 ± 1.23 across the patient sample used. Furthermore, the continuous ABP signal is estimated with a root mean square error of 6.042 ± 3.26 and correlation coefficient of 0.95 ± 0.045. Our method enables designing robust Remote Health Monitoring Systems (RHMS) for Heart Failure patients without requiring traditional blood pressure monitors.

7.2.1 Introduction

Cardiovascular Disease (CVD) has been the leading cause of death in the United States over the last few decades. Statistics from the American Heart Association demonstrate that over 2,150 Americans die each day due to CVD [126]. In fact, in 2009 CVD was responsible for 31.3% of the total deaths in the U.S. CVD is also prevalent in Europe, and statistics in the European Heart Journal [127] report almost 4.1 million deaths per year due to CVD. Among all types of heart failure, blood pressure and heart rate changes are among the most significant non-invasive indicators of a change in a patient's condition [128].

Remote Health Monitoring Systems (RHMS) have shown great promise in managing and preventing CVD. RHMS are clinical information systems designed to monitor individuals outside of traditional healthcare environments. Data from sensors are col-

lected (usually by the patient himself) and transmitted wirelessly to a remote server for analysis. Clinicians and automated algorithms process the data to identify abnormal patterns. A schematic of such a system can be seen in Figure 7.10. RHMS systems, however, rely on robust collection of heart rate and blood pressure signals to produce high quality risk predictions. In recent years, continuous heart rate monitoring has been made significantly easier with wireless pulse oximeters where the subject only has to wear a small device on his/her fingertip. Blood pressure monitoring is less convenient due to the complexity of cuff-based monitoring devices. For RHMS scenarios, collecting reliable blood pressure measurements is associated with several major challenges:

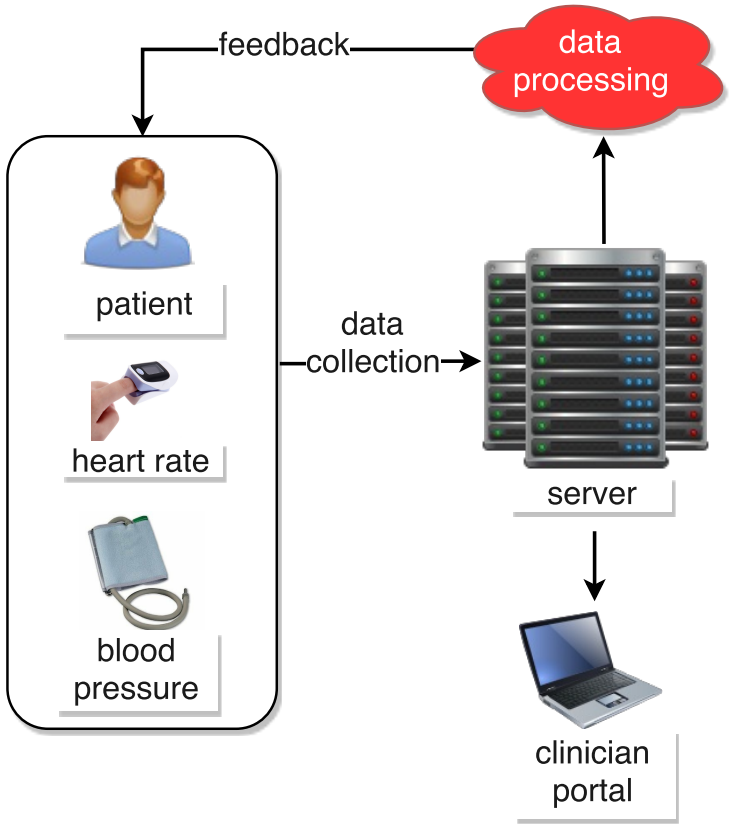

Figure 7.10: Standard architecture of an RHMS. Data collected from the patient is transmitted to a cloud server. The server analyzes and presents the data to clinicians and provides feedback to patients.

- **Patient Condition**: Older patients, or those with severe disabilities may have

difficulty properly collecting blood pressure data. They often forget or are too weak to capture the data themselves.

- **Patient Compliance**: Continuous blood pressure monitoring is challenging outside of a patient's domicile as blood pressure devices are large and visible. Patients often are not motivated or even embarrassed to comply with RHMS data collection protocols.

- **Lack of training**: Finally, even when such data is captured, poor cuff placement and other measuring errors can lead to noisy data. This is a less of an issue with pulse oximeters as they are easier to place and wear.

In this Section, we focus our efforts on developing a methodology that will benefit patients in RHMS by facilitating blood pressure collection. To achieve this, we propose a novel methodology to train accurate, continuous models for inferring blood pressure continuously through pulse oximeters using deep recurrent neural networks. Our work relies on the dynamic temporal behavior of the recurrent networks to learn long and short term characteristics of patient's Photoplethysmography (PPG) data. As a result our system is able to produce high quality approximations of arterial blood pressure signals using input from a finger pulse oximeter.

This work is organized as follows. Section 7.2.2 discusses background and related works. Section 7.2.3 describes our methodology. Section 7.2.4 provides the results and limitations. Finally, we provide concluding remarks in Section 7.2.5.

7.2.2 Background & Related Works

7.2.2.1 Cuffless Blood Pressure monitoring

Cuffless blood pressure monitoring has received a lot of attention in the last decade due to its potential to facilitate blood pressure data collection. This is rendered possible by the fact that blood pressure is highly related with pulse transit time, i.e. the time it

takes the heart beat pulse to propagate from the heart to the peripheral arteries [129]. Most such methods rely on electrocardiograph (ECG) and PPG data to capture the pulse transit time. Such methods include those of Kachuee et al. [130] and Wang et al. [131]. Their results are promising, but ECG data collection is not without challenges as electrodes have to be attached to several parts of the patient's body. Other researchers attempted to model systolic and diastolic blood pressure using only PPG data. Ruiz-Rodriguez et al. [132] used deep networks without temporal behavior and reported promising results albeit with high variance in accuracy. Samria et al. [133] do not report the actual prediction error but rather correlation with measurements. Our proposed system explicitly models the time dependency in the PPG signal which leads to increased accuracy in modeling arterial blood pressure. Furthermore, previous methodologies are limited to predicting only specific metrics of the blood pressure waveform (systolic, diastolic) while our proposed system can reliably output a continuous ABP signal.

7.2.2.2 Remote Health Monitoring Systems

In the last decade, early successes coupled with advances in sensors have evolved Heart Failure RHMS systems from very basic forms (phone interaction, written reports) to advanced end-to-end systems [134]. Among successful applications of RHMS, the system designed by Antonicelli et al. [135] both reduced mortality as well as readmission rates for congestive heart failure patients in RHMS. Another RHMS study carried out by Morguet et al.[136] concluded that a 50% reduction in hospital admissions (38 versus 77/100 patient years, P = 0.034) and a 54% reduction in hospital length of stay is achievable for congestive heart failure patients with RHMS. A few representative solutions are presented to demonstrate the evolution of RHMS systems. An early study by Chaudhry et al. [137] required participants to make daily phone calls to an automated telemonitoring system for a period of 6 months. Each call played a prerecorded voice message that consisted of a series of questions about symptoms and weight for which

the participants had to provide answers using the keypad on the phone. The responses were then downloaded from the telemonitoring system to an Internet website for daily review by clinicians. Another heart failure study conducted by Soran [138, 139] included an electronic scale and an individualized symptom response system connected to a computer database via a standard phone line. Patients were instructed to weigh themselves and answer a series of questions daily. Nurses reviewed the transmitted data on a daily basis and immediately contacted patients whenever the data fell out of a healthy range.

As later studies and systems evolved [140, 134], they employed more sophisticated data collection methodologies as well as data analysis algorithms. In contrast with conventional RHMS, these analytics-based RHMS employ machine learning algorithms to predict the risk of an adverse medical event. It can be concluded from the evidence [87] that analytics-based RHMS work better than threshold-based ones and can help further reduce treatment costs.

Regardless of the algorithms used in a RHMS, accuracy is limited by the data quality. Achieving high-quality blood pressure measurements will enable more reliable monitoring of CVD patients outside of the hospital.

7.2.3 Methodology

7.2.3.1 Data

To validate our approach, we collected data from the MIMIC database [141]. The database was collected from patients in the intensive care unit (ICU). As a result, the dataset contains highly varied blood pressure measurements as the patients are undergoing treatment and receiving drugs. As such, it is a good benchmark for our algorithm's accuracy. We examined signals from 200 patients in the dataset. After excluding short signals and signals with unacceptable blood pressure values (due to being collected in the ICU), we trained and validated regression models for 42 patients. The extracted

data contain two signals per patient. The PPG from the fingertip and invasive arterial blood pressure (mmHg). Both signals are recorded at 125 Hz frequency.

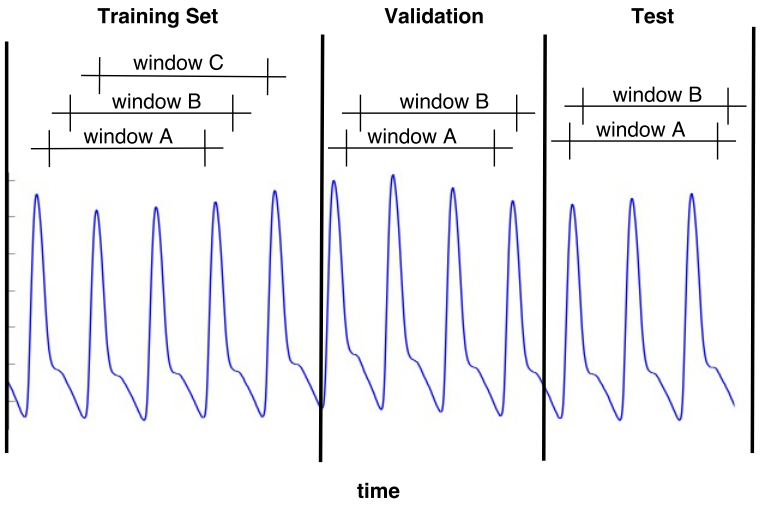

Figure 7.11: A depiction of the training and test sets used

7.2.3.2 Long-Short Term Memory Neural Networks

Deep (or multilayer) neural networks research originates in the 1980s with the seminal papers of Hornik et al. [142] as well as that of Hinton et al. [143]. A neural network is a model loosely based on biological neural networks represented by a set of "neurons" connected with edges with numerical weights. While artificial neural networks initially received a lot of attention from researchers, there were technological and algorithmic limitations that prohibited training very deep networks.

The research field was revived around 2006 with the work of Hinton et al. [144]. In the recent years, advancements in distributed and parallel computing and a new set of training algorithms led to a proliferation of new approaches and applications with state of the art performance in many prediction and classification tasks. For a more thorough understanding of deep neural networks we refer the reader to the book of Bengio et al. [145] and the review papers of Arel et al. [146] and Bengio et al. [147].

Our work relates closely to a variation of deep neural networks, called recurrent

neural networks. In this class of artificial neural networks, the connections between the "neurons" form a directed cycle. This enables them to learn patterns in time-dependent sequences. In fact, they have been applied successfully in handwriting [148] and speech recognition [149] among others. The variation of recurrent networks we utilized are the Long Short-Term Memory (LSTM) models [150]. These models have the ability to learn long term dependencies without the issues that affect traditional recurrent networks. The complete network we used consists of an input layer of nodes, an LSTM and a fully connected output layer with one output node. The complete network is shown in Figure 7.12.

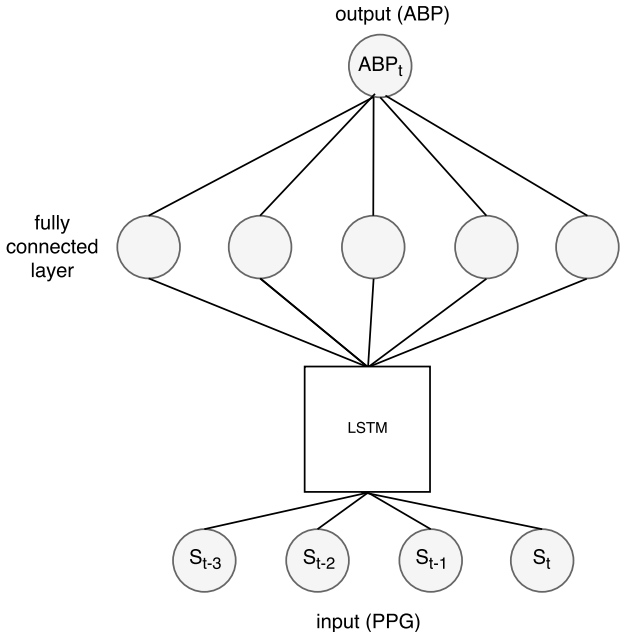

Figure 7.12: The input of the network is the processed, windowed PPG signal and the output is the ABP value at the current time step.

For each patient, we trained a single recurrent neural network. Performing per patient training allows achieving high quality results, as the blood pressure signal depends on the specific properties of the peripheral system of each patient. In an RHMS, calibration does not pose an issue as it can be done when the patient enrolls in the RHMS (usually done at the hospital). Alternatively, a non-invasive, continuous blood pressure

signal can be used. It has been shown to correlate well [151] with invasive arterial blood pressure measurements.

The slow drift component in each signal (PPG and ABP) was removed by subtracting the result of a linear, least-squares fit from the data. Subsequently, each patient record was split into training, validation and test parts using an 80% - 10% - 10% non-overlapping split across time (Figure 7.11). For each of these sets, we extracted overlapping signal windows from the PPG signal. As output, we used the value of the ABP signal that corresponds to the last datapoint in each window.

7.2.4 Results

7.2.4.1 Arterial Blood Pressure Estimation

The network was optimized using the RMSprop algorithm [152] and mean square error as its objective. To prevent over-fitting, Dropout [153] was used during training. With this technique, network nodes and their connections are randomly dropped to minimize learned feature dependencies (co-adaptation). From the estimated arterial blood pressure signal, we compute the systolic and diastolic blood pressure values as the local maxima and minima respectively. Over successive epochs, we update the trained model if the current systolic blood pressure validation error is less than the current best (Algorithm 1).

while *maxepochs* $>$ *current epoch* **do**
    network optimization over the MSE of the ABP
    compute validation MSE of SBP
    if *MSE of SBP* $<$ *current best* **then**
        update model
    else
        continue
    end
end

Algorithm 1: Training algorithm

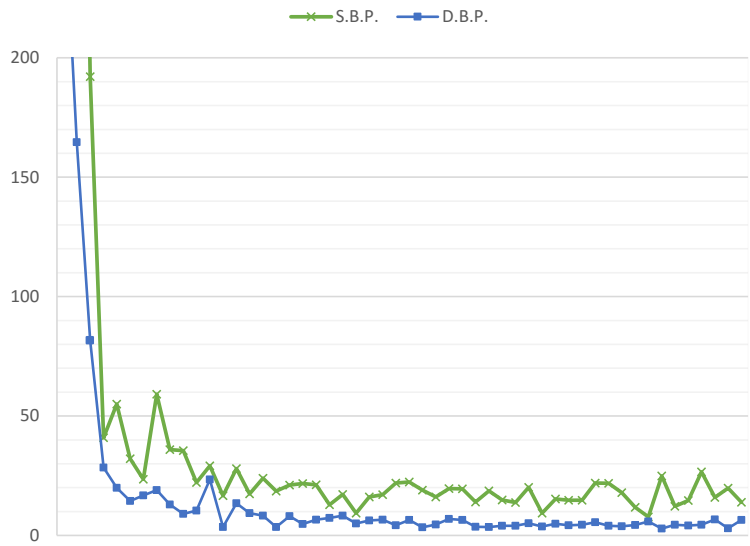

Figure 7.13: Systolic and diastolic blood pressure validation mean square error over training epochs (single patient)

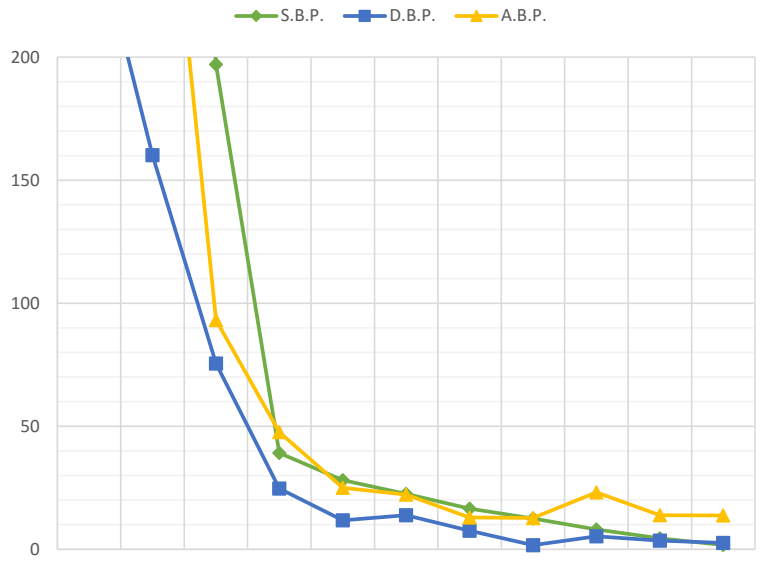

Figure 7.14: Systolic, diastolic and arterial blood pressure test mean square error over successive model updates (single patient)

The full signal MSE or the diastolic blood pressure MSE can also be used as targets depending on the application. Training is stopped after a predetermined number of epochs. Figures 7.13 and 7.14 demonstrate the evolution of the validation and test mean square error during the training of the network. The validation error decreases epoch after epoch up to a certain limit and fluctuates thereafter.

Detailed regression results for each of the examined patients are presented in Tables 7.3, 7.4. The results presented are for the continuous arterial blood pressure signal. Overall, we were able to achieve high quality predicted blood pressure signals with an RMSE of 6.042 ± 3.26. The largest reconstruction errors are observed in the big slope regions of the blood pressure signal (Figure 7.18). These regions are usually less important than local maxima and minima, which correspond to the systolic and diastolic blood pressure.

Finally, Figures 7.17 and 7.18 show the output of the network on the test dataset in the beginning and the end of training respectively. It can be seen that the predicted signal closely follows the actual arterial blood pressure signal.

Table 7.3: Regression Results

patient	root mean square error			correlation	error σ	avg. error
	SBP	DBP	ABP	ABP		
1	1.753	2.806	7.140	0.951	6.980	1.504
2	3.945	1.865	6.671	0.953	6.668	-0.194
3	2.607	2.218	5.217	0.964	5.216	0.064
4	1.324	1.605	3.708	0.985	3.518	1.173
5	2.242	2.908	5.089	0.969	5.065	-0.496
6	2.584	1.465	4.294	0.971	4.284	-0.303
7	2.022	0.988	3.665	0.979	3.660	0.206
8	4.071	1.891	3.429	0.984	3.429	0.030
9	3.392	1.629	3.521	0.984	3.521	0.006
10	1.989	1.360	5.432	0.970	5.349	0.943
11	3.493	1.528	4.216	0.985	4.183	0.525
12	2.736	5.986	5.856	0.909	5.780	0.939
13	3.009	3.251	7.174	0.944	7.172	-0.183
14	6.187	2.422	7.847	0.930	7.846	0.099
15	3.151	1.773	22.850	0.791	22.843	0.541
16	1.250	1.663	5.903	0.973	5.784	-1.181
17	1.041	0.925	3.491	0.991	3.424	-0.682
18	1.554	3.214	9.435	0.926	9.427	0.388
19	0.892	0.990	9.536	0.849	9.536	-0.124
20	1.095	1.792	9.236	0.816	9.217	0.586

Table 7.4: Regression Results (continued)

patient	root mean square error			correlation	error σ	avg. error
	SBP	DBP	ABP	ABP		
21	2.453	0.655	3.735	0.964	3.508	-1.282
22	3.097	2.177	5.380	0.961	5.069	-1.804
23	4.394	3.340	5.134	0.958	5.054	-0.901
24	1.859	1.087	4.175	0.976	4.142	-0.523
25	1.752	1.107	5.100	0.947	4.867	1.524
26	1.857	1.740	4.185	0.904	4.145	-0.580
27	5.835	0.960	6.476	0.951	6.463	-0.405
28	2.113	0.489	7.170	0.930	7.170	0.091
29	4.640	2.164	7.793	0.927	7.753	-0.791
30	1.344	1.798	6.374	0.978	6.235	-1.324
31	2.150	3.828	6.854	0.975	6.800	-0.858
32	2.409	3.666	5.455	0.985	5.210	-1.619
33	3.914	1.775	4.430	0.984	4.425	0.204
34	2.317	2.714	9.070	0.917	8.870	-1.896
35	2.710	3.284	6.192	0.958	6.181	-0.366
36	2.930	2.065	9.105	0.900	9.102	-0.235
37	1.076	1.441	4.187	0.977	4.179	-0.262
38	0.784	0.658	3.764	0.984	3.760	-0.158
39	1.396	1.578	4.748	0.977	4.648	-0.968
40	2.300	1.027	2.993	0.965	2.991	-0.118
41	4.120	1.740	2.448	0.977	2.448	-0.026
42	2.376	1.458	5.268	0.982	5.240	-0.542

7.2.4.2 Comparison with Linear Regression

To evaluate the learning ability of our deep learning network, we compared it against linear regression. As shown in Figures 7.15 and 7.16, both systolic and diastolic root mean square error is significantly larger in linear regression than our proposed methodology. Some extreme values for the error of linear regression are omitted from the graphs for readability.

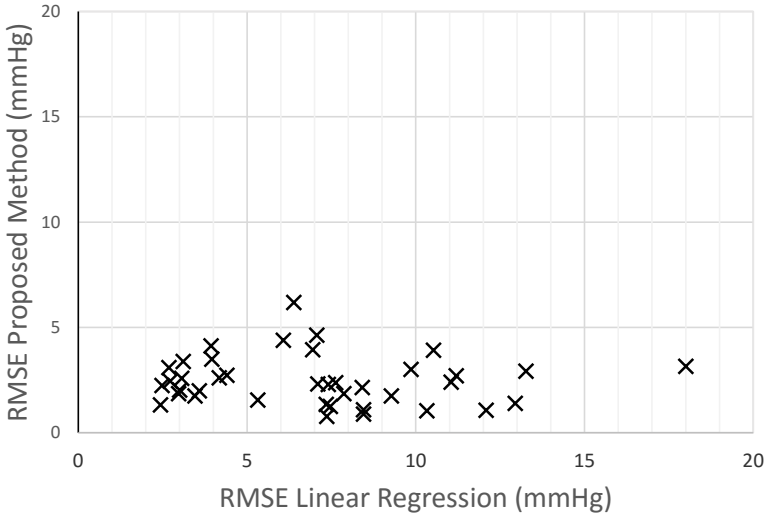

Figure 7.15: Systolic Blood Pressure RMSE in linear regression vs our proposed methodology

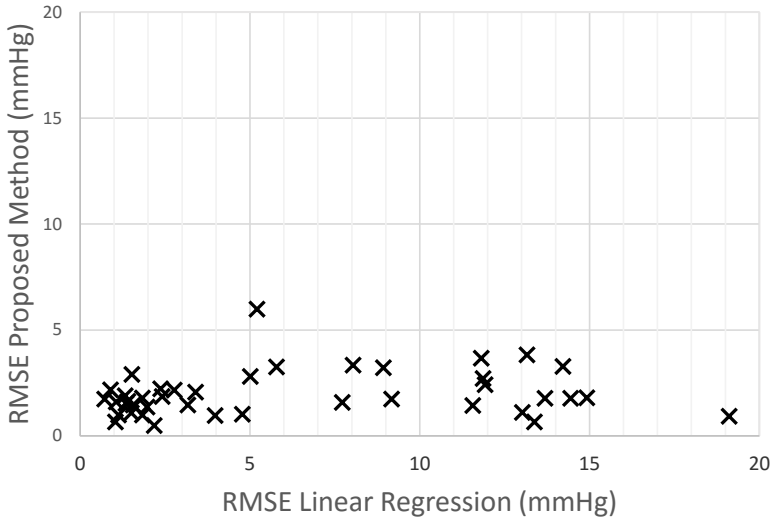

Figure 7.16: Diastolic Blood Pressure RMSE in linear regression vs our proposed methodology

7.2.4.3 Limitations

The methodology and results we presented correspond to data collected from ICU patients. Tuning the network and the learning parameters may be necessary to generalize to patients outside the ICU. In addition, the dataset used did not contain age or other contextual information that could improve output accuracy. Finally, optimizing the window size, the number of hidden nodes and the network architecture was beyond the scope of this work. Our experiments indicate that further gains can be made by exploring those parameters as well.

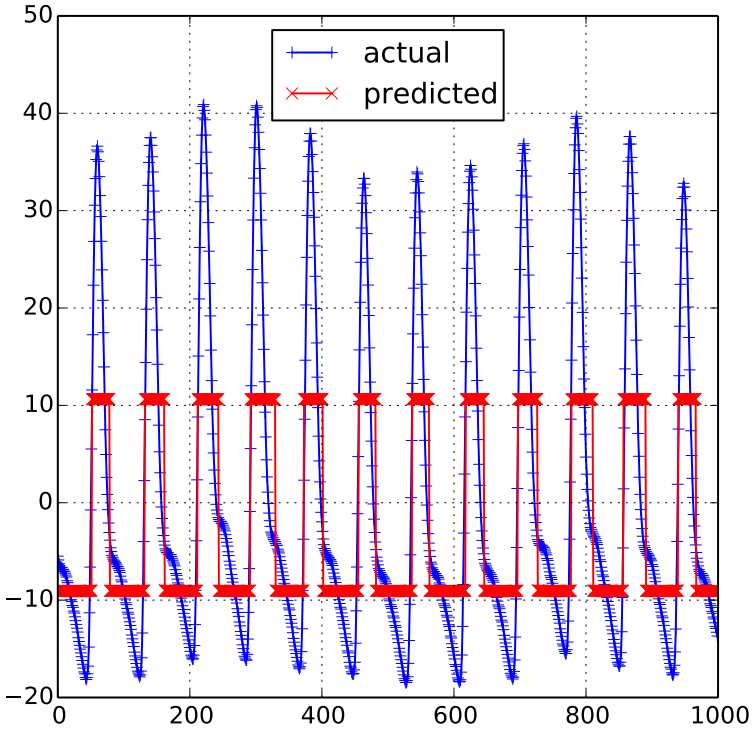

Figure 7.17: Arterial blood pressure signal prediction (mean subtracted) at the beginning of the training (subject 7)

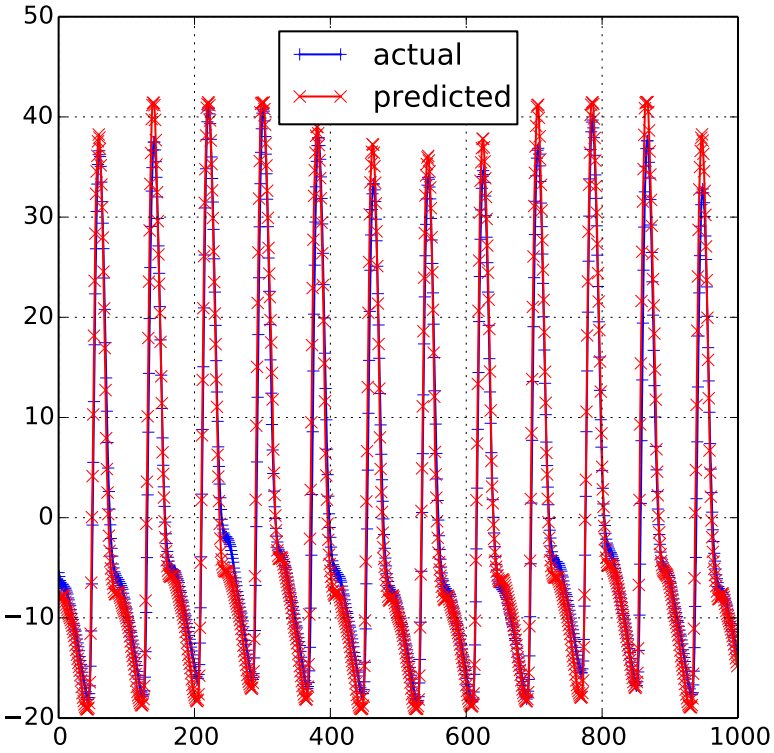

Figure 7.18: Arterial blood pressure signal prediction (mean subtracted) at the end of the training (subject 7)

7.2.5 Conclusions

We have presented a methodology for developing highly-accurate continuous models for inferring arterial blood pressure from finger photoplethysmography. The presented methodology enables continuous blood pressure monitoring for patients in RHMS without the inconvenience of a blood pressure cuff or the ECG sensor. Such a system has the potential to increase patient compliance and provide more accurate risk classification and prediction. In turn, this can lead to better management of heart failure.

CHAPTER 8

Conclusion and Future Works

This dissertation is trying to provide new methodologies in time series analysis of wrist-worn systems' data. Wrist-worn systems have provided a new horizon in remote health monitoring systems. Many activity sensing module are now built for wearing on wrist. A lot of companies such as Fitbit, Apple, Samsung are investing on health tracking based upon the wrist data by implementing new sensors and algorithms on their systems. Being comfortably tightened to the skin provides high sensing capabilities for many vital signs including heart rate, PPG and Spo2 compared to many other health tracking systems. Although, wrist-worn sensing has become very popular in the past few years due to all these advantages, there has been many limitations and challenges introduced when it comes to taking full advantage of them. Chapter II of this dissertation provides a full summary of these challenges specifically focusing on activity recognition. This manuscript is an effort to tackle these challenges and provide methods and techniques to mitigate the these limitations of wrist-worn sensing systems to improve the baseline for both accuracy and battery performance.

Chapter III of this work is proposing the idea of using wrist-worn devices for activity classification. A proof of concept system has been designed and tested for activity state detection. We have shown that smartwatches are as capable as smartphones, if not better, in detecting transitions between sit, stand and lie states. Although this achievement seemed very exciting, it all came from in-lab data collection. The story is very different when wrist-worn systems are tested in-field. Unwanted hand motions confuses classification models by generating false positive and negatives when it comes to activ-

ity recognition. Chapter IV proposed looking to the context information to mitigate this issue and eventually boost both precision of classification and battery performance. We proposed the idea of using the "location" probability distribution information as a context to predict the activity of a person by adjusting the prior probability in the statistical model and showed improvement of up to 7% in the total accuracy of activity classification. We have also shown that "current state" can be used as a context to switch between different sensing modules in order to provide better accuracy and dynamically improve battery lifetime of modules in which power recourse are scarce. An improvement of 5% in accuracy and 7 hours in smartwatch battery lifetime was proved to be achievable. As another effort to deal with unwanted hand noise, we investigated the extent of its effect on gait quality of a person when wearing a smartwatch. Noticing the phenomena of over and under-counting of steps while walking with a wrist device, we realized complex time series analysis methods are necessary. We took advantage of Kalman Filter to estimate the timing information of each step. Then we used this information to correct for the missing peaks taken place due to hand motion noise. We have shown huge improvement in detecting walking steps while proposing models to estimate gait distance, velocity and symmetry. In Chapter VI, a two-layer classification scheme is proposed to further improve of accuracy of activity state recognition. We have used combination of "Random Forest" and "Majority Voting" algorithms to reduce the false positives for the classification of activities with long duration. This idea is proposed to replace using large window size in time series analysis (recalling that using large window size makes detection of short-duration activities more troublesome. An 8% improvement in detection accuracy was observed using this technique which seems very promising when it comes to classification between a combination of short and long-duration activities.

Although this work has tried to identify some of the limitations and challenges of wrist-worn sensing systems in activity recognition, there are still a lot of work could be done. More applications, in addition to activity recognition could be targeted to investigate. With more sensors being embedded in wrist devices. More contextual

information could be used to further improve the inference accuracy. More time series analysis could be applied and tested based upon the targeted application to resolve the challenges to come. Perhaps comparing different analysis techniques and proposing a combination of different time series methods could be a good potential for investigation. Although this dissertation is not claiming to provide a thorough and clear picture of wrist-sensing for activity recognition which tackles all the issues in hand, it serves as a starting point in the new horizon of wrist-based sensing. And with more dominance of these modules in both commercial and clinical settings, there seems to be an enormous demand for better characterization and utilization of wrist-worn sensing systems.

Another big direction for the future work is to investigate and re-evaluate the designed systems and implemented algorithms to involve real patients. Perhaps investing in collecting a new set of data from real patients for the system in Chapter III and tweaking the model including the new dataset is one step. Or perhaps the information regarding prediction capability of Smartphone and Smartwatch based on the "current state" context could be a matter of change in Chapter IV, when the patient data is used. Maybe implementing a new inference architecture which includes a calibration phase before testing, in generating the model (tuned to every subject), would be substantial in improving gait quality estimation when patients (and specially elderly patients) are under assessment in Chapter V. And eventually some key assumptions from elderly patients could be determinant in adjusting some parameters in the 2nd layer of algorithm in Chapter VI (for example the window size in majority voting algorithm).

BIBLIOGRAPHY

[1] Wan He, Manisha Sengupta, Victoria A Velkoff, Kimberly A DeBarros, et al. *65+ in the United States: 2005*. Citeseer, 2005.

[2] Jessie Gerteis, David Izrael, Deborah Deitz, Lisa LeRoy, Richard Ricciardi, Therese Miller, and Jayasree Basu. Multiple chronic conditions chartbook. *Rockville, MD: Agency for Healthcare Research and Quality*, 2014.

[3] Melonie P Heron. Deaths: leading causes for 2012. 2015.

[4] Rebecca L Siegel, Kimberly D Miller, and Ahmedin Jemal. Cancer statistics, 2016. *CA: a cancer journal for clinicians*, 66(1):7–30, 2016.

[5] Roozbeh Jafari, Foad Dabiri, Philip Brisk, and Majid Sarrafzadeh. Adaptive and fault tolerant medical vest for life-critical medical monitoring. In *Proceedings of the 2005 ACM symposium on Applied computing*, pages 272–279. ACM, 2005.

[6] NSRK Prasad and Arepalli Rajesh. Rfid-based hospital real time patient management system. *International Journal of Computer Trends and Technology*, 3(3):1011–1016, 2012.

[7] Prathamesh Dinkar, Abhishek Gulavani, Sourabh Ketkale, Pratik Kadam, and Sheetal Dabhade. Remote health monitoring using wireless body area network. *International Journal of Engineering and Advanced Technology (IJEAT) ISSN*, 2249:8958, 2013.

[8] Ling Bao and Stephen Intille. Activity recognition from user-annotated acceleration data. *Pervasive computing*, pages 1–17, 2004.

[9] Nishkam Ravi, Nikhil Dandekar, Preetham Mysore, and Michael L Littman. Activity recognition from accelerometer data. In *Aaai*, volume 5, pages 1541–1546, 2005.

[10] Sarwat I Chaudhry, Christopher O Phillips, Simon S Stewart, Barbara Riegel, Jennifer A Mattera, Anthony F Jerant, and Harlan M Krumholz. Telemonitoring for patients with chronic heart failure: a systematic review. *Journal of cardiac failure*, 13(1):56–62, 2007.

[11] Myung-kyung Suh, Chien-An Chen, Jonathan Woodbridge, Michael Kai Tu, Jung In Kim, Ani Nahapetian, Lorraine S Evangelista, and Majid Sarrafzadeh. A remote patient monitoring system for congestive heart failure. *Journal of medical systems*, 35(5):1165–1179, 2011.

[12] Bobak Jack Mortazavi, Mohammad Pourhomayoun, Gabriel Alsheikh, Nabil Alshurafa, Sunghoon Ivan Lee, and Majid Sarrafzadeh. Determining the single best axis for exercise repetition recognition and counting on smartwatches. In *Wearable and Implantable Body Sensor Networks (BSN), 2014 11th International Conference on*, pages 33–38. IEEE, 2014.

[13] Nabil Alshurafa, Wenyao Xu, Jason J Liu, Ming-Chun Huang, Bobak Mortazavi, Majid Sarrafzadeh, and Christian Roberts. Robust human intensity-varying activity recognition using stochastic approximation in wearable sensors. In *Body Sensor Networks (BSN), 2013 IEEE International Conference on*, pages 1–6. IEEE, 2013.

[14] Mohammad Pourhomayoun, Zhanpeng Jin, and Mark L Fowler. Indoor localization, tracking and fall detection for assistive healthcare based on spatial sparsity and wireless sensor network. *International Journal of Monitoring and Surveillance Technologies Research (IJMSTR)*, 1(2):72–83, 2013.

[15] Sidney Katz, Amasa B Ford, Roland W Moskowitz, Beverly A Jackson, and Marjorie W Jaffe. Studies of illness in the aged: the index of adl: a standardized measure of biological and psychosocial function. *Jama*, 185(12):914–919, 1963.

[16] JoAnn E Manson, David M Nathan, Andrzej S Krolewski, Meir J Stampfer,

Walter C Willett, and Charles H Hennekens. A prospective study of exercise and incidence of diabetes among us male physicians. *Jama*, 268(1):63–67, 1992.

[17] Martin M Oken, Richard H Creech, Douglass C Tormey, John Horton, Thomas E Davis, Eleanor T McFadden, and Paul P Carbone. Toxicity and response criteria of the eastern cooperative oncology group. *American journal of clinical oncology*, 5(6):649–656, 1982.

[18] Alan M Jette. Functional status index: reliability of a chronic disease evaluation instrument. *Archives of physical medicine and rehabilitation*, 61(9):395–401, 1980.

[19] H Schipper, J_ Clinch, A McMurray, and M Levitt. Measuring the quality of life of cancer patients: the functional living index-cancer: development and validation. *Journal of clinical Oncology*, 2(5):472–483, 1984.

[20] Wenyao Xu, Ming-Chun Huang, Navid Amini, Jason J Liu, Lei He, and Majid Sarrafzadeh. Smart insole: A wearable system for gait analysis. In *Proceedings of the 5th International Conference on PErvasive Technologies Related to Assistive Environments*, page 18. ACM, 2012.

[21] Jiaqi Gong, Karen Moomaw Rose, Ifat Afrin Emi, Janet P Specht, Enamul Hoque, Dawei Fan, Sriram Raju Dandu, Robert F Dickerson, Yelena Perkhounkova, John Lach, et al. Home wireless sensing system for monitoring nighttime agitation and incontinence in patients with alzheimer's disease. In *Proceedings of the conference on Wireless Health*, page 5. ACM, 2015.

[22] Tschepo Rasekaba, AL Lee, MT Naughton, TJ Williams, and AE Holland. The six-minute walk test: a useful metric for the cardiopulmonary patient. *Internal medicine journal*, 39(8):495–501, 2009.

[23] Mikael Andersson, Linda Moberg, Ulla Svantesson, Ann Sundbom, Henrik Johansson, and Margareta Emtner. Measuring walking speed in copd: test-retest

reliability of the 30-metre walk test and comparison with the 6-minute walk test. *Primary Care Respiratory Journal*, 20(4):434–440, 2011.

[24] Kara K Patterson, William H Gage, Dina Brooks, Sandra E Black, and William E McIlroy. Evaluation of gait symmetry after stroke: a comparison of current methods and recommendations for standardization. *Gait & posture*, 31(2):241–246, 2010.

[25] Stephanie Studenski, Subashan Perera, Kushang Patel, Caterina Rosano, Kimberly Faulkner, Marco Inzitari, Jennifer Brach, Julie Chandler, Peggy Cawthon, Elizabeth Barrett Connor, et al. Gait speed and survival in older adults. *Jama*, 305(1):50–58, 2011.

[26] Susan E Hardy, Subashan Perera, Yazan F Roumani, Julie M Chandler, and Stephanie A Studenski. Improvement in usual gait speed predicts better survival in older adults. *Journal of the American Geriatrics Society*, 55(11):1727–1734, 2007.

[27] Robert V Levine and Ara Norenzayan. The pace of life in 31 countries. *Journal of cross-cultural psychology*, 30(2):178–205, 1999.

[28] Constantine Glaros and Dimitrios I Fotiadis. Wearable devices in healthcare. In *Intelligent Paradigms for Healthcare Enterprises*, pages 237–264. Springer, 2005.

[29] Ebrahim Nemati, M Jamal Deen, and Tapas Mondal. A wireless wearable ecg sensor for long-term applications. *IEEE Communications Magazine*, 50(1), 2012.

[30] Alex Huang, Andrew Campion, Daniel C Lu, Eunjeong Park, Jordan H Garst, Majid Sarrafzadeh, Marie Espinal, Marwa Afridi, Meelod Daneshvar, Nima Jahanforouz, et al. Identifying predictors for postoperative clinical outcome in

lumbar spinal stenosis patients using smart-shoe technology. *Journal of neuroengineering and rehabilitation*, 14(1):77, 2017.

[31] Uwe Maurer, Asim Smailagic, Daniel P Siewiorek, and Michael Deisher. Activity recognition and monitoring using multiple sensors on different body positions. In *Wearable and Implantable Body Sensor Networks, 2006. BSN 2006. International Workshop on*, pages 4–pp. IEEE, 2006.

[32] Alexandros Pantelopoulos and Nikolaos G Bourbakis. A survey on wearable sensor-based systems for health monitoring and prognosis. *IEEE Transactions on Systems, Man, and Cybernetics, Part C (Applications and Reviews)*, 40(1):1–12, 2010.

[33] Statista DMO. Smartphone penetration rate as share of the population in the united states from 2010 to 2022.

[34] Anind K Dey, Katarzyna Wac, Denzil Ferreira, Kevin Tassini, Jin-Hyuk Hong, and Julian Ramos. Getting closer: an empirical investigation of the proximity of user to their smart phones. In *Proceedings of the 13th international conference on Ubiquitous computing*, pages 163–172. ACM, 2011.

[35] Ebrahim Nemati, Christina Batteate, and Michael Jerrett. Opportunistic environmental sensing with smartphones: a critical review of current literature and applications. *Current Environmental Health Reports*, 4(3):306–318, 2017.

[36] Yuriy Kurylyak, Francesco Lamonaca, and Domenico Grimaldi. Smartphone based photoplethysmogram measurement. *Digital image and signal processing for measurement systems*, pages 135–164, 2012.

[37] Blaine Reeder and Alexandria David. Health at hand: a systematic review of smart watch uses for health and wellness. *Journal of biomedical informatics*, 63:269–276, 2016.

[38] William Omar Contreras Lopez, Carlos Andres Escalante Higuera, Erich Talamoni Fonoff, Carolina de Oliveira Souza, Ulrich Albicker, and Jairo Alberto Espinoza Martinez. Listenmee® and listenmee® smartphone application: Synchronizing walking to rhythmic auditory cues to improve gait in parkinsonŠs disease. *Human movement science*, 37:147–156, 2014.

[39] Vinod Sharma, Kunal Mankodiya, Fernando De La Torre, Ada Zhang, Neal Ryan, Thanh GN Ton, Rajeev Gandhi, and Samay Jain. Spark: personalized parkinson disease interventions through synergy between a smartphone and a smartwatch. In *International Conference of Design, User Experience, and Usability*, pages 103–114. Springer, 2014.

[40] Juliana Lockman, Robert S Fisher, and Donald M Olson. Detection of seizure-like movements using a wrist accelerometer. *Epilepsy & Behavior*, 20(4):638–641, 2011.

[41] Anahita Hosseini, Chris M Buonocore, Sepideh Hashemzadeh, Hannaneh Hojaiji, Haik Kalantarian, Costas Sideris, Alex AT Bui, Christine E King, and Majid Sarrafzadeh. Hipaa compliant wireless sensing smartwatch application for the self-management of pediatric asthma. In *Wearable and Implantable Body Sensor Networks (BSN), 2016 IEEE 13th International Conference on*, pages 49–54. IEEE, 2016.

[42] Haik Kalantarian and Majid Sarrafzadeh. Audio-based detection and evaluation of eating behavior using the smartwatch platform. *Computers in biology and medicine*, 65:1–9, 2015.

[43] Eirik Årsand, Miroslav Muzny, Meghan Bradway, Jan Muzik, and Gunnar Hartvigsen. Performance of the first combined smartwatch and smartphone diabetes diary application study. *Journal of diabetes science and technology*, 9(3):556–563, 2015.

[44] Sougata Sen, Vigneshwaran Subbaraju, Archan Misra, Rajesh Krishna Balan, and Youngki Lee. The case for smartwatch-based diet monitoring. In *Pervasive Computing and Communication Workshops (PerCom Workshops), 2015 IEEE International Conference on*, pages 585–590. IEEE, 2015.

[45] Nicholas Micallef, Lynne Baillie, and Stephen Uzor. Time to exercise!: an aide-memoire stroke app for post-stroke arm rehabilitation. In *Proceedings of the 18th International Conference on Human-Computer Interaction with Mobile Devices and Services*, pages 112–123. ACM, 2016.

[46] Costas Boletsis, Simon McCallum, and Brynjar Fowels Landmark. The use of smartwatches for health monitoring in home-based dementia care. In *International Conference on Human Aspects of IT for the Aged Population*, pages 15–26. Springer, 2015.

[47] Haik Kalantarian, Nabil Alshurafa, and Majid Sarrafzadeh. Detection of gestures associated with medication adherence using smartwatch-based inertial sensors. *IEEE Sensors Journal*, 16(4):1054–1061, 2016.

[48] Haik Kalantarian, Nabil Alshurafa, Ebrahim Nemati, Tuan Le, and Majid Sarrafzadeh. A smartwatch-based medication adherence system. In *Wearable and Implantable Body Sensor Networks (BSN), 2015 IEEE 12th International Conference on*, pages 1–6. IEEE, 2015.

[49] Harishchandra Dubey, Jon C Goldberg, Mohammadreza Abtahi, Leslie Mahler, and Kunal Mankodiya. Echowear: smartwatch technology for voice and speech treatments of patients with parkinson's disease. In *Proceedings of the conference on Wireless Health*, page 15. ACM, 2015.

[50] Maulik R Kamdar and Michelle J Wu. Prism: A data-driven platform for monitoring mental health. In *PSB*, pages 333–344, 2016.

[51] Ozgur Akyazi, Sahin Batmaz, Bilgin Kosucu, and Bert Arnrich. Smokewatch: A smartwatch smoking cessation assistant. In *Signal Processing and Communications Applications Conference (SIU), 2017 25th*, pages 1–4. IEEE, 2017.

[52] Eduardo Casilari and Miguel A Oviedo-Jiménez. Automatic fall detection system based on the combined use of a smartphone and a smartwatch. *PloS one*, 10(11):e0140929, 2015.

[53] Martine Duclos, Gérard Fleury, Philippe Lacomme, Raksmey Phan, Libo Ren, and Sylvie Rousset. An acceleration vector variance based method for energy expenditure estimation in real-life environment with a smartphone/smartwatch integration. *Expert Systems with Applications*, 63:435–449, 2016.

[54] Vijayalakshmi Ahanathapillai, James D Amor, Zoe Goodwin, and Christopher J James. Preliminary study on activity monitoring using an android smart-watch. *Healthcare technology letters*, 2(1):34–39, 2015.

[55] Emil Jovanov. Preliminary analysis of the use of smartwatches for longitudinal health monitoring. In *Engineering in Medicine and Biology Society (EMBC), 2015 37th Annual International Conference of the IEEE*, pages 865–868. IEEE, 2015.

[56] Stewart G Trost, Yonglei Zheng, and Weng-Keen Wong. Machine learning for activity recognition: hip versus wrist data. *Physiological measurement*, 35(11):2183, 2014.

[57] John J Guiry, Pepijn van de Ven, and John Nelson. Multi-sensor fusion for enhanced contextual awareness of everyday activities with ubiquitous devices. *Sensors*, 14(3):5687–5701, 2014.

[58] Gary M Weiss, Jessica L Timko, Catherine M Gallagher, Kenichi Yoneda, and Andrew J Schreiber. Smartwatch-based activity recognition: A machine learn-

ing approach. In *Biomedical and Health Informatics (BHI), 2016 IEEE-EMBS International Conference on*, pages 426–429. IEEE, 2016.

[59] Marian Haescher, John Trimpop, Denys JC Matthies, Gerald Bieber, Bodo Urban, and Thomas Kirste. ahead: Considering the head position in a multi-sensory setup of wearables to recognize everyday activities with intelligent sensor fusions. In *International Conference on Human-Computer Interaction*, pages 741–752. Springer, 2015.

[60] Sébastien Faye, Raphael Frank, and Thomas Engel. Adaptive activity and context recognition using multimodal sensors in smart devices. In *International Conference on Mobile Computing, Applications, and Services*, pages 33–50. Springer, 2015.

[61] Saisakul Chernbumroong, Anthony S Atkins, and Hongnian Yu. Activity classification using a single wrist-worn accelerometer. In *Software, Knowledge Information, Industrial Management and Applications (SKIMA), 2011 5th International Conference on*, pages 1–6. IEEE, 2011.

[62] John Paul Varkey, Dario Pompili, and Theodore A Walls. Human motion recognition using a wireless sensor-based wearable system. *Personal and Ubiquitous Computing*, 16(7):897–910, 2012.

[63] Harvey Weinberg. Using the adxl202 in pedometer and personal navigation applications. *Analog Devices AN-602 application note*, 2(2):1–6, 2002.

[64] Inge Bylemans, Maarten Weyn, and Martin Klepal. Mobile phone-based displacement estimation for opportunistic localisation systems. In *Mobile Ubiquitous Computing, Systems, Services and Technologies, 2009. UBICOMM'09. Third International Conference on*, pages 113–118. IEEE, 2009.

[65] Hemin Zhang, Weizheng Yuan, Qiang Shen, Tai Li, and Honglong Chang. A

handheld inertial pedestrian navigation system with accurate step modes and device poses recognition. *IEEE Sensors Journal*, 15(3):1421–1429, 2015.

[66] Dae-Ki Cho, Min Mun, Uichin Lee, William J Kaiser, and Mario Gerla. Autogait: A mobile platform that accurately estimates the distance walked. In *Pervasive computing and communications (PerCom), 2010 IEEE international conference on*, pages 116–124. IEEE, 2010.

[67] Valérie Renaudin, Melania Susi, and Gérard Lachapelle. Step length estimation using handheld inertial sensors. *Sensors*, 12(7):8507–8525, 2012.

[68] Bobak Mortazavi, Ebrahim Nemati, Kristina VanderWall, Hector G Flores-Rodriguez, Jun Yu Jacinta Cai, Jessica Lucier, Arash Naeim, and Majid Sarrafzadeh. Can smartwatches replace smartphones for posture tracking? *Sensors*, 15(10):26783–26800, 2015.

[69] Rajesh Krishna Balan, Youngki Lee, Tan Kiat Wee, and Archan Misra. The challenge of continuous mobile context sensing. In *Communication Systems and Networks (COMSNETS), 2014 Sixth International Conference on*, pages 1–8. IEEE, 2014.

[70] AA Aaldriks, E Maartense, S Le Cessie, EJ Giltay, HACM Verlaan, LGM van der Geest, WM Kloosterman-Boele, MT Peters-Dijkshoorn, BA Blansjaar, HW Van Schaick, et al. Predictive value of geriatric assessment for patients older than 70 years, treated with chemotherapy. *Critical reviews in oncology/hematology*, 79(2):205–212, 2011.

[71] Ulrich Steinhoff and Bernt Schiele. Dead reckoning from the pocket-an experimental study. In *Pervasive Computing and Communications (PerCom), 2010 IEEE International Conference on*, pages 162–170. IEEE, 2010.

[72] Nabil Alshurafa, Jo-Ann Eastwood, Mohammad Pourhomayoun, Suneil Nyamathi, Lily Bao, Bobak Mortazavi, and Majid Sarrafzadeh. Anti-cheating: De-

tecting self-inflicted and impersonator cheaters for remote health monitoring systems with wearable sensors. In *Wearable and Implantable Body Sensor Networks (BSN), 2014 11th International Conference on*, pages 92–97. IEEE, 2014.

[73] Diego Alvarez, Rafael C González, Antonio López, and Juan C Alvarez. Comparison of step length estimators from weareable accelerometer devices. In *Engineering in Medicine and Biology Society, 2006. EMBS'06. 28th Annual International Conference of the IEEE*, pages 5964–5967. IEEE, 2006.

[74] Reza Rawassizadeh, Martin Tomitsch, Manouchehr Nourizadeh, Elaheh Momeni, Aaron Peery, Liudmila Ulanova, and Michael Pazzani. Energy-efficient integration of continuous context sensing and prediction into smartwatches. *Sensors*, 15(9):22616–22645, 2015.

[75] Mi Zhang and Alexander A Sawchuk. A feature selection-based framework for human activity recognition using wearable multimodal sensors. In *Proceedings of the 6th International Conference on Body Area Networks*, pages 92–98. ICST (Institute for Computer Sciences, Social-Informatics and Telecommunications Engineering), 2011.

[76] Jhun-Ying Yang, Jeen-Shing Wang, and Yen-Ping Chen. Using acceleration measurements for activity recognition: An effective learning algorithm for constructing neural classifiers. *Pattern recognition letters*, 29(16):2213–2220, 2008.

[77] Henri Vähä-Ypyä, Tommi Vasankari, Pauliina Husu, Jaana Suni, and Harri Sievänen. A universal, accurate intensity-based classification of different physical activities using raw data of accelerometer. *Clinical physiology and functional imaging*, 35(1):64–70, 2015.

[78] Mark Hall, Eibe Frank, Geoffrey Holmes, Bernhard Pfahringer, Peter Reutemann, and Ian H Witten. The weka data mining software: an update. *ACM SIGKDD explorations newsletter*, 11(1):10–18, 2009.

[79] Leslie S Prichep, Arnaud Jacquin, Julie Filipenko, Samanwoy Ghosh Dastidar, Stephen Zabele, Asmir Vodencarevic, and Neil S Rothman. Classification of traumatic brain injury severity using informed data reduction in a series of binary classifier algorithms. *IEEE transactions on neural systems and rehabilitation engineering*, 20(6):806–822, 2012.

[80] Bülent Üstün, Willem J Melssen, and Lutgarde MC Buydens. Facilitating the application of support vector regression by using a universal pearson vii function based kernel. *Chemometrics and Intelligent Laboratory Systems*, 81(1):29–40, 2006.

[81] Bobak Mortazavi, Mohammad Pourhomayoun, Suneil Nyamathi, Brandon Wu, Sunghoon Ivan Lee, and Majid Sarrafzadeh. Multiple model recognition for near-realistic exergaming. In *Pervasive Computing and Communications (PerCom), 2015 IEEE International Conference on*, pages 140–148. IEEE, 2015.

[82] Marina Sokolova and Guy Lapalme. A systematic analysis of performance measures for classification tasks. *Information Processing & Management*, 45(4):427–437, 2009.

[83] Bijan Najafi, David G Armstrong, and Jane Mohler. Novel wearable technology for assessing spontaneous daily physical activity and risk of falling in older adults with diabetes, 2013.

[84] Gerald Bieber, Marian Haescher, and Matthias Vahl. Sensor requirements for activity recognition on smart watches. In *Proceedings of the 6th International Conference on PErvasive Technologies Related to Assistive Environments*, page 67. ACM, 2013.

[85] Isabelle Guyon and André Elisseeff. An introduction to variable and feature selection. *Journal of machine learning research*, 3(Mar):1157–1182, 2003.

[86] Leo Breiman. Random forests. *Machine learning*, 45(1):5–32, 2001.

[87] Sunghoon Ivan Lee, Hassan Ghasemzadeh, Bobak Mortazavi, Mars Lan, Nabil Alshurafa, Michael Ong, and Majid Sarrafzadeh. Remote patient monitoring: what impact can data analytics have on cost? In *Proceedings of the 4th Conference on Wireless Health*, page 4. ACM, 2013.

[88] Mohammad Pourhomayoun and Mark L Fowler. An svd approach for data compression in emitter location systems. In *Signals, Systems and Computers (ASILOMAR), 2011 Conference Record of the Forty Fifth Asilomar Conference on*, pages 257–261. IEEE, 2011.

[89] Neeraj K Gupta and Ram Dantu. Evaluation of respiration quality using smart phone. In *Proceedings of the 6th International Conference on PErvasive Technologies Related to Assistive Environments*, page 28. ACM, 2013.

[90] SH Shin, CG Park, HS Hong, and JM Lee. Mems-based personal navigator equipped on the user's body. 2005.

[91] Lauro Ojeda and Johann Borenstein. Non-gps navigation for security personnel and first responders. *The Journal of Navigation*, 60(3):391–407, 2007.

[92] Angelo M Sabatini, Chiara Martelloni, Sergio Scapellato, and Filippo Cavallo. Assessment of walking features from foot inertial sensing. *IEEE Transactions on biomedical engineering*, 52(3):486–494, 2005.

[93] Jasper Jahn, Ulrich Batzer, Jochen Seitz, Lucila Patino-Studencka, and Javier Gutiérrez Boronat. Comparison and evaluation of acceleration based step length estimators for handheld devices. In *Indoor Positioning and Indoor Navigation (IPIN), 2010 International Conference on*, pages 1–6. IEEE, 2010.

[94] Xiaoxu Wu, Yan Wang, and Gregory Pottie. A robust step length estimation system for human gait using motion sensors. In *Proceedings of the conference on Wireless Health*, page 14. ACM, 2015.

[95] Shinji Miyazaki. Long-term unrestrained measurement of stride length and walking velocity utilizing a piezoelectric gyroscope. *IEEE transactions on Biomedical Engineering*, 44(8):753–759, 1997.

[96] Young Soo Suh, Ebrahim Nemati, and Majid Sarrafzadeh. Kalman-filter-based walking distance estimation for a smart-watch. In *Connected Health: Applications, Systems and Engineering Technologies (CHASE), 2016 IEEE First International Conference on*, pages 150–156. IEEE, 2016.

[97] Ebrahim Nemati, Young Soo Suh, Babak Motamed, and Majid Sarrafzadeh. Gait velocity estimation for a smartwatch platform using kalman filter peak recovery. In *Wearable and Implantable Body Sensor Networks (BSN), 2016 IEEE 13th International Conference on*, pages 230–235. IEEE, 2016.

[98] Arthur D Kuo and J Maxwell Donelan. Dynamic principles of gait and their clinical implications. *Physical therapy*, 90(2):157–174, 2010.

[99] Lely A Luengas, Esperanza Camargo, and Giovanni Sanchez. Modeling and simulation of normal and hemiparetic gait. *Frontiers of Mechanical Engineering*, 10(3):233–241, 2015.

[100] Nihat Özkaya, Dawn Leger, David Goldsheyder, and Margareta Nordin. *Fundamentals of biomechanics: equilibrium, motion, and deformation*. Springer, 2016.

[101] Stephen Boyd and Lieven Vandenberghe. *Convex optimization*. Cambridge university press, 2004.

[102] Robert Grover Brown and Patrick YC Hwang. Introduction to random signals and applied kalman filtering: with matlab exercises and solutions. *Introduction to random signals and applied Kalman filtering: with MATLAB exercises and solutions, by Brown, Robert Grover.; Hwang, Patrick YC New York: Wiley, c1997.*, 1997.

[103] MICHALINA Błażkiewicz, Ida Wiszomirska, and ANDRZEJ Wit. Comparison of four methods of calculating the symmetry of spatial-temporal parameters of gait. *Acta of bioengineering and biomechanics*, 16(1):29–35, 2014.

[104] Young Soo Suh and Sangkyung Park. Pedestrian inertial navigation with gait phase detection assisted zero velocity updating. In *Autonomous Robots and Agents, 2009. ICARA 2009. 4th International Conference on*, pages 336–341. IEEE, 2009.

[105] Eric Foxlin. Pedestrian tracking with shoe-mounted inertial sensors. *IEEE Computer graphics and applications*, 25(6):38–46, 2005.

[106] Mengyuan Liu, Hong Liu, Chen Chen, and Maryam Najafian. Energy-based global ternary image for action recognition using sole depth sequences. In *3D Vision (3DV), 2016 Fourth International Conference on*, pages 47–55. IEEE, 2016.

[107] Muhammad Shoaib, Stephan Bosch, Ozlem Durmaz Incel, Hans Scholten, and Paul JM Havinga. Complex human activity recognition using smartphone and wrist-worn motion sensors. *Sensors*, 16(4):426, 2016.

[108] Meera Viswanathan, Carol E Golin, Christine D Jones, Mahima Ashok, Susan J Blalock, Roberta CM Wines, Emmanuel JL Coker-Schwimmer, David L Rosen, Priyanka Sista, and Kathleen N Lohr. Interventions to improve adherence to self-administered medications for chronic diseases in the united statesa systematic review. *Annals of internal medicine*, 157(11):785–795, 2012.

[109] Tamara L Hayes, John M Hunt, Andre Adami, and Jeffrey A Kaye. An electronic pillbox for continuous monitoring of medication adherence. In *Engineering in Medicine and Biology Society, 2006. 28th Annual International Conference of the IEEE*, pages 6400–6403. IEEE, 2006.

[110] R Brian Haynes, K Ann McKibbon, and Ronak Kanani. Systematic review of randomised trials of interventions to assist patients to follow prescriptions for medications. *The Lancet*, 348(9024):383–386, 1996.

[111] Chen Chen, Nasser Kehtarnavaz, and Roozbeh Jafari. A medication adherence monitoring system for pill bottles based on a wearable inertial sensor. In *Proceedings of the* 36^{th} *Annual International Conference of the IEEE Engineering in Medicine and Biology Society*, pages 4983–4986, Chicago, IL, August 2014.

[112] E. S. Sazonov, O. Makeyev, S. Schuckers, P. Lopez-Meyer, E. L. Melanson, and M. R. Neuman. Automatic detection of swallowing events by acoustical means for applications of monitoring of ingestive behavior. *IEEE Trans Biomed Eng*, 57(3):626–633, Mar 2010.

[113] Oliver Amft, Martin Kusserow, and Gerhard Troster. Bite weight prediction from acoustic recognition of chewing. *IEEE Trans. Biomed. Engineering*, 56(6):1663–1672, 2009.

[114] Vitality glowcap, 2014.

[115] Lindsey Dayer, Seth Heldenbrand, Paul Anderson, Paul O Gubbins, and Bradley C Martin. Smartphone medication adherence apps: Potential benefits to patients and providers. *Journal of the American Pharmacists Association*, 53(2), 2013.

[116] Bradi B Granger and Hayden Bosworth. Medication adherence: emerging use of technology. *Current Opinion in Cardiology*, 26(4):279, 2011.

[117] Glenn Vonk, Richard Rumbaugh, and Colleen Ryan. Medication adherence system, 2013. US Patent 8417381.

[118] Jeannette Y Lee, John W Kusek, Paul G Greene, Steve Bernhard, Keith Norris, Delia Smith, Beth Wilkening, and Jackson T Wright. Assessing medication ad-

herence by pill count and electronic monitoring in the african american study of kidney disease and hypertension (aask) pilot study. *American Journal of Hypertension*, 9(8):719–725, 1996.

[119] Jean-Michel Mallion, Jean-Philippe Baguet, Jean-Philippe Siche, Frederic Tremel, R De Gaudemaris, et al. Compliance, electronic monitoring and antihypertensive drugs. *Journal of hypertension. Supplement: Official Journal of the International Society of Hypertension*, 16(1):S75–9, 1998.

[120] M. Valin, J. Meunier, A. St-Arnaud, and J. Rousseau. Video surveillance of medication intake. In *Engineering in Medicine and Biology Society, 2006. EMBS '06. 28th Annual International Conference of the IEEE*, pages 6396–6399, Aug 2006.

[121] H. H. Huynh, J. Meunier, J.Sequeira, and M.Daniel. 3(12):260 – 267, 2009.

[122] Guillaume-Alexandre Bilodeau and Soufiane Ammouri. Monitoring of medication intake using a camera system. *J. Med. Syst.*, 35(3):377–389, June 2011.

[123] Amiko - medication management made easy, 2014.

[124] Smart blister, 2014.

[125] Haik Kalantarian, Nabil Alshurafa, Tuan Le, and Majid Sarrafzadeh. Non-invasive detection of medication adherence using a digital smart necklace. In *IEEE PerCom: Smart Environments Workshop*, 2015.

[126] Dariush Mozaffarian, Emelia J Benjamin, Alan S Go, Donna K Arnett, Michael J Blaha, Mary Cushman, Sarah de Ferranti, Jean-Pierre Després, Heather J Fullerton, Virginia J Howard, et al. Heart disease and stroke statistics: 2015 update a report from the american heart association. *Circulation*, 131(4):e29–e322, 2015.

[127] Melanie Nichols, Nick Townsend, Peter Scarborough, and Mike Rayner. Cardiovascular disease in europe: epidemiological update. *European heart journal*, 34(39):3028–3034, 2013.

[128] Azza AbuDagga, Helaine E Resnick, and Majd Alwan. Impact of blood pressure telemonitoring on hypertension outcomes: a literature review. *Telemedicine and e-Health*, 16(7):830–838, 2010.

[129] Lukáš Peter, Norbert Noury, and M Cerny. A review of methods for non-invasive and continuous blood pressure monitoring: Pulse transit time method is promising? *IRBM*, 35(5):271–282, 2014.

[130] Mohamad Kachuee, Mohammad Mahdi Kiani, Hoda Mohammadzade, and Mahdi Shabany. Cuff-less high-accuracy calibration-free blood pressure estimation using pulse transit time. In *Circuits and Systems (ISCAS), 2015 IEEE International Symposium on*, pages 1006–1009. IEEE, 2015.

[131] Ruiping Wang, Wenyan Jia, Zhi-Hong Mao, Robert J Sclabassi, and Mingui Sun. Cuff-free blood pressure estimation using pulse transit time and heart rate. In *Signal Processing (ICSP), 2014 12th International Conference on*, pages 115–118. IEEE, 2014.

[132] Juan C Ruiz-Rodríguez, Adolf Ruiz-Sanmartín, Vicent Ribas, Jesús Caballero, Alejandra García-Roche, Jordi Riera, Xavier Nuvials, Miriam de Nadal, Oriol de Sola-Morales, Joaquim Serra, et al. Innovative continuous non-invasive cuffless blood pressure monitoring based on photoplethysmography technology. *Intensive care medicine*, 39(9):1618–1625, 2013.

[133] Rohan Samria, Ridhi Jain, Ankita Jha, Sandeep Saini, and Shubhajit Roy Chowdhury. Noninvasive cuff'less estimation of blood pressure using photoplethysmography without electrocardiograph measurement. In *Region 10 Symposium, 2014 IEEE*, pages 254–257. IEEE, 2014.

[134] Mars Lan, Lauren Samy, Nabil Alshurafa, Myung-Kyung Suh, Hassan Ghasemzadeh, Aurelia Macabasco-O'Connell, and Majid Sarrafzadeh. Wanda: An end-to-end remote health monitoring and analytics system for heart failure patients. In *Proceedings of the conference on Wireless Health*, page 9. ACM, 2012.

[135] Roberto Antonicelli, Paolo Testarmata, Liana Spazzafumo, Cristina Gagliardi, Grzegorz Bilo, Mariaconsuelo Valentini, Fabiola Olivieri, and Gianfranco Parati. Impact of telemonitoring at home on the management of elderly patients with congestive heart failure. *Journal of Telemedicine and Telecare*, 14(6):300–305, 2008.

[136] Andreas J Morguet, Paul Kühnelt, Antje Kallel, Markus Jaster, and Heinz-Peter Schultheiss. Impact of telemedical care and monitoring on morbidity in mild to moderate chronic heart failure. *Cardiology*, 111(2):134–139, 2007.

[137] Sarwat I Chaudhry, Barbara Barton, Jennifer Mattera, John Spertus, and Harlan M Krumholz. Randomized trial of telemonitoring to improve heart failure outcomes (tele-hf): study design. *Journal of cardiac failure*, 13(9):709–714, 2007.

[138] Ozlem Z Soran, Arthur M Feldman, Ileana L Piña, Gervasio A Lamas, Sheryl F Kelsey, Faith Selzer, John Pilotte, and Judith R Lave. Cost of medical services in older patients with heart failure: those receiving enhanced monitoring using a computer-based telephonic monitoring system compared with those in usual care: the heart failure home care trial. *Journal of cardiac failure*, 16(11):859–866, 2010.

[139] Ozlem Z Soran, Ileana L Piña, Gervasio A Lamas, Sheryl F Kelsey, Faith Selzer, John Pilotte, Judith R Lave, and Arthur M Feldman. A randomized clinical trial of the clinical effects of enhanced heart failure monitoring using a computer-

based telephonic monitoring system in older minorities and women. *Journal of cardiac failure*, 14(9):711–717, 2008.

[140] J. T. Black, P. S. Romano, B. Sadeghi, A. D. Auerbach, T. G. Ganiats, S. Greenfield, S. Kaplan, and M. K. Ong. A remote monitoring and telephone nurse coaching intervention to reduce readmissions among patients with heart failure: study protocol for the better effectiveness after transition - heart failure (beat-hf) randomized controlled trial. *Trials*, 15, 2014.

[141] George B Moody and Roger G Mark. A database to support development and evaluation of intelligent intensive care monitoring. In *Computers in Cardiology, 1996*, pages 657–660. IEEE, 1996.

[142] Kurt Hornik, Maxwell Stinchcombe, and Halbert White. Multilayer feedforward networks are universal approximators. *Neural networks*, 2(5):359–366, 1989.

[143] Geoffrey E Hinton. Deterministic boltzmann learning performs steepest descent in weight-space. *Neural computation*, 1(1):143–150, 1989.

[144] Geoffrey E Hinton, Simon Osindero, and Yee-Whye Teh. A fast learning algorithm for deep belief nets. *Neural computation*, 18(7):1527–1554, 2006.

[145] Yoshua Bengio, Ian J Goodfellow, and Aaron Courville. Deep learning, book in preparation for mit press (2015). *Disponıvel em http://www. iro. umontreal. ca/˜ bengioy/dlbook*.

[146] Itamar Arel, Derek C Rose, and Thomas P Karnowski. Deep machine learning-a new frontier in artificial intelligence research [research frontier]. *Computational Intelligence Magazine, IEEE*, 5(4):13–18, 2010.

[147] Yoshua Bengio, Aaron Courville, and Pierre Vincent. Representation learning: A review and new perspectives. *Pattern Analysis and Machine Intelligence, IEEE Transactions on*, 35(8):1798–1828, 2013.

[148] Alex Graves, Marcus Liwicki, Santiago Fernández, Roman Bertolami, Horst Bunke, and Jürgen Schmidhuber. A novel connectionist system for unconstrained handwriting recognition. *Pattern Analysis and Machine Intelligence, IEEE Transactions on*, 31(5):855–868, 2009.

[149] Hasim Sak, Andrew Senior, and Françoise Beaufays. Long short-term memory recurrent neural network architectures for large scale acoustic modeling. In *Proceedings of the Annual Conference of International Speech Communication Association (INTERSPEECH)*, 2014.

[150] Sepp Hochreiter and Jürgen Schmidhuber. Long short-term memory. *Neural computation*, 9(8):1735–1780, 1997.

[151] Sameer Sethi et al. Correlation of invasive and non-invasive blood pressure: A must for management. *Indian journal of anaesthesia*, 54(6):581, 2010.

[152] Tijmen Tieleman and Geoffrey Hinton. Lecture 6.5-rmsprop: Divide the gradient by a running average of its recent magnitude. *COURSERA: Neural Networks for Machine Learning*, 4, 2012.

[153] Nitish Srivastava, Geoffrey Hinton, Alex Krizhevsky, Ilya Sutskever, and Ruslan Salakhutdinov. Dropout: A simple way to prevent neural networks from overfitting. *The Journal of Machine Learning Research*, 15(1):1929–1958, 2014.